

## Author's response to reviewer's comments

We thank the two reviewers for their constructive comments and suggestions, which have helped to improve the manuscript. Below, we provide detailed discussion of the changes made to the manuscript in response to the reviewers comments, and include a track-changes version of the manuscript and supplemental material so that all changes can be easily identified. We believe that we have addressed all reviewer comments thoroughly.

Before responding to the specific individual comments from the reviewers, we note that, we have made substantial changes to the manuscript based on the reviewer comments. Specifically, we changed the focus from looking at the relationship between sea spray aerosol particle hygroscopicity and ATOFMS cluster-type fractions to one between hygroscopicity and organic matter volume fractions ( $\epsilon_{\text{org}}$ ). The OM volume fractions were estimated from the AMS organic matter/PM<sub>1</sub> mass fractions that were presented in the original manuscript. In the original manuscript, we did not use the  $\epsilon_{\text{org}}$  quantitatively, as there are concerns regarding the detection efficiency of the AMS for these marine derived organics as particles containing a large fraction of sea salt have a higher susceptibility to particle bounce and organic matter contained in these particles may be inefficiently vaporized (as is suggested by the results presented by Frossard et al. (2014)). That said, in one of the references mentioned by Reviewer #2 (Ovadnevaite et al. (2012)), it was determined that sea salt aerosol had a collection efficiency ( $CE$ ) in the AMS of 0.25. We have therefore now corrected the AMS organic matter/PM<sub>1</sub> mass fractions using a  $CE$  of 0.25, and the mass fractions were converted to  $\epsilon_{\text{org}}$  assuming a density of 1 g/cm<sup>3</sup> for organic matter. The resulting  $\epsilon_{\text{org}}$  are therefore relatively uncertain in terms of absolute magnitude, but the trends with time should be reasonably robust under the assumption that the  $CE$  did not change substantially across the measurement campaign. A thorough discussion of the uncertainties in  $\epsilon_{\text{org}}$  as estimated from AMS organic matter/PM<sub>1</sub> mass fractions and the details for calculating  $\epsilon_{\text{org}}$  has been added to section 2.2.1.

“It is important to note that while the temporal trends of the AMS NR-OM/PM<sub>1</sub> fractions are likely reflective of the general behavior, the absolute values are more difficult to quantify because NR-OM associated with particles containing high sea salt fractions may not be vaporized efficiently by the AMS due to the refractory nature of sea salt (Frossard et al., 2014) and to the susceptibility of SSA particles to particle “bounce” in the AMS. Consequently, the SSA particles, including the NR-OM component, are detected with a collection efficiency ( $CE$ ) lower than unity (Frossard et al., 2014). One previous study (Ovadnevaite et al., 2012) determined the  $CE$  value for organic-free sea salt sampled when  $RH < 70\%$  is approximately 0.25. However, they also note that the  $CE$  is potentially instrument dependent, and further may not be applicable to the organic fraction in sea spray particles due to differences in ionization efficiency (which is a component of the overall  $CE$ ) (Ovadnevaite et al., 2012). It is also possible that the  $CE$  differs between particles that have differing relative amounts of OM and sea salt. Despite such uncertainties in quantification of NR-OM by the AMS for sea spray particles, the NR-OM mass concentrations for the sampled SSA particles were determined in this study assuming  $CE = 0.25$ . The measured NR-OM mass concentrations were used to calculate

NR-OM volume concentrations assuming a density ( $\rho$ ) of  $1.0 \text{ g/cm}^3$ . A value of  $1.0 \text{ g/cm}^3$  for  $\rho_{\text{OM}}$  is consistent with that of fatty acids ( $\rho < 1 \text{ g/cm}^3$ ), which are a significant fraction of marine-derived OM (Mochida et al., 2002; Cochran et al., 2016). However, this value serves as a lower bound for  $\rho_{\text{OM}}$  because OM with higher densities, such as sugars ( $\rho \sim 1.7 \text{ g/cm}^3$ ), have also been observed in SSA (Quinn et al., 2015). The NR-OM volume fractions of SSA ( $\epsilon_{\text{org}}$ ) were calculated as the ratio between the observed NR-OM volume concentrations and the integrated total particle volume concentrations from the size distribution measurements. Given the use of a lower-limit value for  $\rho_{\text{OM}}$  the  $\epsilon_{\text{org}}$  are likely upper limits (not accounting for uncertainty in the assumed *CE*).”

The CE-corrected  $\epsilon_{\text{org}}$  are now used as the primary compositional metric for understanding both the depression in *GF*(85%) values relative to inorganic sea salt and their temporal variability. Figures 3 and 5 have been updated to show the CE-corrected  $\epsilon_{\text{org}}$  values. Discussion regarding the temporal variability in and absolute magnitude of the CE-corrected  $\epsilon_{\text{org}}$  has been added.

“The NR-OM volume fractions of SSA varied from 0.29 to 0.50 throughout the course of the indoor MART microcosm experiment (Figure 3). The observation of such large  $\epsilon_{\text{org}}$  values is consistent with the substantial depressions in the *GF*(85%) values relative to pure, inorganic sea salt (2.1). The temporal variation in the  $\epsilon_{\text{org}}$  was generally similar to that of the *GF*(85%) values, with smaller *GF*(85%) values corresponding to larger  $\epsilon_{\text{org}}$  values, although the peak in  $\epsilon_{\text{org}}$  is somewhat sharper than the dip in the *GF*(85%). The inverse relationship between the *GF*(85%) and  $\epsilon_{\text{org}}$  is consistent with organic compounds being less hygroscopic than sea salt.”

The original Figure 4, which showed the relationship between the *GF*(85%) values and the ATOFMS non-sea salt cluster fractions, has been replaced. The new Fig. 4 now shows the relationship between *GF*(85%) and the CE-corrected  $\epsilon_{\text{org}}$ . We now use the Zdanovskii-Stokes-Robinson (ZSR) mixing rules to estimate a *GF*(85%) value for the organic matter component of the SSA particles specifically. The fitting procedure is described on Page 16 Lines 12-20 in the updated manuscript.

There has also been an evolution in our understanding of the ATOFMS clusters determined for nascent sea spray since the manuscript was originally submitted. A portion of the non-sea salt (sodium-depleted) clusters can be explained by the incomplete ionization of sea salt particles (Sultana et al., In Prep.). This change in our understanding of ATOFMS cluster types further supports our decision to use the CE-corrected  $\epsilon_{\text{org}}$  from the AMS in place of ATOFMS cluster types to understand the dependence of the *GF*(85%) on variations in particle composition. A brief discussion of this new understanding regarding the ATOFMS clusters for nascent sea spray has been added to the manuscript in the methods section.

“It is important to note, however, that dried SSA particles sampled by the ATOFMS can be spatially chemically heterogeneous, with shells depleted in Na and rich in Mg, K, and Ca (Ault et al., 2013). Thus, some fraction of the particles identified as having Mg or SSOC type spectra may be partially explained by the incomplete ionization of sea salt particles (Sultana et al., In Prep.). However, variations in the thickness of this Na-

depleted shell likely reflect variations in the total particle organic content. Therefore, increases in the fraction of SSOC or Mg type mass spectra generated suggest a net increase in SSA particle organic content.”

We made other changes, where deemed appropriate and added additional figures and tables as supplemental materials. Our point-to-point response to both reviewers follows below.

**Key: Black = Reviewer, Blue = Response**

### **Response to Reviewer #1**

The paper by Forestieri et al. presents results from two microcosm experiments on the properties of sea spray aerosols, focusing on their hygroscopic and optical properties, as a function of the seawater composition. The seawater composition was artificially modified in the microcosms by the addition of nutrients. The authors infer an average hygroscopic growth factor (HGF) for the whole sea spray aerosol population, from the measurement of the aerosol extinction enhancement due to the uptake of water vapour at 85% humidity. Results show a decrease of the HGF by 10 to 19% relative to pure inorganic sea salt. The authors then infer an average chemical composition from the HGF with the hypothesis that the organic fraction is hydrophobic. No linear link between the increase of Chl-a levels and the change in aerosol chemical composition (organic content, mainly) was observed. The study of the impact of the presence of organic matter in primary sea spray on its optical properties through the effect of a decreased water uptake has never been investigated in the past to my knowledge. Whether this has an important impact or not is important. In this view this is a very valuable study. However, the measurement methodology rely on several hypothesis and approximations that could be better justified (see detailed comments), and the article is more focusing on inferring the organic fraction of primary organic aerosol than on evaluating this impact, which could be more emphasised (the impact on scattering is only mentioned in the conclusion as a range from 10 to 35% for 85% humidities). I would have expected a time series of the extinction (wet and dry) in order to directly evaluate the impact of a phytoplanktonic bloom on the optical properties of sea salt aerosol. I recommend publication after major revisions.

Regarding the reviewers comment as to presentation of a time-series of extinction (wet and dry), we note that for this study the absolute values of extinction are not nearly as important as the relative values between the humidified and dried extinction (i.e.  $f(RH) = \text{wet extinction/dry extinction}$ ). Although MARTs produce particles with size distributions that are similar to particles produced from breaking waves in the ocean, the absolute particle concentrations (and therefore the absolute scattering) is different than what would be observed in the ambient marine atmosphere, as the absolute values depend on the sample flow rates, MART size, plunging frequency, etc. (Stokes et al., 2013). Thus, a focus on the extensive properties (e.g. dry and wet scattering) is, in our opinion, not as important as a focus on the intensive properties (e.g.  $f(RH)$ ). In the original manuscript, we presented a time-series only growth factor values that were derived from the  $f(RH)$  measurements and the size distribution measurements, not the  $f(RH)$  measurements themselves. However, to address the reviewers concern, we have now added to the supplemental material a time-series of measured wet and dry extinction measurements and of the associated  $f(RH)$ .

Regarding discussion of the limited evaluation of the impact of organic material on scattering, we intentionally kept this discussion “simple”. The reason for this is that the ultimate impacts depend on not only variability in the organic fraction, but also in real variations in relative humidity fields. Thus, a comprehensive evaluation would likely require assessment within a climate model, which is outside the scope of this work. To address the reviewers suggest that we emphasize the potential impact to a greater extent, we have added the following sentences to the conclusions:

“Regardless, the results presented here suggest that OM in SSA particles may have a non-negligible, yet variable impact on the light scattering by SSA particles in the ambient atmosphere. Most likely, the simulated cooling effect of SSA particles due to aerosol-radiation interactions (i.e. the “direct effect”) would be decreased relative to the assumption that all SSA behaves as sea salt.”

Therefore,  $f(\text{RH})$  (= wet scattering/dry scattering), which is an intensive parameter, is used to assess radiative impacts. A figure comparing the  $f(\text{RH})$  of particles observed in this study to the  $f(\text{RH})$  expected for pure, inorganic sea salt calculated using average size distributions for both microcosm experiments has been added to the supplementary material (Figure S8).

Page 4, lines 6-7 : “SSA particles sampled from the MARTs are primary, since the average residence time in the MARTs is much shorter than the time scale required for secondary processing of SSA particles (e.g. heterogeneous gas-phase reactions) (Lee et al., 2015).” What is the residence time in the microcosm headspace, what are briefly the results from Lee et al. 2015 to support this hypothesis ? How can the absence of any photochemical reactions producing condensing organic matter be excluded?

Oxidants which accompany secondary processes, such sulfates and nitrates, were not present in the ATOFMS spectra. This is as expected as zero air (particle, ozone, and volatile organic species free) was used to feed the MART headspace, so secondary processes should be highly minimized even over extended periods. Hydroxyl radicals should not be generated by the lamps used here, as the higher-energy UV radiation needed to photolyze water would be filtered by the acrylic chamber walls. The residence time in the headspace is particle size dependent (as discussed in Stokes et al., 2013). At the flow rate used here, for particles in the size range 400-600 nm the e-folding lifetime was 11 minutes and in the size range 1-2 microns was 8.5 minutes.

Page 5 lines 13\_18 : “The same seawater as used in the indoor MART was added to a separate MART and sampled immediately after collection and before nutrient addition. However, the resulting particle size distribution from this MART differed substantially from those measured from the indoor MART, with a much greater contribution of large particles. Thus, the measurements from this separate MART are not directly comparable to the measurements from the indoor MART and are not considered further” Is there any explanation for this ? Could it be that the same difference in original size distribution (before enrichment) was observed in the outdoor experiment ?

The large supermicron mode observed during in the pre-nutrient period may be due to differences in MART conditions, such as water level or sampling tube length, but we cannot entirely rule out that it is some difference due to the nutrient addition. Unlike the indoor MART, the outdoor MART was not sampled prior to enrichment, and thus we cannot directly address the reviewers' second question. In separate (unpublished) MART experiments, strong differences in the size distributions before/after nutrient addition are not observed, suggesting that in this particular case the size distribution difference was driven by external factors (which resulted from the somewhat more complex experimental setup during the IMPACTS study due to the large number of instruments involved).

Page 6, line 10 : "Group 1 sampled for 1.5 h, group 2 sampled for 2 h, and Group 3 for sampled 1 h each day that sampling was conducted" Was sampling always performed in this order ? Can there be a bias due to the position of the sampling period during the day ? Has this been tested ?

On all days, except for 7/9, the instruments sampled at the same time each day. It is possible that the composition differed when the cavity-ringdown (CRD) sampled versus when the ATOFMS sampled, but this has not been systematically tested. In fact, some differences are to be expected given that the observations suggest changes in composition and  $f(RH)$  from one day to the next. However, the correlation between the ATOFMS organic markers and the CRD growth factors indicates that compositional changes were gradual and the composition of particles sampled by both instruments was consistent on a given day, even though the ATOFMS sampled 9 hours after the CRD.

Page 6, line 25 : "The SEMS and APS distributions were merged using the SEMS distribution up to 1  $\mu\text{m}$  and the (dp,m equivalent) APS distribution at larger diameters." How did the two instrument compare on their common size range ? Why was the SEMS preferred over the APS on the 1-1.9 micron size range ?

A comparison between the SEMS and APS suggests that the SEMS under-counted particles with mobility diameters  $> 1$  micron. This was characterized during separate experiments in which substantial fractions of supermicron particles were sampled. At just above 1100 nm, the SEMS undercounted by  $\sim 20\%$  and at 1.5  $\mu\text{m}$ , the SEMS undercounted by  $\sim 90\%$ . We suspect that this difference resulted from the SEMS not being optimized in these experiments to transmit larger particles, and thus internal losses increased as size increased. It is for this reason that we chose to use the merged distribution, as opposed to the SEMS distribution by itself. However, in the size region that is most relevant to the experiments considered here, namely below  $\sim 1$  micron, there was no substantial difference between the SEMS and merged SEMS + APS distributions. Since the fraction of supermicron particles was very small for these MART studies the impact of SEMS vs. APS differences at larger sizes is negligible.

Page 7, line 2 : "Light absorption by the SSA particles was negligible, and thus extinction is equal to scattering, i.e.  $b_{\text{ext}} = b_{\text{sca}}$ ." Was this assumption validated ? Can Brown carbon contribute the SSA absorption ?

The SSA absorption was measured by a UC Davis photoacoustic spectrometer (Lack et al., 2011; Cappa et al., 2012) and the observed absorption was 0 Mm<sup>-1</sup> (within uncertainty), whereas the measured extinction was ~250 Mm<sup>-1</sup>.

Page 9, lines 16-17: "Unlike f(RH), GF values are independent of the dry particle size, and thus only depend on composition" This is only true for larger particles, the smaller the particles the highest the kelvin effect is. Maybe it is useful to argue that this hypothesis is true for the sizes of particles relevant here.

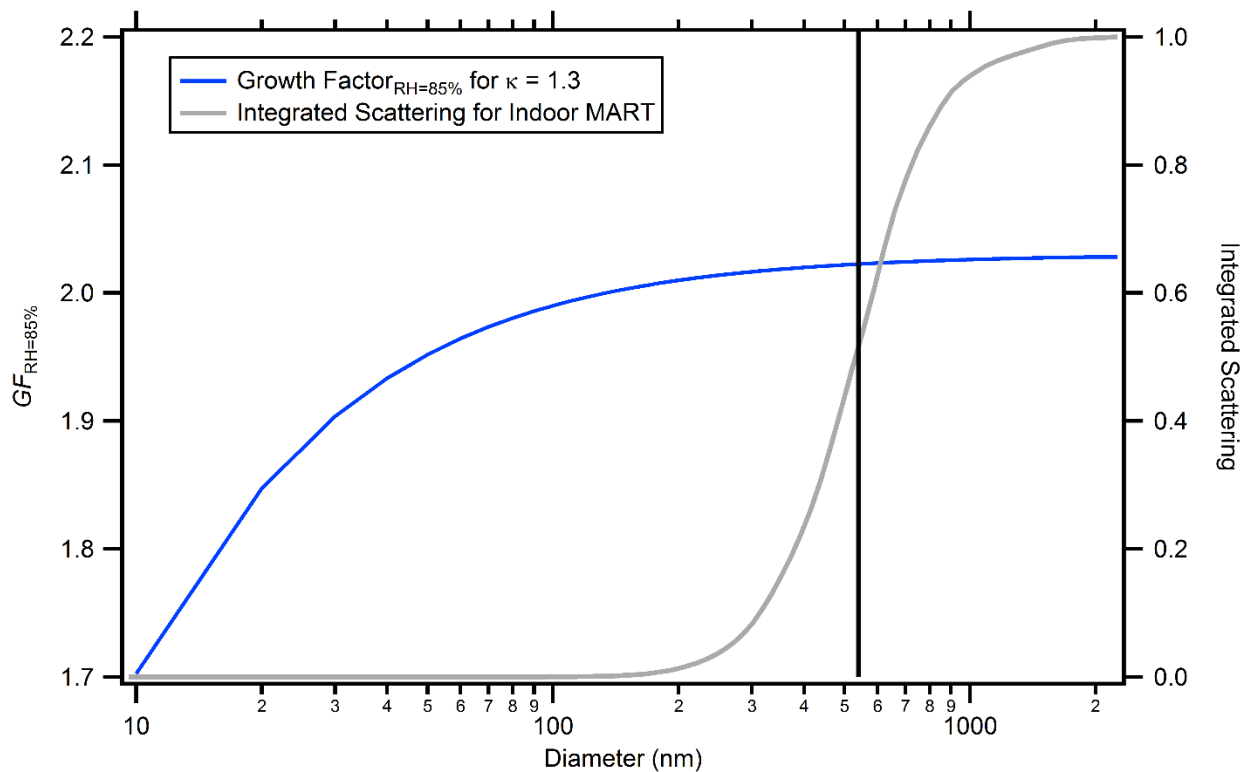
The reviewer raises an important point. We have therefore calculated theoretical growth factors as a function of particle diameter using equation 11 from Petters and Kreidenweis (2007), assuming 85% and assuming  $\kappa = 1.3$ . The relevant equation is:

$$\frac{RH}{\exp\left(\frac{A}{D_{dry}} \cdot GF\right)} = \frac{GF^3 - 1}{GF^3 - (1 - \kappa)}$$

The Kelvin effect is inherent in the  $A$  term in the above equation since:

$$A = \frac{4 \cdot \sigma \cdot MW_{H_2O}}{RT \cdot \rho_{H_2O}}$$

where  $\sigma$  = surface tension,  $MW_{H_2O}$  is the molecular weight of water and  $\rho_{H_2O}$  is the density of water. Results of these calculations are shown in the figure below. The black line indicates where the median (50%) integrated scattering occurred in our experiments. The  $GF(85\%)$  values change by only ~1% over the range of sizes that contributed substantially to the observed scattering and thus changes in the measured GF values should only depend on composition. (To the extent that composition depends on size, size will play a role. But the Kelvin effect can be ignored for these experiments.)

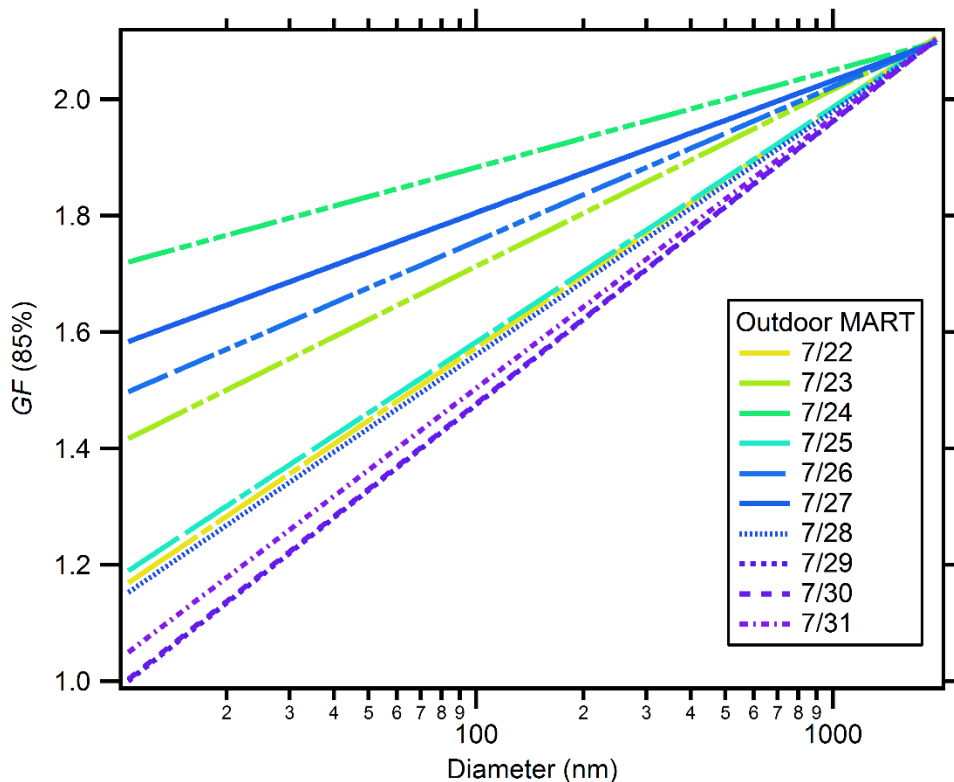


Pages 9 and 10 : calculation of  $GF(RH)$  : the underlying hypothesis for such a iterative calculation is that the chemical composition of the aerosol is homogeneous over the whole range of sizes (independent of the particle diameter). Figure S6 does not show this. How does this impact the results ?

This simplification has no major impact on our results. The iterative approach used in our analysis can be modified to allow  $GF$  values to vary with size. If a functional form is assumed then one can allow the parameters describing this relationship to vary, as opposed to a single average value, to match the observed  $f(RH)$  values. We have actually made this model modification, assuming that  $GF$  values are a linear function of  $\log(d_p)$ , increasing as  $d_p$  increases. Specifically, we assumed that  $GF(d_p) = a + b \cdot \log(d_p)$  with the added constraint that  $GF(1800 \text{ nm}) = 2.1$ , i.e. that these particles are pure sodium chloride and that all values must be  $\geq 1$ . It was fully possible to adjust the  $a$  and  $b$  coefficients for each day to match the calculated and observed  $f(RH)$  values. One then finds that the lines (and  $a$  and  $b$  coefficients) vary day-to-day in a manner consistent with the derived variations in the optically-weighted  $GF$  values. The results of this approach are shown in the figure below for the Outdoor MART. The reason that this approach was not adopted as the default approach is that we did not want to introduce another assumption regarding the form of the  $GF$  vs. diameter relationship, and thus opted for the simpler (albeit, potentially less physically realistic) approach. We now discuss this further in the manuscript in Section 2.2.2 and have added the following text.

“It is assumed that the growth factors are size independent, namely that  $GF_x = GF$  for all  $d_p$ . Thus, this method retrieves an effective, optically-weighted  $GF$  value that explains the observed influence of water uptake on light scattering for the sampled size distribution. An alternative approach was considered in which the  $GF_x$  were assumed to vary with

size, specifically as  $GF_x = 2.1 - b (\log(1.8 \mu\text{m}) - \log(d_{p,m}))$ , and where the value of  $b$  was allowed to vary during the optical closure, with the condition that  $GF_x \geq 1$ . (This expression assumes that particles with  $d_{p,m} = 1.8$  have a  $GF_x = 2.1$ , i.e. that of NaCl. The  $GF_x$  decrease as size decreases.) The derived  $b$  values exhibit a similar temporal dependence as the derived optically-weighted  $GF$  values. The general conclusions reached in this study are therefore independent of the assumptions made regarding the size-dependent behavior of  $GF_x$ . Thus, rather than introducing an uncertain functional form, the simpler assumption (namely, size-independent  $GF_x$  values) is used here.”



Page 10, lines 1ç-21 : "The measured GF(85%) for NaCl was 2.09 +/- 0.03 and for (NH4)2SO4 was 1.59 +/- 0.05, which compare very well with literature values of ~2.1 for NaCl (Cruz and Pandis, 2000; Laskina et al., 2015; Hansson et al., 1998) and ~1.55 for ammonium sulfate (Laskina et al., 2015; Wise et al., 2003)." The literature values should be reported for a given aerosol size (or size range).

The aerosol size ranges have been added to the manuscript.

Page 12 , lines 13\_14 : "Uncertainty in the assumed RI value for the dry particles may explain a small fraction (<5%) of the difference." How was this assessed ? Has the chemical analysis of the aerosol been used to estimate the real RI? All hypothesis for possible discrepancies addressed in this paragraph should be detailed in the methodology section (or at least in the supplementary material). An overall uncertainty on the HGF retrievals procedure should be calculated and

compared to the measured HGF variability and consequent Org frac variability, so the reader can be convinced that the measured time variations are real. The uncertainty on the calculation method should be less than the 10 to 19% decrease in HGF for the results of the paper to be significant.

The uncertainties in the measured  $f(\text{RH})$ , relative humidity, refractive index, and diameter all contribute to uncertainty in GF retrieval. A fuller discussion of the contributions of uncertainty in each term to the uncertainty in the retrieved GF values, and how this was determined, has been added to the supplementary material. The precision of the GF values for each experimental day ranged from 1.7 to 2.2% (determined as the standard deviation of the individual measurements over each sampling period), which is far less than the 5 to 15% (in the updated manuscript the GF(85%) for pure sea salt is assumed to be 2.1 instead of 2.2) decrease in GF relative to pure, inorganic sea salt.

Page 12, lines 21-24 : "We have tested the sensitivity of the retrieval method to an 8% increase in the particle diameters. The retrieved GF values are increased by a marginal amount (0.015-0.03) when the diameters are increased, and thus such potential sizing uncertainty does not affect the main conclusions presented here" Does this mean that a particle diameter increase of 8% was actually applied to the data set ?

This statement refers only to the sensitivity tests. In the sensitivity test, the particle diameters were all increased by 8%, and then the retrieval was performed. No adjustment was applied to the "data set" beyond this sensitivity test.

Page 17, lines 10-12 : "By using a campaign-average scaling factor, it is implicitly assumed that the actual variations in  $f_{\text{SS},0.75\mu\text{m}}$  are captured by  $f_{\text{SS},\text{avg}}$ , which seems reasonable given the general constancy of the size distributions over the course of each of the microcosm experiments, c.f. Fig. 2." Why would the relative stability of the size distribution shown on fig 2 insure that the non-sea salt content of the aerosol (shown to increase in the course of the experiment) evolves uniformly with size ?

The ATOFMS sea salt fractions are no longer used quantitatively, so we no longer adjust the sea salt fraction to a vacuum aerodynamic diameter  $0.75 \mu\text{m}$ .

Page 17, lines 19-24 : ". . . organic volume fraction ( $\epsilon_i$ ) of 0.56 – 0.88 for these particle types if it is assumed that volume mixing rules apply (i.e. the Zdanovskii-StokesRobinson mixing rules (Stokes and Robinson, 1966)). Since the non-SS values range from 0.53 – 0.74, if it is assumed that the SS-type and non-SS particle types have similar size distributions, then the implied ensemble average  $\epsilon_i$  would be about 0.33 – 0.52." I understand that the first time that  $\epsilon_i$  is used it refers to the fraction of hydrophobic material in the non-SS fraction, while the second time it is used it refers to the fraction of hydrophobic material in the overall aerosol. If this is right, the same terminology should not be used for both.

We now have an estimate for the organic volume fraction ( $\epsilon_{\text{org}}$ ) of the SSA particles and no longer estimate the non-SS organic fraction. Thus, there is no longer a need to change the terminology.

Page 18, lines 9-12: "Both DOC and heterotrophic bacteria concentrations increased as the bloom progressed until they stabilized around the point when Chl-a concentrations had returned approximately to their pre-bloom levels, with DOC concentrations ranging from 200 to 300  $\mu\text{M}$  C and heterotrophic bacteria concentrations from  $1 \times 10^6$  to a peak of  $1.7 \times 10^7$   $\text{mL}^{-1}$  (Figure S5B)." Are those values realistic for natural seawaters ?

As noted on Page 13 Lines 5-6 in the original manuscript, the peak DOC range is somewhat larger than values typically observed for blooms in the ocean, which are only  $\sim 130 - 250 \mu\text{M}$  C (Kirchman et al., 1991; Norrman et al., 1995). Regarding heterotrophic bacteria, the range of heterotrophic bacteria concentrations in surface ocean waters range from around 1 to  $5 \times 10^6$  cells per mL (Li, 1998), which is comparable to the bacteria concentrations observed in the MART, although the peak MART concentrations exceed those in the ocean. This has been added to the manuscript.

Technical comments

Page 5, line 8 : mesocosm or microcosm ?

"Mesocosm" has been replaced with "microcosm" to keep terminology consistent.

Figure 3 (B) : description of Org not in the figure text. "the reported uncertainties for all properties is 1 sigma: : "should be "the reported standard deviations for all properties is 1 sigma: : " as those are not uncertainties on the measurements

This has been updated in the manuscript.

\*\*\*\*\*

## Response to Reviewer #2

The paper by Forestieri et al. reports on hygroscopicity of sea spray particles generated in lab conditions during various stages of phytoplankton bloom development. Lab generated sea spray studies are being pursued by many research groups during recent years trying to uncover the mechanisms and impacts of organic matter enrichment in sea spray particles. The hygroscopic properties of sea spray were studied by measuring scattering properties of wet versus dry particles. As it measures bulk sea spray population it is missing on the important aspect of size dependent chemical composition which is critical in uncovering organic matter enrichment processes. The results of the study are not particularly new and the authors could increase its significance by assessing radiative forcing impacts.

Reductions in hygroscopicity have indeed been linked to SSA particle composition changes during phytoplankton blooms in the ocean during field studies, but (to our knowledge) this is the first time this has been quantified for particles produced during a phytoplankton bloom that is completely isolated from anthropogenic influence or background particles. Thus, we believe that this work does provide a new contribution to the literature, as noted on Page 3, Lines 19-20.

The goal of this study was not to understand the size dependence of SSA particle composition, but rather to link composition to optically weighted hygroscopic growth factors for submicron particles. A figure showing the observed  $f(\text{RH})$  relative to the  $f(\text{RH})$  of pure sea salt for duration of both microcosm experiments has been added to supplementary material as a complement to the radiative impacts discussion in Section 4.

Finally, regarding a broader assessment of the radiative forcing impacts, although we agree with the reviewer that this would be an interesting extension, it would clearly require doing something like implementing a new scheme in a climate model and running that climate model, which is far outside the scope of this work.

It would be very interesting how the results of this study compare with the study by Vaishya et al. (2013) conducted in marine atmosphere (the study referenced, but not discussed).

We have now added extensive discussion associated with Vaishya et al. in the “Implications and Conclusions” section. Specifically, we now write:

“This was previously suggested by the ambient measurements of Vaishya et al. (2013), who observed substantial differences in  $GF(90\%)$  and  $f(\text{RH})$  values for submicron particles having very different  $\epsilon_{\text{org}}$  fractions in what were identified as clean marine air masses. (Their  $GF(90\%)$  values were measured using a hygroscopic tandem DMA (HT-DMA) for size-selected particles with  $35 \text{ nm} \leq d_{p,m} \leq 165 \text{ nm}$ . Their  $f(\text{RH})$  values were measured for  $\text{PM}_{1.0}$ .) They observed that increases in  $\epsilon_{\text{org}}$  had no effect on the  $GF(90\%)$  until a threshold  $\epsilon_{\text{org}}$  was reached, specifically  $\epsilon_{\text{org}} > \sim 55\%$ . Below this value, they measured  $GF(90\%)$  value of  $\sim 2.3$ , which is the expected value for pure sea salt at  $\text{RH} = 90\%$ . Above this value, the observed a rapid fall off in  $GF(90\%)$  to a plateau at 1.22. This reported behavior differs from that observed for nascent SSA particles sampled in the current study. Here, substantial depressions in  $GF(85\%)$  (and  $f(\text{RH})$ ) relative to inorganic sea salt were observed when the  $\epsilon_{\text{org}}$  was only  $\sim 25\%$ , and a co-variation between  $GF(85\%)$  and  $\epsilon_{\text{org}}$  (and the ATOFMS SS spectral-type fraction) was observed. One plausible reason for this difference is that nascent (freshly-emitted) SSA particles are measured here whereas Vaishya et al. (2013) measured ambient particles that could be subject to photochemical processing. Secondary organic aerosol formed from gases, such as monoterpenes and isoprene, emitted from the ocean (Shaw et al., 2010) could have contributed to the NR-OM, although Vaishya et al. (2013) argue that this influence was negligible based on the literature. Emission rates of such species from the ocean and their relationship with oceanic processes are not well established. Although Vaishya et al. (2013) attempted to remove the influence of secondary organics in their analysis (as well as the influence of non-sea salt sulfate), it is possible that their analysis was complicated by the impacts of atmospheric processing. Another key difference is that relationship between the  $GF(85\%)$  values and  $\epsilon_{\text{org}}$  observed in the current study is consistent with ZSR behavior, while Vaishya et al. reported “bistable” behavior of the  $GF(90\%)$  values as a function  $\epsilon_{\text{org}}$  (i.e. the flat behavior at  $\epsilon_{\text{org}} < 55\%$  and the steep fall off above). The physical basis of this bistable behavior, and the functional form implied by their measurements, is not easily explained. Finally, the  $GF(90\%)$  measurements by Vaishya et al. were made for particles with  $d_{p,m} < 165 \text{ nm}$ , while the composition was characterized

with an HR-AMS. It is possible that size mismatch between these measurements influenced their analysis. Mass-weighted size distributions were not shown by Vaishya et al. (2013), however Frossard et al. show mass-weighted size distributions for ambient particles sampled in the remote marine boundary layer that suggest that much of the organic mass is contained in particles  $> 165$  nm. Our results clearly indicate that compositional changes to nascent SSA particles, driven by variation in physical and biochemical processes in seawater, can impact the influence of water uptake on scattering by submicron SSA even when  $\epsilon_{\text{org}} < 55\%$ . The comparison with the Vaishya et al. (2013) measurements suggests that this initial state can be further modified through atmospheric processing.”

The most confusing aspect of this study is that a significant change in hygroscopicity of sea spray particles is only loosely connected to chemical composition. AMS did not detect the amount of organic matter required to explaining the observed change in GF. While the authors speculate about the bounce and refractory nature of sea spray particles (providing no references) the published evidence is in favour of AMS being able to quantitatively measure sea spray e.g. (Allan et al., 2004; Ovadnevaite et al., 2012; Schmale et al., 2013) to mention a few.

As discussed in detail at the beginning of this document, we believe that the reviewer’s suggestion of better utilizing AMS data improves understanding of the observed  $GF(85\%)$  values. Despite the uncertainties in quantifying organic matter in sea spray aerosol (SSA) particles by the AMS, we estimated organic matter volume fractions ( $\epsilon_{\text{org}}$ ) for the particles sampled during this study. The range of  $\epsilon_{\text{org}}$  was 0.25 to 0.50, which is consistent with the observed depressions in growth factors relative to inorganic sea salt.

Frossard et al. (2014) was provided as a reference for the refractory nature of sea salt in the original manuscript (Page 15 Lines 1).

ATOFMS results seem to correlate with the observed GF, but ATOFMS lacks quantitative estimate as its sensitivity to sea spray is rather poor. As the mixed-in organic matter in sea spray would increase ATOFMS sensitivity, the amount of non-sea-salt particles would be biased high. Also considering ATOFMS size range and MART sea spray particle size peaking at a size where ATOFMS just starting to detect particles, it appears that ATOFMS measured only a fraction of sea spray population. As it currently stands, the data do not corroborate each other.

It is true that the ATOFMS results are semi-quantitative. However, trends in the data are still informative and are indicative of changes in the chemistry of the particles. Therefore, increases in the number of SSOC type spectra are indicative of chemical changes in the particle population, specifically higher organic content. Though we cannot say quantitatively the degree of organic enrichment, we can say that it occurred. Also, not all organic matter would necessarily increase the ATOFMS sensitivity. If it was very lipid rich (with lots of hydrocarbon character) the sensitivity may have even decreased.

While the number-weighted distribution peaked at 100 nm, the CRD optically weighted GFs are most sensitive to particles with  $d_{p,m}$  between 400 nm to 800 nm (see Page 11 Lines 13-14 and Figure 2) . The ATOFMS counts are maximum at a vacuum aerodynamic diameter of 1.5  $\mu\text{m}$  (Figure S3), corresponding to a mobility diameter ( $d_{p,m}$ ) of 830 nm, which is a little above this range. However, since the ATOFMS is no longer used quantitatively, it is no longer necessary to adjust ATOFMS cluster fractions to smaller sizes ( $d_{va} = 0.75 \mu\text{m}$ ) as was done in the original manuscript

Page4, Line 24. I wonder if the flow was split isokinetically (equal face velocities) between instruments sampling from MART as that could affect sampled particle sizes of individual instruments. The authors mentioned laminar conditions, but laminar conditions limit particle losses to tubing walls while isokinetic split maintains the same particle population into each sampling line.

The reviewer raises an important question about the comparability of the measurements between instruments due to differences in sampling. During these experiments, flow was not split isokinetically. The particle-laden air from the MART was sampled into a manifold. The individual instruments sampled from this manifold from one of a many “ports”. The flow rate to each instrument (or group of instruments), and thus the flow from each port, varied. For example, for Group 1 the CRD + SEMS sampled a much higher flow rate (3 LPM) than the AMS and ATOFMS (~ 0.7 to 1 LPM) from the manifold. Therefore, it is possible that the instruments sampled particle populations with different sizes. It is difficult to estimate differential losses between the different ports due to flow rate differences in this configuration. The equations describing aspiration efficiency for isoaxial sampling from an air stream typically have a form similar to:

$$\eta_{asp} = 1 + \left[ \frac{U_0}{U} - 1 \right] [other\ terms]$$

where  $\eta_{asp}$  is the aspiration efficiency,  $U_0$  is the ambient gas stream velocity and  $U$  is the sampling velocity (Kulkarni, Baron and Willeke, 2011). The last term in brackets (“other terms”) depends on particle diameter and velocity, but we will not worry about this at this time. For the manifold system here, the effective ambient gas stream velocity is very low, and will be much lower than the sampling velocity to each individual port (due in large part to the substantial difference in size between the manifold and the sampling ports. In the limit of  $U_0 \rightarrow 0$  (or more specifically,  $U_0 \ll U$ ), we can see that  $\eta_{asp} \rightarrow 1$ . Thus, it seems reasonable to think that the particle population will not be strongly influenced by the non-isokinetic sampling conditions here and the lack of explicit isokinetic sampling did not have a substantial impact on the measurements here.

Page 5, Line 12. Peak chlorophyll concentration was mentioned as 10 $\mu\text{g/l}$  in the previous paragraph.

Even though the peak was 10 $\mu\text{g/l}$ , a concentration of 12  $\mu\text{g/l}$  is consistent with MART bloom studies described in Lee et al. (2015). This line has been revised to read “Further sampling was delayed until Chlorophyll-a (Chl-a) concentrations exceeded *approximately* 12  $\mu\text{g L}^{-1}$ ”

Line 17. Was this MART reproducibility issue or else? Considering 3week duration of the whole experiment a substantial degradation of organic matter (rotting) should have occurred at ambient temperatures in excess of 25C. Was bacteria growth monitored to inform on such process and if not informative, how could that be related to real world environment?

The reason for the greater contribution of larger particles in the pre-nutrient size distribution is unknown. It may have been due to differences in water level (water was collected for offline sampling once per day) or sampling tube length.

Bacterial growth in the bulk water was indeed monitored over the course of the 2 week (not 3 week) duration of each individual MART experiment. The time-series of bacterial concentrations was shown in the original manuscript in Figure S6 and was observed to peak after the chlorophyll peak. The method for this measurement has been added to Table 1. The impact of bacteria in the source water on the chemical nature and fraction of organic matter in nascent SSA particles has been discussed in more detail in Wang et al. (2015).

Page 6, Line 27. Were the particles dried? What RH? It seems that APS density was picked based on OM fractional contribution which suggests about 30% depending on OM density. If particles were not dried the picked density would not apply.

As stated in the original manuscript Page 6 Line 13, particles were dried (RH < 20%) prior to sizing. For all instruments mentioned, we stated that they measured “dried” particles.

Page 7, Line 26. Was PM2.5 cyclone operated in dry or wet conditions which could have converted PM2.5 into PM1 or lower size cut if wet?

The PM2.5 cyclone was located prior to the drier and thus operated in “wet” conditions. The RH at the point of the cyclone was around 70%, although this was not constantly monitored. The equivalent size cut for the dried particles was therefore smaller (as suggested by the reviewer), we estimate by ~1.5x (based on our derived GF values). A figure showing the cavity ring-down and SEMS sampling configuration following the manifold has been added to supplementary material (Figure S1). The RH for cyclone sampling has also been added to the manuscript (Page 8 Line 29 and Page 9 Lines 1-4).

Page 8, Line 3. Following the paragraph above referring to minimal contribution of >2.5um particles to the total SSA population it follows that ATOFMS sampled minor fraction of particles considering its transmission efficiency. Given low ATOFMS sensitivity to sea salt particles it transpires that ATOFMS sampled fraction of a fraction of SSA population. This aspect has to be clearly articulated otherwise references to SSA chemical composition is heavily biased towards supermicron particles.

In the original manuscript, the ATOFMS size-dependent counts were shown in Figure S2. As stated in the manuscript (Page 8 Line 17-18) and indicated by this figure, the peak in the particle counts for the ATOFMS is at 1.5  $\mu\text{m}$  vacuum aerodynamic diameter ( $d_{va}$ ). The particle counts fall off rapidly below  $d_{va} = 0.5 \mu\text{m}$ . As discussed in the manuscript, to relate the ATOFMS measurements to the optical property and hygroscopicity measurements requires converting the vacuum aerodynamic diameters into mobility-equivalent diameters ( $d_m$ ). A value of  $d_{va} 1.5 \mu\text{m}$

corresponds to a mobility-equivalent diameter of 830 nm. This value of  $d_m$  is in the upper end of the size range of the particles that most contributed to the observed scattering. However, since we no longer use ATOFMS data in a quantitative way and mainly use this data for understanding temporal changes, it is no longer necessary to adjust the ATOFMS fractions to a more relevant size.

Page 9, Line 2. Is it referred to dry or wet particles? If SEMS was dried, but AMS was not then not same SSA population was measured by the two instruments making diameter match irrelevant. Wet particles entering the AMS inlet are instantly frozen due to adiabatic expansion and segregated by aerodynamic lenses based on their wet diameter. Assuming RH in the MART and subsequent sampling lines 90-100%, wet particle diameter was 2-3 times larger than dry SEMS particles. NR-OM mass was therefore limited to 186-280nm instead of 560nm. The drying issue appears quite central throughout the manuscript, so I suggest it clarifying at the beginning and using notations  $d(\text{dry})$ ,  $d(\text{wet})$  were appropriate. If AMS sampled wet particles that would explain the missing mass discussed few lines below.

As stated on Page 8 Line 18 in the original manuscript, the AMS sampled dried particles. In fact, all of the instruments used in this study ultimately sampled dried particles. Thus, instead of adopting the notation suggested above throughout the manuscript (since wet particle diameters are only discussed in the Instrumentation section), clarification has been added to specify whether particles were dried prior to sampling for each instrument in Table 1.

Also, we should correct the misconception that the RH in the MART and sampling lines was necessarily 90-100%. The RH in the MART is dictated by the balance between the evaporation rate of water and the flow rate and RH of the sampling airstream. The RH in our sampling lines was, in fact, closer to 70% RH and not 90-100%.

Line 8. AMS is typically calibrated with dry  $\text{NH}_4\text{NO}_3$  particles. Why would SS particles bounce more than the calibration particles as AMS chemical species mass is calculated on nitrate equivalent basis?

Particle bounce is not significant for ammonium nitrate because it primarily exists in the liquid phase and thus has a high collection efficiency (CE) of ~100%. On the other hand, solid particles have lower CE values due to particle bounce. Issues of collection bounce for different materials and as a function of phase have been previously addressed by [Matthews et al. 2008]. Sea salt specifically has a CE of 0.25, although may vary by instrument and can depend on the extent of drying (Ovadnevaite et al., 2012).

Page 11, Line 20. Many lab and ambient studies reported chemical composition dependence on particle size which would make GF size dependent too. This study reports size independent (averaged) GF which is rather misleading and, therefore, the issue should be clearly stated.

The reported GF values here are defined as “optically weighted” to indicate just what the reviewer implies, namely that they are an average over different sizes but weighted by the scattering. To further clarify, in the abstract on Page 1 Line 22, “bulk average” has been changed

to “optically-weighted average.” We have also added text to Section 2.2.1 where the  $f(\text{RH})$  to  $GF$  inversion procedure was discussed to make this issue clearer. We now state:

“Unlike  $f(\text{RH})$ ,  $GF$  values are independent of the dry particle size (above about 100 nm diameter) for particles of a given composition. Thus, variations in the optically-weighted  $GF$  values are driven only by variations in particle composition, specifically variations in the average composition of particles in the size range over which the optical measurements are most sensitive. For the measurements here, the sensitive size range is between about 400 nm and 800 nm with particles below 200 nm contributing almost zero to the observed scattering (see Section 3.1 below). SSA particle composition can vary with size (e.g. O’Dowd et al., 2004), and thus the  $GF$  itself may vary with size. The optically-weighted  $GF$  averages across such size-dependent variations in composition to focus on the chemical changes that most influence water uptake by the particles that most contribute to light scattering.”

Line 28. The discrepancy can be partly due to shallow cut-off function of PM2.5 cyclone. Another source of discrepancy can be due to losses of wet particles and corresponding losses in dryers as in general wet particles are lossier. Again the drying of the particle is very unclear throughout the study and difficult to interpret.

We have now clarified the experimental configuration and the drying aspects within the manuscript. In very general terms, all instruments used in this study ultimately sampled dried particles. However, the particles that passed through the cyclone were not dried, but at an  $\text{RH} \sim 70\%$ ; they were subsequently dried prior to sampling. Below is a figure showing the general sampling configuration, and has been added to the supplementary material (Figure S1).

Although the reviewer is correct to note that losses increase with size, it is important to realize that the effect of water uptake on particle losses is not straightforward. Water is typically less dense ( $1 \text{ g cm}^{-3}$ ) than many other common atmospheric materials. Thus, if water uptake leads to a decrease in density then this can offset, at least to some extent, the increase in size in terms of sedimentation losses. Consider an example. If a 1 micron particle has a density of  $2.0 \text{ g cm}^{-3}$  (e.g. sea salt) and doubles in size due to water uptake (e.g.  $GF = 2.0$ ) then the density of the particle will decrease to  $1.22 \text{ g cm}^{-3}$ . The percent loss of a 1 micron particle with density =  $2.0 \text{ g cm}^{-3}$  due to sedimentation in a 10 m long tube at a flow rate of 5 lpm is 9.3%. If the particle size were doubled without changing the density, the loss would increase to 32%. But, if the decrease in density is accounted for the loss only increases to 13%. Thus, the decrease in density offsets a very large fraction of the increase in size. (The above calculations were performed using the Particle Loss Calculator of Von der Weiden et al. (2009).) Now, of course, if the density of the material were closer to water (such as may be the case for organics) this offsetting effect would be smaller. But our premise is that the organic material is relatively non-hygroscopic, and thus the water uptake itself (and associated increase in size) would be smaller, negating the effect in the first place. Consequently, while it is possible that differences in the influence of sedimentation between instruments due to differences in drying, the magnitude of the difference is much smaller than one might intuit based on the size change alone. As such, while it may be possible that the optical closure may have been impacted by differential sedimentation of wet

and dry particles such and impact is limited in scope. Finally, we note that the driers used to dry particles sampled into the CRD-PAS and SEMS were oriented vertically (to minimize sedimentation losses).

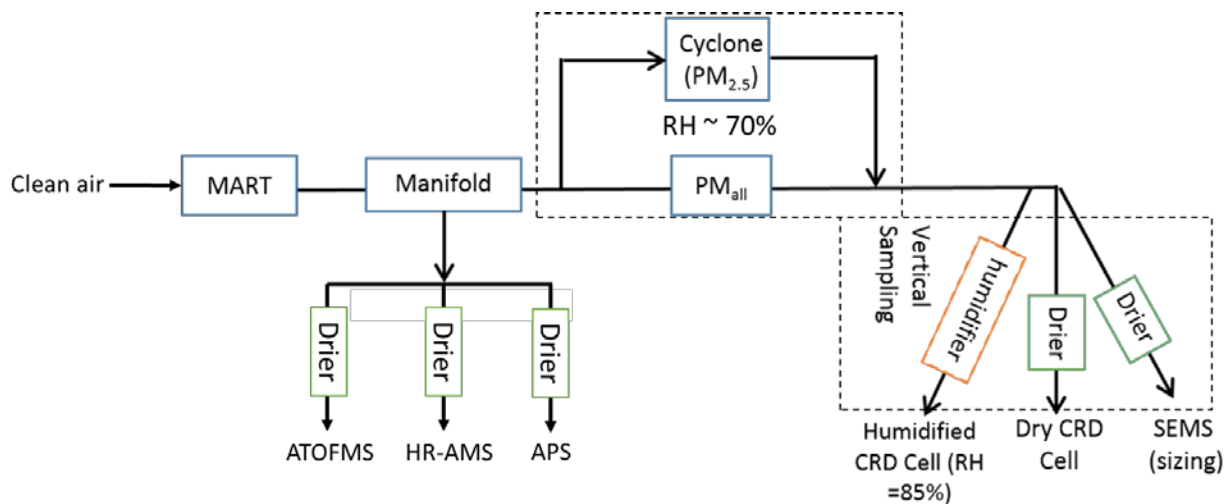


Figure S1. A detailed schematic of the general sampling scheme for the online instruments. Note that not all instruments sampled at the same time (see Table 1). Particles sampled from the MART passed through a manifold from which they were subsampled to the various instrumentation. All instruments included an upstream drier and sampled dried particles. The driers and humidifiers for the CRD and SEMS sampling group (Group 1) were oriented vertically. The particles sampled to the CRD and SEMS alternately passed through a PM<sub>2.5</sub> cyclone. The RH at this point was ~70%.

Page 12, Line 6. Wiedensohler et al. (2012) reported that in general sizing errors of different instruments can be objectively up to 10%.

The reviewer is correct that the sizing errors of different instruments can be objectively up to 10%. In our case, we characterized the sizing accuracy of the SEMS using size-selected PSLs and found that the particle sizes were characterized to within 1% of the stated PSL size (see Page 12 Lines 7-12 in the original manuscript). Thus, it seems unlikely that large instrumental sizing errors are the primary reason for differences between the observed and calculated dry particle scattering. However, we have added a reference to the Wiedensohler paper to the discussion on Page 12 as motivation for considering the possibility of sizing errors. “Wiedensohler et al. (2012) reported that sizing errors between instruments can be up to 10%.”

Page 13, Line 13. 2.2 at 85% or 90%? Also on page 10, GF(85%) of NaCl was referred to as 2.1.

A GF(85%) of 2.2 was originally used as a value for sea salt and not NaCl. However, a value of 2.1 is a better estimate for sea salt (Ming and Russell, 2001) at 85% relative humidity and the manuscript has been updated using this value for sea salt.

Line 27. Is it possible that the relative abundance of Fe-rich particles was due to higher sensitivity of ATOFMS to Fe-rich versus SSA?

The reviewer raises a good point about differential sensitivity of the ATOFMS. However, here we are confident that the higher relative abundance of Fe-rich particles at the beginning of the experiments is due to the addition of iron rich nutrients to encourage phytoplankton growth. As the reviewer notes, the ATOFMS is very sensitive to iron compared to species such as sodium chloride making exact quantification difficult. However, we emphasize that the *trends* in the particle spectra and the particle type abundances are reflective of changes in the particle composition. During many other "microcosm" experiments using the same methodology, an initial spike in iron signal after nutrient addition was observed, which then declines as the bloom progresses and nutrients are likely taken up into the proliferating microbiology. Finally, we note that while differences in sensitivity between particle types would certainly give rise to errors in particle type quantification (relative abundance) at a given point in time, it should not give rise to time-dependent changes in the relative abundance.

Page 14, Line 23. This is only true if ATOFMS and CRD size ranges were exactly the same which was not the case as ATOFMS cannot reliably detect 100nm particles, especially SSA.

The reviewer again raises a good point about particle size and comparability. Here, we reemphasize that we have measured optically-weighted growth factors and, for the size distributions from the MART, particles with  $d_{p,m} \leq 100$  nm contributed very little to overall scattering measured by the CRD. As stated on Page 11 Lines 16-20 in the original manuscript, the optically-weighted GF measurements were most sensitive to  $d_{p,m}$  (mobility diameters) between 400 to 800 nm, with median scattering occurring at  $d_{p,m} = 530$  nm. As such, we compared the optically-weighted GF values to the ATOFMS composition for particle having  $d_{va} \sim 0.75$   $\mu\text{m}$ , which corresponds to a  $d_{p,m} = 420$  nm.

Page 16, Line 13. Page 10 referred to 2.1 GF(85%). Why GF=1 is expected as the minimum combined value? Any reference to backup? Marine gels and micelles have been reported to process some water despite being generally hydrophobic (Ellison et al., 1999; Chakraborty and Zachariah, 2007). Fatty acid is only one of the many possible compounds and necessarily entirely hydrophobic.

While it is true that many types of marine organic matter have  $GF > 1$ , we assume a  $GF = 1$  as a lower bound. Although a lower bound, this assumption is consistent with GFs for fatty acids often found in marine aerosols (e.g. Cochrane et al., 2016). That said, we have revised the sentence to read (added text in italics): "The line connecting  $GF_{SS}(85\%) = 2.2$  and  $GF_{non-SS}(85\%) = 1.0$  provides the minimum value (*lower bound*) expected for any combination of SS and non-SS particles."

Line 20. It has been demonstrated in numerous studies that OM fraction in sea spray is size dependent. Should the GF value of 1.39 be interpreted as a bulk average of highly enriched and poorly enriched SS particles?

As noted above, we are now using  $\epsilon_{\text{org}}$  instead of the fraction of ATOFMS non-SS particles to examine the relationship between particle hygroscopicity,  $GF(85\%)$ , and composition. Therefore, we now estimate GF values for the organic fraction of the sampled PM specifically, i.e. the  $GF(85\%)$  values after extrapolation of our fits to  $\epsilon_{\text{org}} = 1$ . We find values of  $GF_{\text{org}}(85\%) = 1.16$  and  $1.23$  for the two MART experiments, which are optically weighted averages. One can assume that the GF is constant with size or that it varies with size, perhaps with an inverse relationship between GF and size, since OM fraction typically increases with decreasing size, within the optically-weighted size range. As discussed in detail in response to Reviewer #1, it is fully possible to assume some relationship between particle size and GF to come up with an optically-weighted average value. To clarify, we have added the following sentence: “This value for  $GF_{\text{org}}$  can be interpreted as an optically-weighted average for the OM component of the SSA particles sampled here.”

Page 17, Line 20. There is an issue regarding size dependent chemical composition. As scattering is dominated by larger submicron sizes and the smaller submicron particles tend to be more enriched in OM, averaged GF of this study missing out on the important aspect of size dependent chemical composition.

We do not dispute that the GF may be size dependent (O'Dowd et al., 2004; Prather et al., 2013). However, we emphasize again that we have measured the *optically-weighted average GF*. Thus, the measured optically-weighted GF is directly relevant to the actual impact of composition variations on SSA particle light scattering. Put another way, composition changes of e.g. 50 nm particles are almost completely irrelevant to the magnitude of light scattering by SSA particles and the direct effect (although critical to understanding the impact of SSA particles on clouds via their ability to act as CCN). It is instead variations in the average composition within the optically-relevant range, which is around 400-800 nm in this study given the size distribution, that is most important to consider when considering the total scattering. Had we instead measured size-dependent GF values explicitly, this would have provided, perhaps, greater process-level information. However, without considering which particles in the size distribution do most of the scattering, such process-level information is limited in nature. Since the MART system generates particle size distributions that are very similar to those generated from real wave breaking (Prather et al., 2012; Stokes et al., 2014), our optically-weighted measurements are of direct relevance to understanding the impact that compositional variations have on overall light scattering. As noted above, we have revised Section 2.2.1 to more clearly address this issue of size-dependent composition.

Line 24. How this volume fraction compared with AMS chemical composition? Did AMS record any substantial organics as 0.33-0.52 volume fraction would suggest? Figures show that AMS OM fraction was 0.05.

The reviewer raises an important question about comparability between the derived organic volume fractions and the AMS measurements. As stated at the beginning of our responses, we estimated  $\epsilon_{\text{org}}$  values from the AMS measurements instead of deriving organic volume fractions from our  $GF$  values. The estimated GFs for the organic component are above 1 indicating that our estimates for  $\epsilon_{\text{org}}$  are reasonable.

Page 18, Line 5. “which was 5 times higher”. Much higher chl was probably due to higher temperature than the ocean (what was the T range?) and plentiful nutrients.

In the manuscript, we attribute the larger Chl-a concentrations to larger photosynthetically active radiation. However, temperature and nutrients could have also played a role. The temperature of the water in the MART was ~26°C, which is larger than the 20 to 23°C measured for seawater at the Scripps pier (Table 2).

‘Page 19, Line 3. Consider different size ranges sampled if AMS was not dried. Table 1. AMS size range is missing.

As stated above, particles sampled by the AMS were dried. The size range is now included in Table 1.

## References

- Ault, A. P., Guasco, T. L., Ryder, O. S., Baltrusaitis, J., Cuadra-Rodriguez, L. A., Collins, D. B., Ruppel, M. J., Bertram, T. H., Prather, K. A., and Grassian, V. H.: Inside versus Outside: Ion Redistribution in Nitric Acid Reacted Sea Spray Aerosol Particles as Determined by Single Particle Analysis, 135, 14528-14531, doi:10.1021/ja407117x, 2013.
- Cappa, C. D., Onasch, T. B., Massoli, P., Worsnop, D. R., Bates, T. S., Cross, E. S., Davidovits, P., Hakala, J., Hayden, K. L., Jobson, B. T., Kolesar, K. R., Lack, D. A., Lerner, B. M., Li, S.-M., Mellon, D., Nuaaman, I., Olfert, J. S., Petäjä, T., Quinn, P. K., Song, C., Subramanian, R., Williams, E. J., and Zaveri, R. A.: Radiative Absorption Enhancements Due to the Mixing State of Atmospheric Black Carbon, 337, 1078-1081, doi:10.1126/science.1223447, 2012.
- Cochran, R., Laskina, O., Jayarathne, T., Laskin, A., Laskin, J., Lin, P., Sultana, C. M., Moore, K. A., Cappa, C., Bertram, T., Prather, K. A., and Grassian, V. H.: Analysis of Organic Anionic Surfactants in Fine (PM<sub>2.5</sub>) and Coarse (PM<sub>10</sub>) Fractions of Freshly Emitted Sea Spray Aerosol, 50 2477-2486, doi:10.1021/acs.est.5b04053, 2016.
- Frossard, A. A., Russell, L. M., Massoli, P., Bates, T. S., and Quinn, P. K.: Side-by-side comparison of four techniques explains the apparent differences in the organic composition of generated and ambient marine aerosol particles, 48, v-x, doi:10.1080/02786826.2013.879979, 2014.
- Kirchman, D. L., Suzuki, Y., Garside, C., and Ducklow, H. W.: High turnover rates of dissolved organic carbon during a spring phytoplankton bloom, 352, 612-614, doi:10.1038/352612a0, 1991.
- Lack, D. A., Richardson, M. S., Law, D., Langridge, J. M., Cappa, C. D., McLaughlin, R. J., and Murphy, D. M.: Aircraft Instrument for Comprehensive Characterization of Aerosol Optical Properties, Part 2: Black and Brown Carbon Absorption and Absorption Enhancement Measured with Photo Acoustic Spectroscopy, 46, 555-568, doi:10.1080/02786826.2011.645955, 2011.
- Lee, C., Sultana, C. M., Collins, D. B., Santander, M. V., Axson, J. L., Malfatti, F., Cornwell, G. C., Grandquist, J. R., Deane, G. B., Stokes, M. D., Azam, F., Grassian, V. H., and Prather, K. A.: Advancing Model Systems for Fundamental Laboratory Studies of Sea Spray Aerosol using the Microbial Loop, 119 8860–8870, doi:10.1021/acs.jpca.5b03488, 2015.
- Li, W. K.: Annual average abundance of heterotrophic bacteria and *Synechococcus* in surface ocean waters, 43, 1746-1753, doi:10.4319/lo.1998.43.7.1746, 1998.

Ming, Y. and Russell, L. M.: Predicted hygroscopic growth of sea salt aerosol, 106, 28259-28274, doi:10.1029/2001JD000454, 2001.

Mochida, M., Kitamori, Y., Kawamura, K., Nojiri, Y., and Suzuki, K.: Fatty acids in the marine atmosphere: Factors governing their concentrations and evaluation of organic films on sea-salt particles, 107, AAC 1-1–AAC 1-10, 2002.

Norrman, B., Zwiefel, U. L., Hopkinson, C. S., and Brian, F.: Production and utilization of dissolved organic carbon during an experimental diatom bloom, 40, 898-907, doi:10.4319/lo.1995.40.5.0898, 1995.

O'Dowd, C. D., Facchini, M. C., Cavalli, F., Ceburnis, D., Mircea, M., Decesari, S., Fuzzi, S., Yoon, Y. J., and Putaud, J.-P.: Biogenically driven organic contribution to marine aerosol, 431, 676-680, doi:10.1038/nature02959, 2004.

Ovadnevaite, J., Ceburnis, D., Canagaratna, M., Berresheim, H., Bialek, J., Martucci, G., Worsnop, D. R., and O'Dowd, C.: On the effect of wind speed on submicron sea salt mass concentrations and source fluxes, 117, doi:10.1029/2011jd017379, 2012.

Petters, M. and Kreidenweis, S.: A single parameter representation of hygroscopic growth and cloud condensation nucleus activity, 7, 1961-1971, doi:10.5194/acp-7-1961-2007, 2007.

Prather, K. A., Bertram, T. H., Grassian, V. H., Deane, G. B., Stokes, M. D., DeMott, P. J., Aluwihare, L. I., Palenik, B. P., Azam, F., and Seinfeld, J. H.: Bringing the ocean into the laboratory to probe the chemical complexity of sea spray aerosol, 110, 7550-7555, doi:10.1073/pnas.1300262110, 2013.

Quinn, P. K., Collins, D. B., Grassian, V. H., Prather, K. A., and Bates, T. S.: Chemistry and Related Properties of Freshly Emitted Sea Spray Aerosol, doi: 10.1021/cr500713g, 2015. doi:10.1021/cr500713g, 2015.

Shaw, S. L., Gantt, B., and Meskhidze, N.: Production and Emissions of Marine Isoprene and Monoterpenes: A Review, *Adv. Meteorol.*, 2010, doi:10.1155/2010/408696, 2010.

Stokes, M. D., Deane, G. B., Prather, K., Bertram, T. H., Ruppel, M. J., Ryder, O. S., Brady, J. M., and Zhao, D.: A Marine Aerosol Reference Tank system as a breaking wave analogue for the production of foam and sea-spray aerosols, *Atmos. Meas. Tech.*, 6, 1085-1094, doi:10.5194/amt-6-1085-2013, 2013.

Sultana, C. M., Collins, D. B., Lee, C., Axson, J. L., Santander, M. V., and Prather, K. A.: Exploration of the Effect of Biological Activity on the Chemical Mixing State of Sea Spray Aerosols During a Laboratory Phytoplankton Bloom, In Prep., In Prep.

Von der Weiden, S., Drewnick, F., and Borrmann, S.: Particle Loss Calculator—a new software tool for the assessment of the performance of aerosol inlet systems, 2, 479-494, 2009.

Wang, X., Sultana, C. M., Trueblood, J., Hill, T. C. J., Malfatti, F., Lee, C., Laskina, O., Moore, K. A., Beall, C. M., McCluskey, C. S., Cornwell, G. C., Zhou, Y., Cox, J. L., Pendergraft, M. A., Santander, M. V., Bertram, T. H., Cappa, C. D., Azam, F., DeMott, P. J., Grassian, V. H., and Prather, K. A.: Microbial Control of Sea Spray Aerosol Composition: A Tale of Two Blooms, 1, 124-131, doi:10.1021/acscentsci.5b00148, 2015.

# Linking variations in sea spray aerosol particle hygroscopicity to composition during two microcosm experiments

Sara D. Forestieri<sup>1</sup>, Gavin C. Cornwell<sup>2</sup>, Taylor M. Helgestad<sup>1</sup>, Kathryn A. Moore<sup>2</sup>, Christopher Lee<sup>2</sup>, Gordon A. Novak<sup>3</sup>, Camille M. Sultana<sup>2</sup>, Xiaofei Wang<sup>2</sup>, Timothy H. Bertram<sup>2,3</sup>, Kimberly A. Prather<sup>2,4</sup>, Christopher D. Cappa<sup>1,\*</sup>

<sup>1</sup>Department of Civil and Environmental Engineering, University of California, Davis, CA 95616

<sup>2</sup> Department of Chemistry and Biochemistry, University of California, San Diego, La Jolla, CA 92093

<sup>3</sup> Department of Chemistry, University of Wisconsin, Madison, WI 53706

<sup>4</sup> Scripps Institution of Oceanography, 9500 Gilman Drive, La Jolla, CA 92093

\* Correspondence to: E-mail: cdcappa@ucdavis.edu

**Abstract.** The extent to which water uptake influences the light scattering ability of marine sea spray aerosol (SSA) particles depends critically on SSA chemical composition. The organic fraction of SSA can increase during phytoplankton blooms, decreasing the salt content and therefore the hygroscopicity of the particles. In this study, subsaturated hygroscopic growth factors at 85% relative humidity ( $GF(85\%)$ ) of predominately submicron SSA particles were quantified during two induced phytoplankton blooms in marine aerosol reference tanks (MARTs). One MART was illuminated with fluorescent lights and the other was illuminated with sunlight, referred to as the “indoor” and “outdoor” MARTs, respectively. Optically weighted  $GF(85\%)$  values for SSA particles were derived from measurements of light scattering and particle size distributions. The mean optically weighted SSA diameters were 530 nm and 570 nm for the indoor and outdoor MARTs, respectively. The  $GF(85\%)$  measurements were made concurrently with online particle composition measurements, including bulk composition (using an Aerodyne high-resolution aerosol mass spectrometer) and single particle (using an aerosol time-of-flight mass spectrometer) measurement, and a variety of water-composition measurements. During both microcosm experiments, the observed optically-weighted  $GF(85\%)$  values were depressed substantially relative to pure, inorganic sea salt, by 5 to 15%. There was also a time lag between  $GF(85\%)$  depression and the peak chlorophyll-a (Chl-a) concentrations, by either one (indoor MART) and three-to-six (outdoor MART) days. The fraction of organic matter in the SSA particles generally increased after the Chl-a peaked, also with a time lag, and ranged from about 0.25 to 0.5 by volume. The observed depression in the  $GF(85\%)$  values (relative to pure sea salt) is consistent

Deleted: .

Deleted: single

Deleted: and bulk aerosol

Deleted: .

Deleted: bulk average

Deleted: 10

Deleted: 19%, with a one (indoor MART) and six (outdoor MART) day

Deleted: .

Deleted: -containing

Deleted: peak of the phytoplankton blooms.

Deleted: were inversely correlated

with the large observed volume fractions of non-refractory organic matter (NR-OM) comprising the SSA. The  $GF(85\%)$  values exhibited a reasonable negative correlation with the SSA NR-OM volume fractions after the peak of the blooms (i.e. Chl-a maxima), i.e. the  $GF(85\%)$  values generally decreased when the NR-OM volume fractions increased. The  $GF(85\%)$  versus NR-OM volume fraction relationship was interpreted using the Zdanovskii-Stokes-Robinson (ZSR) mixing rule, and used to estimate the  $GF(85\%)$  of the organic matter in the nascent SSA. The estimated pure NR-OM  $GF(85\%)$  values were  $1.16 \pm 0.09$  and  $1.23 \pm 0.10$  for the indoor and outdoor MARTS, respectively. These measurements demonstrate a clear relationship between SSA particle composition and the sensitivity of light scattering to variations in relative humidity. The implications of these observations to the direct climate effects of SSA particles are discussed.

**Deleted:** of particles containing organic or other biological markers. This indicates these particles were less hygroscopic than the particles identified as predominately sea salt containing and demonstrates

## 1 Introduction

Aerosols impact climate directly by scattering and absorbing solar radiation and indirectly by modifying cloud properties (IPCC, 2013). Sea spray aerosol (SSA) particles are a major source of natural aerosols to the atmosphere and dominate the pre-industrial clear-sky direct radiative effects over the ocean (Haywood et al., 1999). Breaking waves in the ocean entrain air into seawater leading to the formation of bubbles, which burst at the ocean's surface, producing SSA particles (Lewis and Schwartz, 2004). The climate impacts of SSA particles depend critically on their composition, shape, and size (Carslaw et al., 2013; Pilinis et al., 1995). Given typical size distributions for particles in the marine boundary layer, both the submicron (300-1000 nm) and supermicron (~1-5 µm) size ranges contribute to light scattering, with the relative contributions varying depending on location and conditions (Kleefeld et al., 2002). Under humidified conditions, the size of SSA particles is modified through water uptake and loss, which are a strong function of chemical composition (Saxena et al., 1995). The overall mass of SSA particles is dominated by sodium chloride and other inorganic ions, but organic compounds can also contribute substantially to the total mass, especially in the submicron size regime (Facchini et al., 2008; Keene et al., 2007; O'Dowd et al., 2004). Larger organic matter-to-salt ratios occur in the submicron mode through the formation of film drops, since surface-active organics can become enriched in the thin film prior to bubble bursting (Skop et al., 1994; Stefan and Szeri, 1999; Tseng et al., 1992), but it has also been shown that supermicron particles can also contain organic and biological markers (Quinn et al., 2015). Since organic compounds are universally less hygroscopic than inorganic sea salt (Petters and Kreidenweis, 2007), their transfer to SSA will lead to less water uptake and, thus, less scattering than in the case of pure inorganic sea salt particles of the same size.

Previous studies have linked the suppression of water uptake of ambient SSA particles to increasing fractions of marine-derived organic matter in the ambient atmosphere (Vaishya et al., 2013; Ovadnevaite et al., 2011; Lawler et al., 2014; Hegg et al., 2008; Zhang et al., 2014). Phytoplankton blooms lead to chemical changes in seawater and serve as a source of particulate and dissolved organic carbon (DOC) to the system, which is then processed by other microorganisms as part of the microbial loop (Pomeroy et al., 2007). These chemical and biological changes in the seawater can impact SSA particle composition (Prather et al., 2013; Lee et al., 2015; O'Dowd et al., 2004). The organic fraction of SSA particles has been correlated to metrics for high biological activity, such as chlorophyll-a, in some studies (O'Dowd et al., 2004; Facchini et al.,

Deleted: µm

2008), but not others (Quinn et al., 2014). Some lab studies have observed small depressions in water uptake by SSA particles produced from natural seawater relative to synthetic, inorganic seawater (Sellegrri et al., 2008; Modini et al., 2010; Fuentes et al., 2011; Park et al., 2014). However, all of these studies have focused on particles smaller than ~150 nm, for which variations in composition have bigger impacts on cloud condensation nuclei concentrations (Dusek et al., 5 2006; Farmer et al., 2015). Substantially less is understood about the connections between seawater composition and the water uptake properties of the larger submicron particles that contribute more to light scattering. The connection between biological and chemical characteristics of seawater and the resulting SSA particle composition, and consequently hygroscopicity, has 10 therefore not been fully established.

To better understand the connection between SSA particle composition and water uptake as it relates to light scattering in particular, two microcosm experiments were conducted in July 2014 as part of IMPACTS (Investigation into Marine Particle Chemistry and Transfer Science). Through the addition of light and nutrients, phytoplankton blooms were induced in natural seawater. Marine aerosol reference tanks (MARTs) were used to produce SSA particles via intermittent plunging of 15 a sheet of water, which reproduces the bubble size distribution of whitecaps in the ocean (Lee et al., 2015; Stokes et al., 2013). Studying the SSA particles produced during these microcosm studies can provide insights into the linkage between hygroscopicity of nascent SSA particles and ocean biology in an environment that is isolated from anthropogenic influence or background particles. 20 The simultaneous measurement of submicron SSA particle water uptake and of particle composition here demonstrate that variations in seawater biology and composition influence water uptake by SSA particles.

## 2 Methods

### 2.1 MART Description and Operation

25 Two separate experiments were conducted during July 2014 utilizing MARTs. Detailed information on the performance and operation of MARTs can be found in Stokes et al. (2013) and only a brief description will be provided here. SSA particles were generated in an enclosed 210 L acrylic tank via an intermittent plunging sheet of water operated on a computer-controlled 4-seconds-on, 4-seconds-off cycle to allow for surface foam evolution and dissipation close to what

would be observed for natural whitecaps in the ocean. The plunging cycle creates a constant, reproducible concentration of nascent SSA particles in the 90 L headspace, with SSA particle size distributions produced in the MARTs generally consistent with those observed for SSA particles from lab generated breaking waves (Stokes et al., 2013). SSA particles sampled from the MARTs are primary, since the average residence time in the MARTs is much shorter than the time scale required for secondary processing of SSA particles (e.g. heterogeneous gas-phase reactions) (Lee et al., 2015). SSA particles from the headspace were sampled periodically each day by instruments that characterized SSA particle size distributions, composition, and optical and hygroscopic properties. SSA were sampled from the MART headspace and transported through an approximately 2 m long line of 3/8 in. conductive tubing into a laminar flow manifold from which the instruments sampled. Due to the limited headspace volume and flow restrictions, not all instruments in this study could sample simultaneously. During individual sampling periods, only a subset of the full instrument suite sampled from the MARTs. The flow rate of zero air going into the MART and the flow being pulled from the MART by the instruments, as well as sampling times for each group of instruments, are provided in Table 1. The flow into the MART was always 1 LPM greater than the combined instrument pull to ensure positive pressure in the headspace, which eliminated possibility of sampling of room air. The shape of the measured particle size distributions were relatively independent of flow rate for the range of flow rates considered while sampling from the MARTs, although the residence time of individual particles decreases as the flow rate increases (Stokes et al., 2013). The air pushed into the MART was produced by a zero air generator (Sabio Instruments, Model 1001), with air flow controlled by a mass flow controller. The excess flow was released through a vent on the MART. The different flow rates through the MART and through the sample tubing for each sampling configuration led to some differences in the size distribution sampled by the downstream instrumentation.

The procedure for inducing phytoplankton blooms inside of the MARTs will be briefly described here; further general details can be found in Lee et al. (2015). The MARTs were filled with ~120 L of seawater each collected from the SIO pier in La Jolla, California, USA (32°51'56.8"N: 117° 15'38.48"W). Debris and zooplankton were filtered out of the seawater with 50 µm mesh. Phytoplankton growth was induced by exposure to artificial or natural light and the addition of growth media, which is described further in Lee et al. . The two independent MART experiments will be referred to according to the MART location during the growth phase, either

**Deleted:** in the ocean

**Deleted:** the addition of Guillard's f medium (a diatom growth medium) and Na<sub>2</sub>SiO<sub>3</sub> solutions, both of which were diluted by a factor of 2, and

"indoor" or "outdoor". The indoor MART was illuminated using 5700 K full spectrum lights, while the outdoor MART was illuminated with sunlight. A key difference between these two experiments is the intensity of the photosynthetically active radiation (PAR) during growth. The PAR was much greater for the outdoor MART compared to the indoor MART (PAR~1000-1500  $\mu\text{E m}^{-2} \text{s}^{-1}$  (Bouvet et al., 2002) versus  $\sim 70 \mu\text{E m}^{-2} \text{s}^{-1}$ ), which likely resulted in a much larger peak Chl-a concentration for the outdoor MART, 51  $\mu\text{g L}^{-1}$  (outdoor) versus 10  $\mu\text{g L}^{-1}$  (indoor). An additional difference between the two microcosms was that the seawater was collected on different days, 8 July for the indoor MART and 19 July for the outdoor MART. The conditions of the seawater at time of collection are detailed in Table 2.

Deleted:  $\mu\text{g}$

Deleted: mesocosms

10 On 9 July, particles from the indoor MART were sampled immediately following nutrient addition. Further sampling was delayed until Chlorophyll-a (Chl-a) concentrations exceeded approximately 12  $\mu\text{g L}^{-1}$ , which occurred seven days after nutrient addition. (The same seawater as used in the indoor MART was added to a separate MART and sampled immediately after collection and before nutrient addition. However, the resulting particle size distribution from this  
15 MART differed substantially from those measured from the indoor MART, with a much greater contribution of large particles. Thus, the measurements from this separate MART are not directly comparable to the measurements from the indoor MART and are not considered further.) The outdoor MART was only sampled after Chl-a concentrations exceeded approximately 12  $\mu\text{g L}^{-1}$ ,  
20 which occurred three days after nutrient addition. This delay in sampling from when the water and nutrients were first added to the MARTs is necessary because the plunging process can lead to lysis of the phytoplankton cells during this vulnerable growth period, which will inhibit phytoplankton growth (Lee et al., 2015). Ultimately, SSA from the initially collected water from the indoor MART was sampled on 9 July, and subsequent sampling commenced periodically from 19 July through 31 July, i.e. beginning 11 days after the water was collected. Sampling from the  
25 outdoor MART did not commence until 22 July, continuing through 1 August. During the growth period and the off-sampling periods, air was gently bubbled through the tank to provide aeration. Sampling from the MARTs was performed daily once the threshold chlorophyll-a concentrations were reached.

Deleted:  $\mu\text{g}$

Deleted:  $\mu\text{g}$

## 2.2 Instrumentation

A variety of online and offline measurements were made to characterize water composition and particles generated within the MARTs. A general sampling schematic is shown in Figure 1 and a list of the instrumentation used is given in Table 1. As only a limited number of instruments were able to sample concurrently from the MART due to flow limitations, the individual sampling configurations (i.e. groupings of instruments sampling at the same time) are indicated; three specific instrument groupings are considered. The sampling times of each group relative to Group 1 are listed in Table 1 [and a more detailed schematic of Group 1 optical and sizing measurements is provided in Figure S1](#). (The specific timing was dictated by the broader goals of IMPACTS.) A general description of the key instrumentation used as part of this study is provided below. Group 1 sampled for 1.5 h, group 2 sampled for 2 h, and Group 3 for sampled 1 h each day that sampling was conducted.

### 2.2.1 Online particle measurements

Size distributions for dried particles ( $RH < 20\%$ ) were measured with a scanning electrical mobility sizer (SEMS; BMI; model 2002), and an aerodynamic particle sizer (APS; TSI Inc.; Model 3321). The SEMS combines a differential mobility analyzer (DMA) and a mixing condensation particle counter (MCPC) to characterize particles according to their mobility diameter ( $d_{p,m}$ ). The APS characterizes particles according to their aerodynamic diameter ( $d_{p,a}$ ). The SEMS characterized particles over the range  $10 \text{ nm} < d_{p,m} < 1900 \text{ nm}$  and the APS over the range  $0.7 \text{ }\mu\text{m} < d_{p,a} < 20 \text{ }\mu\text{m}$ . The SEMS size distributions were corrected for the influence of multiply charged particles using software provided by the manufacturers. No diffusion correction was performed, which has negligible influence on this study because the smallest particles ( $< 100 \text{ nm}$ ), which are sensitive to diffusion corrections, contribute negligibly to the observed scattering. The APS had a time resolution of 1 minute, while the SEMS had a time resolution of 5 minutes and the APS distributions were accordingly averaged to 5 minutes to facilitate generation of a merged size distribution. The SEMS and APS distributions were merged using the SEMS distribution up to  $1 \text{ }\mu\text{m}$  and the ( $d_{p,m}$  equivalent) APS distribution at larger diameters. The APS  $d_{p,a}$  values were converted to mobility equivalent values assuming a particle density of  $1.8 \text{ g cm}^{-3}$ .

The hygroscopicity of the SSA particles was characterized through simultaneous measurement of light extinction coefficients ( $b_{ext}$ ) for particles that were either dried to  $RH < 20\%$

Deleted: .

(“dry”) or humidified to RH ~85% (“wet”) using the UC Davis cavity ringdown spectrometer (CRD) (Langridge et al., 2011; Cappa et al., 2012). Light absorption by the SSA particles was negligible, and thus extinction is equal to scattering, i.e.  $b_{\text{ext}} = b_{\text{sca}}$ . The dry particle measurements were made at wavelengths of 532 nm and 405 nm, while the wet particle measurements were made only at 532 nm. It should be noted that the humidified particle stream was generated without first drying the particles, and thus it is unlikely that the sampled particles had effloresced. Humidification was achieved by passing the particles through a Nafion humidifier (Permapure, MD-110-12) while drying was achieved by passing the particles through a diffusion denuder filled with Drierite. Both the humidifier and drier were oriented vertically to prevent differential losses due to sedimentation, which could bias the measurements. The fundamental performance of the CRD method for wet particles is the same for dry particles, but variations and uncertainty in the relative humidity (RH) contribute to the uncertainty in the measured  $b_{\text{ext}}$ . The RH for the humidified channel varied between 80-87% due to challenges in maintaining a constant temperature in the open-air Scripps Hydraulics Lab; these variations are accounted for in the analysis as described below. The RH of the air was measured directly in the CRD cells using RH probes (Vaisala, HMP50) that were calibrated against saturated salt solutions. The wet (high RH) and dry (low RH) particle measurements are combined to provide a characterization of the extent of water uptake at a given RH, which causes particles to grow through the parameter  $f(\text{RH})$ , where:

$$f(\text{RH}) = \frac{b_{\text{ext}}(\text{RH}_{\text{high}})}{b_{\text{ext}}(\text{RH}_{\text{low}})} = \frac{b_{\text{sca}}(\text{RH}_{\text{high}})}{b_{\text{sca}}(\text{RH}_{\text{low}})} \quad (1).$$

The parameter  $f(\text{RH})$  is RH-specific, and is most appropriate when  $\text{RH}_{\text{low}}$  is sufficiently low that there is little, if any particle-phase water. The accuracy of the  $f(\text{RH})$  measurements, as well as the conversion to equivalent growth factors ( $GF$ , Section 2.2.3), were tested through measurements made using sodium chloride and ammonium sulfate particles that were generated using an atomizer.

The CRD (and SEMS) alternated between sampling behind a  $\text{PM}_{2.5}$  cyclone and with no explicit size cut (referred to as  $\text{PM}_{\text{all}}$ ) every ten minutes to try and determine  $f(\text{RH})$  and  $GF$  values separately for smaller and larger particles. Note that particles were sampled through the  $\text{PM}_{2.5}$

Deleted: However,

cyclone prior to being dried (RH~70%) and thus the effective size cut for the subsequently dried particles is somewhat less than 2.5  $\mu\text{m}$ , depending on the exact water content of the particles at 70% RH. Since the measured size distributions indicate minimal contributions from particles with  $d_{p,a} > 2.5 \mu\text{m}$ , the  $\text{PM}_{2.5}$  and  $\text{PM}_{\text{all}}$  measurements will generally be considered together.

**Deleted:**  $\mu\text{m}$

5 An aerosol time of flight mass spectrometer (ATOFMS) (Gard et al., 1998; Pratt et al., 2009) was used to characterize the composition of individual dried SSA particles with vacuum aerodynamic diameters ( $d_{va}$ ) from  $\sim 300$  nm to  $3 \mu\text{m}$ , with the highest transmission and sampling of particles with  $d_{va} \sim 1\text{-}2 \mu\text{m}$  (Wang et al., 2015). The ATOFMS single particle spectra have been analyzed using a statistical clustering algorithm (ART-2a) that groups particles with similar spectra together (Zhao et al., 2008). Six particle mass spectra categories were generated and are described as: sea salt (SS), salt mixed with organic carbon (SSOC), predominately OC containing (OC), containing a large Fe peak (Fe) and containing a large Mg Peak (Mg) (Lee et al., 2015; Sultana et al., In Prep.; Wang et al., 2015). A campaign-average spectrum for each category is shown in Figure S2. The combination of the aerodynamic lens transmission and the input particle size distribution determines the particular weighting of the average fractions of the ATOFMS particle types (see Figure S3); in this study, the results are for the sampling-weighted average, which corresponds approximately to a sampling-weighted average  $d_{va} = 1.5 \mu\text{m}$ .

**Deleted:**  $\mu\text{m}$

**Deleted:** distinct

**Deleted:** types

**Deleted:** identified here

**Deleted:** classified

**Deleted:** . A campaign-average spectrum for each particle type is shown in . Each type is reported as a fraction of the total particles sampled for the following vacuum aerodynamic diameter size bins individually:  $0.5\text{-}1 \mu\text{m}$ ,  $1\text{-}1.5 \mu\text{m}$ ,  $1.5\text{-}2 \mu\text{m}$ ,  $2\text{-}2.5 \mu\text{m}$ , referred to as the  $0.75 \mu\text{m}$ ,  $1.25 \mu\text{m}$ ,  $1.75 \mu\text{m}$  and  $2.25 \mu\text{m}$  bins, respectively. These correspond approximately to mobility diameters of  $420$  nm,  $690$  nm,  $970$  nm and  $1250$  nm, respectively, assuming a density of  $1.8 \text{ g cm}^{-3}$  and spherical particles.

**Deleted:** );

**Deleted:** weighted-average corresponds approximately to particles with  $d_{va} = 1.5 \mu\text{m}$  and, unless otherwise specified, the

20 An Aerodyne high resolution time-of-flight aerosol mass spectrometer (HR-ToF-AMS, henceforth AMS) quantified mass concentrations of non-refractory (NR) components of dried SSA particles, in particular NR organic matter (NR-OM) but also other non-refractory (NR-PM) components (Canagaratna et al., 2007). NR-PM species are defined as those that volatilize at  $\sim 600$   $^{\circ}\text{C}$  on a time scale of a few seconds under vacuum ( $10^{-4}$  torr) conditions. No cyclone was used in front of the AMS, and thus the size range of sampled SSA particles was determined by the size-dependent transmission of the aerodynamic lens, which nominally allowed for quantitative sampling of particles with  $d_{va}$  between  $90$  nm and  $700$  nm (50% cut points at  $\sim 40$  nm and  $\sim 1$  micron), although some fraction of even larger particles were characterized (Wang et al., 2015). The AMS data were analyzed using the SQUIRREL toolkit. The high resolution mass spectra were analyzed using the PIKA toolkit to determine O/C atomic ratios for the NR-OM components. The NR-OM fraction of total sampled PM was estimated by normalizing the NR-OM mass concentrations by  $\text{PM}_1$  concentrations determined from integration of the SEMS particle size distributions using an assumed density of  $1.8 \text{ g cm}^{-3}$ . Since a  $d_{va}$  of  $1 \mu\text{m}$  corresponds

**Moved (insertion) [1]**

**Deleted:** The instrument collection efficiency ( $CE$ ) was assumed to be unity, and thus NR-OM values are likely underestimated for particles containing refractory sea salt .

approximately to a  $d_{p,m} = 560$  nm, the use of the SEMS size distribution is appropriate and the derived NR-OM fractions can be considered reflective of the submicron SSA composition. It is important to note that while the temporal trends of the AMS NR-OM/PM<sub>1</sub> fractions are likely reflective of the general behavior, the absolute values are more difficult to quantify because NR-OM associated with particles containing high sea salt fractions may not be vaporized efficiently by the AMS due to the refractory nature of sea salt (Frossard et al., 2014) and to the susceptibility of SSA particles to particle “bounce” in the AMS. Consequently, the SSA particles, including the NR-OM component, are detected with a collection efficiency (CE) lower than unity (Frossard et al., 2014). One previous study (Ovadnevaite et al., 2012) determined the CE value for organic-free sea salt sampled when RH < 70% is approximately 0.25. However, they also note that the CE is potentially instrument dependent, and further may not be applicable to the organic fraction in sea spray particles due to differences in ionization efficiency (which is a component of the overall CE) (Ovadnevaite et al., 2012). It is also possible that the CE differs between particles that have differing relative amounts of OM and sea salt. Despite such uncertainties in quantification of NR-OM by the AMS for sea spray particles, the NR-OM mass concentrations for the sampled SSA particles were determined in this study assuming CE = 0.25. The measured NR-OM mass concentrations were used to calculate NR-OM volume concentrations assuming a density ( $\rho$ ) of 1.0 g/cm<sup>3</sup>. A value of 1.0 g/cm<sup>3</sup> for  $\rho_{OM}$  is consistent with that of fatty acids ( $\rho < 1$  g/cm<sup>3</sup>), which are a significant fraction of marine-derived OM (Cochran et al., 2016; Mochida et al., 2002). However, this value serves as a lower bound for  $\rho_{OM}$  because OM with higher densities, such as sugars ( $\rho \sim 1.7$  g/cm<sup>3</sup>), have also been observed in SSA (Quinn et al., 2015). The NR-OM volume fractions of SSA ( $\epsilon_{org}$ ) were calculated as the ratio between the observed NR-OM volume concentrations and the integrated total particle volume concentrations from the size distribution measurements. Given the use of a lower-limit value for  $\rho_{OM}$  the  $\epsilon_{org}$  are likely upper limits (not accounting for uncertainty in the assumed CE).

Deleted: likely too low

Deleted: is

Deleted: , i.e. have

Deleted: values <1

Deleted: .

Moved up [1]: The high resolution mass spectra were analyzed using the PIKA toolkit to determine O/C atomic ratios for the NR-OM components.

### 2.2.2 Optical closure methods

The  $f(RH)$  values measured using the CRD instrument have been used to determine optically-weighted physical growth factors ( $GFs$ ). For particles of a given size, the  $GF$  is defined as:

Deleted: converted

Deleted: ),

$$GF(RH) = \frac{d_p(RH_{high})}{d_p(RH_{low})} \quad (2)$$

where  $d_p$  is the geometric particle diameter, which is equivalent to  $d_{p,m}$  for spherical particles. For clarity, in this work the optically-weighted  $GF$  will be indicated simply as  $GF$ , while size-specific  $GF$  values will be indicated as  $GF_x$ . SSA particle composition can vary with size (e.g. O'Dowd et al., 2004), and thus  $GF_x$  values may vary with size. The optically-weighted  $GF$  averages across size-dependent variations in composition and  $GF_x$  to focus on the chemical changes that most influence water uptake by the particles that most contribute to light scattering. Unlike  $f(RH)$ ,  $GF_x$  values are independent of the dry particle size (above about 100 nm diameter) for particles of a given composition. Thus, variations in the optically-weighted  $GF$  values are driven only by variations in particle composition, specifically variations in the average composition of particles in the size range over which the optical measurements are most sensitive. For the measurements here, the sensitive size range is between about 400 nm and 800 nm, with particles below 200 nm contributing almost zero to the observed scattering (see Section 3.1 below).

The observed  $f(RH)$  values are converted to  $GF(RH)$  values via optical closure. The optical closure technique uses spherical particle Mie theory calculations and the measured size distributions and  $f(RH)$  values to derive equivalent  $GF(RH)$  values. This methodology is described in detail in Zhang et al. (2014). In brief, the dry scattering is first calculated from the measured dry particle size distribution assuming a refractive index of 1.55 (the refractive index for NaCl), as:

$$b_{sca} = \int \sigma_{sca}(d_{p,m}) \cdot \frac{dN}{d \log d_{p,m}} d \log d_{p,m} \quad (3)$$

where  $\sigma_{sca}$  is the size-dependent scattering cross section and  $dN/d \log d_{p,m}$  is the number-weighted size distribution. Then, each diameter for the dry distribution is multiplied by a trial value for  $GF(RH)$ , the refractive index of the particles is adjusted to account for the resulting volume fraction of water, and the scattering by the resulting “wet” distribution is calculated, from which a theoretical  $f(RH)$  value is determined. The calculated  $f(RH)$  is compared to the observed  $f(RH)$ , and if the two do not agree to within 0.01 the trial  $GF(RH)$  is increased until closure is obtained.

**Deleted:** Unlike  $f(RH)$ ,  $GF$  values are independent of the dry particle size, and thus only depend on composition.

**Deleted:**  $\sigma_{sca}$

It is assumed that the growth factors are size independent, namely that  $GF_x = GF$  for all  $d_p$ . Thus, this method retrieves an effective, optically-weighted  $GF$  value that explains the observed influence of water uptake on light scattering for the sampled size distribution. An alternative approach was considered in which the  $GF_x$  were assumed to vary with size, specifically as  $GF_x = 2.1 - b (\log(1.8 \mu\text{m}) - \log(d_{p,m}))$ , and where the value of  $b$  was allowed to vary during the optical closure, with the condition that  $GF_x \geq 0$ . (This expression assumes that particles with  $d_{p,m} = 1.8$  have a  $GF_x = 2.1$ , i.e. that of NaCl. The  $GF_x$  decrease as size decreases.) The derived  $b$  values exhibit a similar temporal dependence as the derived optically-weighted  $GF$  values. The general conclusions reached in this study are therefore independent of the assumptions made regarding the size-dependent behavior of  $GF_x$ . Thus, rather than introducing an uncertain functional form, the simpler assumption (namely, size-independent  $GF_x$  values) is used here.

As the RH of the humidified channel was not perfectly constant during measurements, the derived individual  $GF(\text{RH})$  values have been adjusted to 85% by using Equation 4:

$$\frac{RH}{\exp\left(\frac{A}{d_d \cdot GF(\text{RH})}\right)} = \frac{GF(\text{RH})^3 - 1}{GF(\text{RH})^3 - (1 - \kappa)} \quad (4)$$

where  $A$  is a constant, RH is relative humidity,  $d_d$  is the dry particle diameter and  $\kappa$  is the effective hygroscopicity parameter, which is assumed to be RH-independent (Petters and Kreidenweis, 2007). Here, the  $d_d$  values used are the optically-weighted median diameters, which are calculated by integrating the concentration-weighted size-dependent cross-sections  $(\sigma_{\text{sca}}(d_p))$ .  $GF(85\%)$  values were determined by first calculating  $\kappa$  based on the measured  $GF(\text{RH})$  and then recalculating the  $GF$  at 85% RH.

The accuracy of this optical closure method, as well as of the initial  $f(\text{RH})$  measurements, was assessed by comparing the  $GF(85\%)$  values determined for polydisperse distributions of NaCl and  $(\text{NH}_4)_2\text{SO}_4$  test particles, for which  $GF(85\%)$  values are known. The measured  $GF(85\%)$  for NaCl was 2.09 +/- 0.03 and for  $(\text{NH}_4)_2\text{SO}_4$  was 1.59 +/- 0.05, which compare very well with literature values of ~2.1 for NaCl (Cruz and Pandis, 2000; Laskina et al., 2015; Hansson et al., 1998) for particle sizes ranging from 100 nm to 300 nm and ~1.55 for ammonium sulfate (Laskina

Deleted:  $\kappa$

Deleted:  $(\sigma_{\text{sca}}$

Deleted:  $\kappa$

et al., 2015; Wise et al., 2003) for 100 nm particles. (The reported experimental uncertainties are 1 $\sigma$  standard deviations over each measurement period.)

Deleted: .

Deleted: 1 $\sigma$

*GF* calculations for  $PM_{all}$  utilized a combined size distribution from the SEMS and the APS, with the merge point at a  $d_{p,m} = 1000$  nm. The APS sampled at a separate time from the CRD (see Table 1). The CRD set-up also required dilution due to the 3 LPM required for the cyclone and a total pull of ~6.3 LPM. Therefore, a dilution correction was applied to the APS distributions to account for the different sampling scheme. Although this adjustment adds some uncertainty to the  $PM_{all}$  size distributions, the concentrations at larger sizes were very small and thus had minimal influence on the derived *GFs*. For the  $PM_{2.5}$  sampling periods, only SEMS distributions were used.

### 3 Results

#### 3.1 Size Distributions and Dry Particle Optical Closure

The daily and study average merged size distributions for each MART are shown in Figure 2A (indoor MART) and Figure 2B (outdoor MART). The day-to-day variations in the size distributions were generally small. The average SSA particle number-weighted size distributions from both MARTs peaked around  $d_{p,m} = 100$  nm and were relatively broad. The observed concentration of supermicron particles ( $d_{p,m} > 1000$  nm) was somewhat lower than that previously reported from a MART (Stokes et al., 2013) and likely reflects greater gravitational losses of supermicron particles in the long sampling line used here (Figure S4). Since the hygroscopicity measurements discussed in this study are based on measurements made using polydisperse distributions, it is useful to determine the effective, scattering-weighted particle diameters that characterize the MART size distributions. The study average integrated scattering for each MART was calculated from Mie theory using the observed dry particle size distributions (Figure 2C). The  $d_{p,m}$  at which 50% of the total scattering occurs were 570 nm for the outdoor MART and 530 nm for the indoor MART and particles with  $d_{p,m} > 1000$  nm contributed <10% of the total scattering in both MARTs, indicating that the derived *GF*(85%) values for these two experiments are most sensitive to submicron particles with  $d_{p,m}$  values between about 400 nm and 800 nm.

Deleted: ()

Deleted: diameters

Deleted: ..

The extent of agreement between the observed  $b_{sca}$  for dry particles and the values calculated from Mie theory using measured size distributions (Equation 3) has been assessed (Figure S5).

Deleted: ()

The calculated  $b_{sca}$  are ~15% lower than the observed  $b_{sca}$  for both  $PM_{all}$  and  $PM_{2.5}$ , which is outside the combined uncertainty for the CRD and size distribution measurements (which is ~11% from error propagation). Some of the difference may result from differential losses between or within the sizing instruments and the CRD, although this seems generally unlikely to explain the entire difference, as losses of particles in the submicron range should be small. There is greater scatter in the  $PM_{all}$  light scattering comparison than there is from the  $PM_{2.5}$  comparison, which likely results both from the APS measurements being made at a different time than the CRD and SEMS measurements and the need for dilution correction. Some of the difference between the observed and calculated  $b_{sca}$  may be attributable to the assumption of spherical particles in the calculations, although similar closure was obtained (within 16%) between observed and calculated  $b_{sca}$  for atomized NaCl, suggesting that this is unlikely to explain the difference. It is possible that the diameters measured by the SEMS may have been too small. [Wiedensohler et al. \(2012\) reported that sizing errors between instruments can be up to 10%. If the](#) measured diameters are increased by 8%, then a 1:1 agreement between the measured and calculated extinction values is obtained. However, tests conducted during the study in which a 2<sup>nd</sup> DMA was used to size-select monodisperse particles in the range 100-300 nm indicated agreement between the instruments to within 1%. Additional tests after the study using 220 nm monodisperse polystyrene latex spheres (PSLs) demonstrated the SEMS sizing was good to better than 1%, suggesting that sizing inaccuracies cannot explain the difference absent some fundamental problem with the data inversion procedure for size distributions (Lopez-Yglesias et al., 2014), which seems unlikely. Uncertainty in the assumed RI value for the dry particles may explain a small fraction (<5%) of the difference. Additionally, if the dry particles had retained some water in the CRD but not the SEMS, then the observed  $b_{sca}$  would be larger than the calculated value. However, the RH in the CRD dry channel is much lower than the efflorescence RH for NaCl (~45% (Biskos et al., 2006)), and thus it seems unlikely that residual water would have contributed substantially to the difference. Regardless of the explicit reason for the difference in calculated and observed absolute values of  $b_{sca}$ , since the calculation of  $f(RH)$  depends on the ratio between the  $b_{sca}$  for wet and dry particles, such absolute differences do not strongly affect the retrieval of  $GF(85\%)$  values. We have tested the sensitivity of the retrieval method to an 8% increase in the particle diameters. The retrieved  $GF$  values are increased by a marginal amount (0.015-0.03) when the diameters are

Deleted: If

increased, and thus such potential sizing uncertainty does not affect the main conclusions presented here.

### 3.1 Indoor MART

The temporal variation in Chl-a concentrations, the derived  $GF(85\%)$  and various particle composition metrics are shown in Figure 3 for the indoor MART. As has been previously observed in microcosm experiments, the measured Chl-a time series exhibits a distinct peak (Lee et al., 2015), which in this case occurred on 16 July at a value of  $10 \mu\text{g L}^{-1}$ . This Chl-a concentration is around the upper end of values observed for large phytoplankton blooms observed in the oceans, in particular near coastal regions (O'Reilly et al., 1998). After the peak the Chl-a concentration dropped relatively quickly to around  $1.5 \mu\text{g L}^{-1}$  (15% of the peak) and then eventually to  $\sim 1.4 \mu\text{g L}^{-1}$  (14% of the peak). The DOC concentrations varied from 240 to  $350 \mu\text{M C}$ , increasing rapidly when the Chl-a concentration peaked and then staying relatively constant around  $320 \mu\text{M}$  (Figure S6A). The peak DOC range is somewhat larger than values typically observed for blooms in the ocean, which are only  $\sim 130 - 250 \mu\text{M C}$  (Kirchman et al., 1991; Norrman et al., 1995). The temporal variation in heterotrophic bacteria concentration was similar to that for DOC, and heterotrophic bacteria concentrations ranged from  $\sim 1 \times 10^6$  to  $1.2 \times 10^7 \text{ mL}^{-1}$  (Figure S6A), which is comparable to concentrations observed in the ocean (Li, 1998).

The  $GF(85\%)$  values determined for the indoor MART ranged from 1.79 to 1.9 and exhibited distinct temporal variations, decreasing from  $1.88 \pm 0.04$  on 16 July, just as the Chl-a peaked, to a minimum range of  $1.79 \pm 0.03$  to  $1.80 \pm 0.01$  from 17 July to 18 July when the Chl-a concentration dropped to  $3.41 \pm 1.89 \mu\text{g L}^{-1}$ , and then recovering back to  $1.90 \pm 0.03$  on 7/20 (Figure 3A). The range of these values is 10-15% lower than the value of  $\sim 2.1$  for pure (inorganic) sea salt (Ming and Russell, 2001). There is a one day lag between the peak in Chl-a and the (temporary) depression in  $GF(85\%)$ .

The NR-OM volume fractions of SSA varied from 0.29 to 0.50 throughout the course of the indoor MART microcosm experiment (Figure 3). The observation of such large  $\epsilon_{\text{org}}$  values is consistent with the substantial depressions in the  $GF(85\%)$  values relative to pure, inorganic sea salt (2.1). The temporal variation in the  $\epsilon_{\text{org}}$  was generally similar to that of the  $GF(85\%)$  values, with smaller  $GF(85\%)$  values corresponding to larger  $\epsilon_{\text{org}}$  values, although the peak in  $\epsilon_{\text{org}}$  is somewhat sharper than the dip in the  $GF(85\%)$ . The inverse relationship between the  $GF(85\%)$

Deleted:  $\mu\text{g}$

Deleted:  $\mu\text{g}$

Deleted:  $\mu\text{M}$

Deleted:  $\mu\text{M (A)}$

Deleted: (A).

Deleted: 14-19

Deleted: 2

Deleted: , which is primarily NaCl.

Deleted: With the exception of the measurements made just after nutrient addition on 9 July, the temporal variations in  $GF(85\%)$  showed a strong, positive correlation ( $R^2 = 0.83$ ) with the relative fraction of SS-type particles ( $f_{\text{SS}}$ ) from the ATOFMS (Figure 3A). This key observation suggests that the predominant non-SS particle types during this period (SSOC, Mg and Other, listed in order of decreasing fractional abundance) are, on average, less hygroscopic than the SS-type particles. However, very different behavior was observed on 9 July, and if the measurements from this day are included the correlation between  $GF(85\%)$  and  $f_{\text{SS}}$  decreases dramatically ( $R^2 \sim 0$ ). This is because on this day only the Fe-type particles comprised a substantial fraction of the total particles ( $f_{\text{Fe}} = 0.32 \pm 0.01$ ); on all other days the Fe-type particle fraction was negligible. Consequently, the  $f_{\text{SS}}$  on 9 July was much smaller, only 0.32. The sum of  $f_{\text{SS}}$  and  $f_{\text{Fe}}$  on 9 July is similar to the  $f_{\text{SS}}$  values on the other sampling days. The  $GF(85\%)$  values, including 9 July, therefore show a reasonable correlation with  $f_{\text{SS}} + f_{\text{Fe}}$  ( $R^2 = 0.49$ ). This suggests that the hygroscopicity of the Fe-type particles is similar to that of the  $f_{\text{SS}}$  particles. However, the observed  $GF(85\%)$  value on 9 July is somewhat smaller than expected given the correlation observed on the other days and the  $f_{\text{SS}} + f_{\text{Fe}}$  value on this day. This therefore suggests that the Fe-type particles are more hygroscopic than the other non-SS-type particles but that they are not as hygroscopic as sea salt. These Fe-type particles result from nutrient addition at the beginning of the experiment, as the Guillard's f medium contains iron citrate. The Fe-type particles are characterized by their large  $\text{Fe}^+$  peak, along with peaks corresponding to  $\text{Na}^+$ ,  $\text{Cl}^-$ ,  $\text{Mg}^{2+}$  and, notably,  $\text{PO}_4^{3-}$ . Accordingly, the Fe-type particles may be composed of substantial amounts of sea salt with a clump of insoluble Fe-rich particulates, i.e. might be reasonably considered as SS+Fe-type particles. Although the Fe-type particles clearly have an influence on the observed  $GF(85\%)$  values when present with high relative abundance, their large fraction on 9 July is a result of nutrient addition and not biological changes in the seawater, and thus the measurements on 9 July are excluded from subsequent analysis. ¶ As noted above, the non-SS particle types (excluding the Fe type) are, on average, less hygroscopic than the SS-type particles. Correlations with individual other particle types were generally weaker, although the minimum  $GF(85\%)$  values observed on 17 July-18 July are coincident with maxima in SSOC, Mg type and, to a lesser extent, "Other" particle type, which suggests some sort of anti-correlation between  $GF(85\%)$  and these particle types (Figure 3B). It should be recognized, however, that since the ATOFMS ...

and  $\epsilon_{org}$  is consistent with organic compounds being less hygroscopic than sea salt. The O:C ratio of the NR-OM had an average value of  $0.25 \pm 0.05$  ( $1\sigma$ ), which is similar to the value of  $0.20 \pm 0.08$  reported by Frossard et al. (2014) for primary NR-OM that was generated from the open ocean using the “sea sweep” (Bates et al., 2012). The O:C ratio of NR-OM in the indoor MART generally increased with time, from 0.17 to 0.30, but also exhibited a temporary decrease on 17 July, the day when the  $GF(85\%)$  and  $\epsilon_{org}$  both first dropped. Since O:C often correlates with hygroscopicity for organics (at least for multi-component mixtures), this behavior may indicate a general increase in the hygroscopicity of the NR-OM with time (Cappa et al., 2011; Massoli et al., 2010). However, since the hygroscopicity of organic aerosol with O:C values in this range has generally been found to be small, the observed variations in O:C may not have a noticeable impact on the overall behavior of the  $GF(85\%)$  values.

The explicit co-variation of  $\epsilon_{org}$  and the  $GF(85\%)$  values is shown in Figure 4. Assuming that volume mixing rules apply (i.e. the Zdanovskii-Stokes-Robinson (ZSR) mixing rules (Stokes and Robinson, 1966)), the overall, effective  $GF$  ( $GF_{obs}$ ) can be estimated as:

$$GF_{obs} = \sqrt[3]{(1 - \epsilon_{org}) \cdot GF_{sea\ salt}^3 + \epsilon_{org} \cdot GF_{org}^3} \quad (5)$$

where  $GF_{org}$  is the  $GF$  value for pure OM and  $GF_{sea\ salt}$  is the  $GF$  value expected for pure sea salt. The ZSR line connecting  $GF_{sea\ salt}(85\%) = 2.1$  and  $GF_{org}(85\%) = 1.0$  provides the minimum value expected for any fraction of OM relative to sea salt. Low  $GF_{org}(85\%)$  values ( $\sim 1.0$ ) have been observed for fatty acids (Vesna et al., 2008), which have been found in SSA particles in the atmosphere (Mochida et al., 2002) and were observed in SSA produced in a related mesocosm experiment (Wang et al., 2015; Cochran et al., 2016). Values above this line indicate that the  $GF$  of the OM in the sampled SSA particles is, on average, greater than 1. Equation 5 was fit to the data shown in Figure 4 to determine an average value for  $GF_{org}(85\%)$  for the indoor MART. The best-fit  $GF_{org}(85\%)$  was  $1.16 \pm 0.09$ , which falls between  $GF_{org} = 1.0$  expected for non-hygroscopic OM, such as fatty acids, and  $GF_{org}$  expected for more soluble OM, such as sugars (e.g.  $GF_{org}(85\%) = 1.24 \pm 0.04$  has been observed for glucose (Mochida and Kawamura, 2004)). (The uncertainty on  $GF_{org}(85\%)$  is the fit uncertainty and does not account for uncertainties in either the CE for SSA particles or in  $\rho_{OM}$ .) This value for  $GF_{org}$  can be interpreted as an optically-weighted

**Deleted:** [Bates et al., 2011].

**Deleted:**  $f_{SS}$

**Deleted:** Under the assumption that the SS-type particles are effectively pure sea salt particles, the  $GF(85\%)$  for these particles should be  $\sim 2.2$ . In contrast, the  $GF(85\%)$  values for the non-SS particle types are not known *a priori*, although reasons for their being less hygroscopic than the SS particle type can be postulated based on their mass spectra. The SSOC particle type is identified in large part by the presence of organic-containing peaks in the mass spectrum (in particular,  $CN^+$  and  $CNO^+$ ; see ). Thus, it makes sense that an increase in the SSOC particle type fraction at the expense of the SS-type particle fraction would suppress  $GF(85\%)$  values, as organic compounds are less hygroscopic than sea salt. The Mg-type particles are characterized by their large  $Mg^+$  peak, but also by large  $Cl^-$  peaks and smaller  $Ca^+$  and  $K^+$  peaks (). It may be that Mg-type particles are sea salt particles in which, during the drying process, NaCl has crystallized first, leaving a Mg-rich shell on the outside of the particles. If these particles then undergo incomplete ionization, the Mg signal may dominate the mass spectra. If this is the case, then the Mg-type particles should be about as hygroscopic as the SS particle type, which appears to run counter to the observations. However, if these Mg-type particles are highly enriched in  $MgCl_2$  over NaCl, then their hygroscopicity would be reduced since  $MgCl_2$  is less hygroscopic than NaCl. An alternative interpretation of the Mg-type is that they are whole or fragmented bacteria cells or possibly strongly associated with organic material such as in marine gels, in which case their hygroscopicity would likely be lower than sea salt. ¶

**Deleted:** the SS-type particle fraction

**Deleted:** of two distinct particle types, with respect to hygroscopicity, and assuming additivity of the individual particle type  $GF$  values,

**Deleted:**  $GF_{tot}$

**Deleted:**  $f_{SS} \cdot GF_{SS} + (1 - f_{SS}) \cdot GF_{non-SS}$

**Deleted:**  $f_{SS}$

**Deleted:** SS-type particle fraction and a single

**Deleted:** is assumed for all non-SS particle types, as discussed above. The

**Deleted:**  $GF_{SS}$

**Deleted:** 2

**Deleted:**  $GF_{non-SS}$

**Deleted:** combination

**Deleted:** SS and non-SS particles

**Deleted:**  $GF_{non-SS}$

**Deleted:** non-SS particle type

**Deleted:**  $GF_{non-SS}(85\%)$  for the indoor MART. The best-fit  $GF_{non-SS}(85\%)$  was  $1.39 \pm 0.03$  when the sampling-weighted average  $f_{SS}$  values from each day were used

average for the OM component of the SSA particles sampled here. Although the derived  $GF_{org}$  values are reasonable, as the  $CE$  is relatively uncertain for sea spray particles (Ovadnevaite et al., 2012; Frossard et al., 2014) and the  $\rho_{OM}$  is also uncertain, the derived value for  $GF_{org}$  should be viewed as suggestive only.

5 One important issue to consider in assessing the quantitative nature of the derived  $GF_{org}(85\%)$  value is that the mass-weighted organic fractions used to determine  $\epsilon_{org}$  do not necessarily have the same weighting with respect to particle size as do the  $GF(85\%)$  values. The scattering-weighted median diameter, relevant to the  $GF(85\%)$  measurements, was  $d_{p,m} = 530$  nm. The mass-weighted size distribution of OM can be estimated from the size distribution of a particular tracer ion in the AMS mass spectrum, specifically the ion at  $m/z = 43$ , which is indicative of total organic mass (Figure S7). (Interference from the large signal contribution from inorganic ions prohibited explicit determination of the total NR-OM size distribution, and thus only the  $m/z = 43$  ion is used.) The peak in the NR-OM mode occurs at  $d_{va} \sim 1$   $\mu\text{m}$ , which corresponds to  $d_{p,m} \approx 560$  nm. This is comparable to the scattering-weighted median diameter, suggesting that the temporal variations in the  $GF(85\%)$  and  $\epsilon_{org}$  can be compared. However, the AMS aerodynamic lens imposes a 50% cut diameter of  $\sim 1$   $\mu\text{m}$  (Canagaratna et al., 2007), and thus the observed peak in  $m/z$  43 likely occurs at a diameter that is somewhat too small compared to the actual distribution.

10 There was also a strong temporal correlation observed between the  $GF(85\%)$  values and the number fractions of ATOFMS mass spectra categories. Specifically, the decrease in  $GF(85\%)$  values after the bloom peak corresponded to a shift from particles that generated mass spectra dominated by sea salt ion markers (SS type) to particles with strong spectral signatures indicative of organic or biological influence (SSOC and Mg type). (The measurements made just after nutrient addition on 9 July are a notable exception, discussed below). The inverse relationship between the  $GF(85\%)$  and the SS type particle spectra is consistent with the inverse relationship between the  $GF(85\%)$  and  $\epsilon_{org}$ , providing additional confidence that the temporal variations in  $GF(85\%)$  are driven by variations in particle composition. The SSOC mass spectral type is identified in large part by the presence of carbon-containing peaks ( $\text{CN}^-$  and  $\text{CNO}^-$ ) and  $\text{K}^+$  and  $\text{Ca}^+$  in the mass spectrum (see Figure S2). The Mg-type spectra are characterized by their large  $\text{Mg}^+$  peak, which has been previously attributed to the presence of biological material (e.g. bacteria) (Guasco et al., 2013; Prather et al., 2013), as well as by smaller  $\text{Ca}^+$  and  $\text{K}^+$  peaks (Figure S2). Both the SSOC and Mg spectral types are depleted in peaks corresponding to Na or NaCl. It

**Deleted:**  $GF_{non-SS}$

**Deleted:** sampling

**Deleted:** number

**Deleted:** above

**Deleted:**  $f_{SS}$

**Deleted:** (For clarity, in the following discussion the sampling-weighted average number fractions will have “avg” appended as a subscript.)

**Deleted:** whereas the sampling

**Deleted:** of the ATOFMS was  $d_{va} \sim 1.5$   $\mu\text{m}$  ( $d_{p,m} \sim 800$  nm). The observed  $f_{SS}$  values generally decreased as particle size decreased (). This suggests

**Deleted:** actual  $f_{SS}$  values most relevant to the  $GF(85\%)$  measurements should be somewhat smaller than the  $f_{SS,avg}$ . To provide for better correspondence between the size sensitivity of the  $f_{SS}$  values and the  $GF(85\%)$  values, the  $f_{SS}$  values have been adjusted by multiplying each  $f_{SS,avg}$  value by the campaign-average of the ratio  $R_{SS} = f_{SS,0.75\mu\text{m}}/f_{SS,avg}$ , where  $f_{SS,0.75\mu\text{m}}$  is the  $f_{SS}$  for the  $d_{va} = 0.75$   $\mu\text{m}$  ( $d_{p,m} \sim 420$  nm) bin. The campaign-average  $R_{SS} = 0.78 \pm 0.05$ . The absolute values of these re-weighted  $f_{SS}$  values (referred to as  $f_{SS^*}$ ) are more representative of the size range relevant to the  $GF$  measurements. The reason for using a campaign-average scaling factor rather than using the measured  $f_{SS,0.75\mu\text{m}}$  values directly is that, although the  $f_{SS,avg}$  and  $f_{SS,0.75\mu\text{m}}$  exhibit generally good correspondence, the counting statistics of particles in the  $0.75$   $\mu\text{m}$  bin was substantially smaller than that in the larger bins, making the individual  $f_{SS,0.75\mu\text{m}}$  points less certain than the campaign average. By using a campaign-average scaling factor, it is implicitly assumed that the actual

**Deleted:**  $f_{SS,0.75\mu\text{m}}$  are captured by  $f_{SS,avg}$ , which seems reasonable given the general constancy of the size distributions over the course of each of the microcosm experiments, c.f. Fig. 2. ¶  
The relationship between  $GF(85\%)$  and  $f_{SS^*}$

**Deleted:** also shown in Fig. 4, along with a separate fit using Eqn. 5. The  $GF_{non-SS}(85\%)$  derived using  $f_{SS^*}$  is  $1.57 \pm 0.03$ , larger than that obtained when  $f_{SS,avg}$  is used. Regardless of whether  $f_{SS}$  or  $f_{SS^*}$  is used, it is apparent that the non-SS particles types have, on average,  $GF(85\%)$  values that are consistent with their being a mixture of less hygroscopic organic and more hygroscopic inorganic (sea salt) components. If it is assumed that the organic fraction is completely non-hygroscopic ( $GF(85\%) = 1.0$ ) and the inorganic fraction is pure sea-salt ( $GF(85\%) = 2.2$ ), the range of derived  $GF_{non-SS}(85\%)$  values implies an average organic volume fraction ( $\epsilon_i$ ) of  $0.56 - 0.88$  for these particle types if it is assumed that volume mixing rules apply (i.e. the Zdanovskii-Stokes-Robinson mixing rules). Since the  $f_{non-SS}$  values range from  $0.53 - 0.74$ , if it is assumed that the SS-type and non-SS particle types have similar size distributions, then the implied ensemble average  $\epsilon_i$  would be about  $0.33 - 0.52$ . If the organics comprising the non-SS particles are somewhat hygroscopic, then the estimated  $\epsilon_i$  ...

is important to note, however, that dried SSA particles sampled by the ATOFMS can be spatially chemically heterogeneous, with shells depleted in Na and rich in Mg, K, and Ca (Ault et al., 2013). Thus, some fraction of the particles identified as having Mg or SSOC type spectra may be partially explained by the incomplete ionization of sea salt particles (Sultana et al., In Prep.). However, variations in the thickness of this Na-depleted shell likely reflect variations in the total particle organic content. Therefore, increases in the fraction of SSOC or Mg type mass spectra generated suggest a net increase in SSA particle organic content. On 9 July a substantial fraction of particles containing large Fe<sup>+</sup> peaks were observed; on all other days the Fe spectral-type particle fraction was negligible. The Fe spectral-type particles may have had an influence on the observed GF(85%) values when present with high relative abundance. However, their large fraction on 9 July is a result of nutrient addition and not biological changes in the seawater.

### 3.2 Outdoor MART

The temporal variation in Chl-a concentrations, the derived GF(85%) values and various particle composition metrics are shown in Figure 5 for the outdoor MART. Like the indoor MART, the Chl-a concentrations exhibited a characteristic rise and fall for the microcosm experiment. However, the maximum Chl-a concentration was 51 µg L<sup>-1</sup>, which 5 times higher than the indoor MART and likely due to greater PAR in the outdoor MART. Such high Chl-a concentrations are well above those typically observed in the ocean. However, the Chl-a concentration rapidly declined to 6 µg L<sup>-1</sup> two days after the peak and then continued to decrease over the next week to <1.5 µg L<sup>-1</sup>. Both DOC and heterotrophic bacteria concentrations increased as the bloom progressed until they stabilized around the point when Chl-a concentrations had returned approximately to their pre-bloom levels, with DOC concentrations ranging from 200 to 300 µM C and heterotrophic bacteria concentrations from 1 x 10<sup>6</sup> to a peak of 1.7 x 10<sup>7</sup> mL<sup>-1</sup> (Figure S6B).

The GF(85%) values ranged from a maximum of 1.99 ± 0.03 to a minimum of 1.78 ± 0.04, again lower than what would be expected for pure sea salt (by 5-15%). Unfortunately, no pre-bloom measurements were possible for this experiment, with the first particle measurements made for all instruments when the Chl-a concentration was peaking. The smallest GF(85%) values were observed towards the end of the microcosm, when the Chl-a concentrations were at their lowest point (< 1.5 µg L<sup>-1</sup>). The GF(85%) values exhibited two sequential decreases after the Chl-a peak,

Deleted: µg

Deleted: µg

Deleted: µM

Deleted: (B

Deleted: 10-19

Deleted: µg

the first after 3 days and the second after 6 days. The range of  $GF(85\%)$  values for the SSA particles from the outdoor MART were similar to those for the indoor MART

The observed  $\epsilon_{org}$  values for the SSA particles were similarly comparable to the indoor MART (0.26 to 0.46). In general, decreases in  $GF(85\%)$  values corresponded to increases in  $\epsilon_{org}$  values, with the exception of the measurements on 7/30 (Figure 5C). Following the peak in Chl-a, the  $\epsilon_{org}$  values increase gradually over a few days, then stabilize, and finally exhibit an additional increase six days after the bloom peak (Figure 5A). The temporal variations in  $\epsilon_{org}$  tracks neither the Chl-a nor DOC concentrations. This suggests that, perhaps, biological processing and its impact on the composition of organics in the sea water, more so than absolute organic concentrations, is important for determining the abundance of organic matter transferred into SSA particles (Rinaldi et al., 2013; Lee et al., 2015; Quinn et al., 2014). However, further experiments will be needed to confirm this hypothesis.

Values of  $GF_{org}(85\%)$  have again been estimated using the ZSR relationship (Eqn. 5) and the observed  $GF(85\%)$  and  $\epsilon_{org}$ . Assuming  $GF_{sea\ salt}(85\%) = 2.1$ , the derived  $GF_{org}(85\%) = 1.23 \pm 0.10$  (Figure 4). This  $GF_{org}(85\%)$  for the outdoor MART is comparable to that obtained from the indoor MART, suggesting that the OM generated from the outdoor MART has similar hygroscopicity as the OM sampled from the indoor MART.

As with the indoor MART, there was a reasonable temporal correlation between the  $GF(85\%)$  values and the number concentration of SS spectral-type particles from the ATOFMS. The two most abundant non-SS particle mass spectra types were SSOC-type and Mg-type, with all other types contributing negligibly. This is again an indication that the temporal variation in the  $GF(85\%)$  values corresponds to an evolution of the composition of the SSA particle population, and is consistent with the variation in  $\epsilon_{org}$ .

#### 4 Implications and Conclusions

The two MART microcosm studies provide two case studies relating variations in the optically-weighted  $GF(85\%)$  values and SSA particle composition, for predominately submicrometer SSA particles. For both microcosms, clear depression of the  $GF(85\%)$  values, relative to that for pure sea salt, occurred following the peak in Chl-a concentrations and upon the death of both phytoplankton blooms, but with differing time lags between peak Chl-a and the minimum  $GF(85\%)$  between the experiments. This depression in  $GF(85\%)$  values is consistent

**Deleted:** The  $f_{SS,avg}$  values for the outdoor MART were generally smaller than those observed for the indoor MART experiment and varied over a wider range (0.32 to 0.58 versus 0.55 to 0.6), most likely a reflection of the higher peak Chl-a concentration and greater overall biological activity, although interestingly the DOC concentrations reached higher levels in the indoor MART. Despite the smaller  $f_{SS,avg}$  for the outdoor MART, the range of  $GF(85\%)$  values was similar to the indoor MART, if not a bit higher. Nonetheless, there is still a moderate, albeit weaker, positive correlation ( $R^2 = 0.48$ ) between the  $GF(85\%)$  values and  $f_{SS,avg}$  (Figure 4 and Figure 5A). The two most abundant non-SS particle types were SSOC-type and Mg-type, with all other types contributing negligibly. The Mg-type particles (...)

**Deleted:** The  $f_{SS,avg}$

**Deleted:** just after the peak in Chl-a, stabilizes

**Deleted:** then exhibits a relatively sharp drop

**Deleted:** that persists for about two days before recovering

**Deleted:** This behavior

**Deleted:**  $f_{SS,avg}$

**Deleted:** behavior, suggesting

**Deleted:** predominant types of particles that are produced (...)

**Deleted:** Equation 5 has

**Deleted:** used to estimate  $GF_{non-SS}(85\%)$  from

**Deleted:**  $f_{SS,avg}$

**Deleted:**  $GF_{SS}$

**Deleted:** 2,

**Deleted:**  $GF_{non-SS}$

**Deleted:** 60

**Deleted:** 03

**Deleted:** If the size-adjusted  $f_{SS^*}$  is instead used, the deriv (...)

**Deleted:** increases to  $1.70 \pm 0.03$ . (The adjustment factor (...)

**Deleted:**  $0.74 \pm 0.06$ .) The  $GF_{non-SS}(85\%)$  values using  $f_{SS}$  (...)

**Deleted:** non-SS particles

**Deleted:** are perhaps slightly more hygroscopic than those

**Deleted:** There is one notable outlier from the general (...)

**Deleted:** results. The estimated range of average organic (...)

**Deleted:** is 0.59-0.68, again assuming that the organics (...)

**Deleted:** are non-hygroscopic while the inorganics behav (...)

**Deleted:** , this

**Deleted:** ensemble average  $\epsilon_i$  of 0.22 - 0.28

**Deleted:** .

**Deleted:** The

with large  $\epsilon_{org}$  (0.25 – 0.50) values estimated using the NR-OM/PM<sub>1</sub>. The similar temporal variations in  $GF(85\%)$  and  $\epsilon_{org}$ , as well as with the ATOFMS particle mass spectra types, demonstrates a clear link between SSA hygroscopicity and composition. For a given microcosm experiment, the estimated hygroscopicity of OM components are similar, with  $GF(85\%) = 1.16$  for the indoor MART and 1.23 for the outdoor MART.

The observations here demonstrate that the climate impacts of marine-derived organic compounds can go beyond their demonstrated ability to influence cloud condensation nuclei efficacy (Quinn et al., 2014; Collins et al., 2013), additionally affecting the efficiency with which SSA particles scatter solar radiation. This was previously suggested by the ambient measurements of Vaishya et al. (2013), who observed substantial differences in  $GF(90\%)$  and  $f(RH)$  values for submicron particles having very different  $\epsilon_{org}$  fractions in what were identified as clean marine air masses. (Their  $GF(90\%)$  values were measured using a hygroscopic tandem DMA (HT-DMA) for size-selected particles with  $35 \text{ nm} \leq d_{p,m} \leq 165 \text{ nm}$ . Their  $f(RH)$  values were measured for PM<sub>1</sub>.) They observed that increases in  $\epsilon_{org}$  had no effect on the  $GF(90\%)$  until a threshold  $\epsilon_{org}$  was reached, specifically  $\epsilon_{org} > \sim 55\%$ . Below this value, they measured  $GF(90\%)$  value of  $\sim 2.3$ , which is the expected value for pure sea salt at  $RH = 90\%$ . Above this value, the observed a rapid fall off in  $GF(90\%)$  to a plateau at 1.22. This reported behavior differs from that observed for nascent SSA particles sampled in the current study. Here, substantial depressions in  $GF(85\%)$  (and  $f(RH)$ ) relative to inorganic sea salt were observed when the  $\epsilon_{org}$  was only  $\sim 25\%$ , and a co-variation between  $GF(85\%)$  and  $\epsilon_{org}$  (and the ATOFMS SS spectral-type fraction) was observed. One plausible reason for this difference is that nascent (freshly-emitted) SSA particles are measured here whereas Vaishya et al. (2013) measured ambient particles that could be subject to photochemical processing. Secondary organic aerosol formed from gases, such as monoterpenes and isoprene, emitted from the ocean (Shaw et al., 2010) could have contributed to the NR-OM, although Vaishya et al. (2013) argue that this influence was negligible based on the literature. Emission rates of such species from the ocean and their relationship with oceanic processes are not well established. Although Vaishya et al. (2013) attempted to remove the influence of secondary organics in their analysis (as well as the influence of non-sea salt sulfate), it is possible that their analysis was complicated by the impacts of atmospheric processing. Another key difference is that relationship between the  $GF(85\%)$  values and  $\epsilon_{org}$  observed in the current study is consistent with ZSR behavior, while Vaishya et al. reported “bistable” behavior of the  $GF(90\%)$

**Deleted:** showed relatively strong correlation with the number fraction of sea salt-type particles

**Deleted:** characterized by ATOFMS,

**Deleted:** lower  $GF(85\%)$  values corresponding to lower  $f_{ss}$  values. This provides evidence that

**Deleted:** non-SS

**Deleted:** are, on average, less hygroscopic than the SS-type particles. The most abundant non-SS particle types identified here were sea salt mixed with organic carbon and Mg-containing.

**Deleted:** hygroscopicity of these different non-SS particle types was generally similar. However, the non-SS particle types between the different microcosm experiments differed somewhat in terms of their

**Deleted:** , with the particles from

**Deleted:** being somewhat less hygroscopic ( $GF(85\%) \sim 1.4$  -

**Deleted:** 6) than the particles from

**Deleted:** ( $GF(85\%) \sim 1.6 - 1.7$ ).

values as a function  $\epsilon_{org}$  (i.e. the flat behavior at  $\epsilon_{org} < 55\%$  and the steep fall off above). The physical basis of this bistable behavior, and the functional form implied by their measurements, is not easily explained. Finally, the  $GF(90\%)$  measurements by Vaishya et al. were made for particles with  $d_{p,m} < 165$  nm, while the composition was characterized with an HR-AMS. It is possible that size mismatch between these measurements influenced their analysis. Mass-weighted size distributions were not shown by Vaishya et al. (2013), however Frossard et al. show mass-weighted size distributions for ambient particles sampled in the remote marine boundary layer that suggest that much of the organic mass is contained in particles  $> 165$  nm. Our results clearly indicate that compositional changes to nascent SSA particles, driven by variation in physical and biochemical processes in seawater, can impact the influence of water uptake on scattering by submicron SSA even when  $\epsilon_{org} < 55\%$ . The comparison with the Vaishya et al. (2013) measurements suggests that this initial state can be further modified through atmospheric processing.

The implications of these results are explored here through calculations of the net decrease (relative to pure sea salt) in the average per particle scattering that would theoretically result from increasing amounts of OM in SSA particles, assuming that the SSA particles follow the ZSR mixing rules (see Figure 6). This has been done for different assumed  $GF(85\%)_{org}$  values as a function of  $\epsilon_{org}$  using the average size distribution for the outdoor MART shown in Figure 2B. Given the particle size distributions measured here, this assessment pertains to submicron SSA, not the entire SSA particle size distribution observed over the ocean (which includes contributions from supermicron particles (Kleefeld et al., 2002)). The range of  $\epsilon_{org}$  and  $GF_{org}(85\%)$  values determined here (about 0.25-0.50 and 1.16-1.23, respectively) correspond to decreases in scattering of about 15 to 30%. Thus, climate models that assume SSA particles behave like pure sea salt or NaCl (Stier et al., 2005; Schmidt et al., 2006) may over-predict SSA particle scattering, dependent upon the exact RH fields in the model. However, the range of  $\epsilon_{org}$  observed here, ~0.25 to 0.50, may be larger than is typical in the ambient marine atmosphere, given that the MART bloom experiments are more representative of regions of the ocean with high biological activity. For example, O'Dowd et al. (2004) observed mass fractions of ~0.40 organic matter for SSA particles with aerodynamic diameters between 0.5 and 1  $\mu\text{m}$  during periods with high biological productivity, but  $< 5\%$  for periods with low productivity. Regardless, the results presented here suggest that OM in SSA particles may have a non-negligible, yet variable impact on the light

- Deleted: substitution
- Deleted: less hygroscopic non-SS
- Deleted: for SS-type
- Deleted:  $GF_{non-SS}$
- Deleted:  $f_{SS}$
- Deleted: For a given  $GF_{non-SS}(85\%)$ , the magnitude of the decrease varies linearly with  $f_{SS}$ .
- Deleted:  $f_{SS}$
- Deleted:  $GF_{non-SS}$
- Deleted: 4
- Deleted: 7
- Deleted: 4
- Deleted: 7
- Deleted: 10
- Deleted: 35
- Deleted:  $f_{SS}$
- Deleted: 4
- Deleted: 6
- Deleted: lower
- Deleted: For example, Lee et al. observed a slightly larger  $f_{SS} \sim 0.72$  in Bodega Bay, CA during a clean atmospheric period. Recent climate modeling studies

scattering by SSA particles in the ambient atmosphere (Figure S8). Most likely, the simulated cooling effect of SSA particles due to aerosol-radiation interactions (i.e. the “direct effect”) would be decreased relative to the assumption that all SSA behaves as sea salt. Recent climate modeling studies (Partanen et al., 2014; O'Dowd et al., 2008) have attempted to account for variability in

5 OM fractions of SSA particles by parameterizing OM fraction as a function of Chl-a. However, relating the OM fraction of SSA particles to simple ocean biological metrics like Chl-a still remains challenging, as these metrics are often insufficient predictors for SSA particle composition (Quinn et al., 2014; Wang et al., 2015), and the measurements reported here indicate a clear lag between the peak in Chl-a and the minimum in the *GF*(85%) values. Quantitative understanding of the  
10 climate impacts of SSA particles will require further understanding of the timing and relationships between ocean biogeochemistry and SSA properties.

## 5 Acknowledgments

This study was funded by the Center for Aerosol Impacts on Climate and Environment (CAICE), a NSF Center for Chemical Innovation (CHE-1305427). The authors thank all IMPACTS  
15 participants and the SIO hydraulics facility staff. SDF and CDC additionally thank the students in ECI 247L during spring quarter 2015 at UC Davis, who validated the SEMS sizing.

## References

20 Ault, A. P., Guasco, T. L., Ryder, O. S., Baltrusaitis, J., Cuadra-Rodriguez, L. A., Collins, D. B., Ruppel, M. J., Bertram, T. H., Prather, K. A., and Grassian, V. H.: Inside versus outside: Ion redistribution in nitric acid reacted sea spray aerosol particles as determined by single particle analysis, *Journal of the American Chemical Society*, 135, 14528-14531, 10.1021/ja407117x, 2013.

25 Bates, T., Quinn, P., Frossard, A., Russell, L., Hakala, J., Petäjä, T., Kulmala, M., Covert, D., Cappa, C., and Li, S. M.: Measurements of ocean derived aerosol off the coast of California, *Journal of Geophysical Research: Atmospheres* (1984–2012), 117, 2012.

Biskos, G., Malinowski, A., Russell, L., Buseck, P., and Martin, S.: Nanosize effect on the deliquescence and the efflorescence of sodium chloride particles, *Aerosol Science and Technology*, 40, 97-106, 10.1080/02786820500484396, 2006.

30 Bouvet, M., Hoepffner, N., and Dowell, M. D.: Parameterization of a spectral solar irradiance model for the global ocean using multiple satellite sensors, *Journal of Geophysical Research: Oceans* (1978–2012), 107, 8-1-8-18, 10.1029/2001JC001126, 2002.

Canagaratna, M. R., Jayne, J. T., Jimenez, J. L., Allan, J. D., Alfarra, M. R., Zhang, Q., Onasch, T. B., Drewnick, F., Coe, H., Middlebrook, A., Delia, A., Williams, L. R., Trimborn, A. M., Northway, M. J., DeCarlo, P. F., Kolb, C. E., Davidovits, P., and Worsnop, D. R.: Chemical and

- microphysical characterization of ambient aerosols with the aerodyne aerosol mass spectrometer, *Mass Spectrometry Reviews*, 26, 185-222, 10.1002/mas.20115, 2007.
- 5 Cappa, C. D., Che, D. L., Kessler, S. H., Kroll, J. H., and Wilson, K. R.: Variations in organic aerosol optical and hygroscopic properties upon heterogeneous oxidation, *Journal of Geophysical Research: Atmospheres*, 116, D15204, 10.1029/2011JD015918, 2011.
- 10 Cappa, C. D., Onasch, T. B., Massoli, P., Worsnop, D., Bates, T. S., Cross, E., Davidovits, P., Hakala, J., Hayden, K., Jobson, B. T., Kolesar, K. R., Lack, D. A., Lerner, B., Li, S. M., Mellon, D., Nuaanman, I., Olfert, J., Petaja, T., Quinn, P. K., Song, C., Subramanian, R., Williams, E. J., and Zaveri, R. A.: Radiative absorption enhancements due to the mixing state of atmospheric black carbon *Science*, 337, 1078-1081, 10.1126/science.1223447, 2012.
- 15 Carslaw, K., Lee, L., Reddington, C., Pringle, K., Rap, A., Forster, P., Mann, G., Spracklen, D., Woodhouse, M., and Regayre, L.: Large contribution of natural aerosols to uncertainty in indirect forcing, *Nature*, 503, 67-71, 10.1038/nature12674, 2013.
- 20 Cochran, R., Laskina, O., Jayarathne, T., Laskin, A., Laskin, J., Lin, P., Sultana, C. M., Moore, K. A., Cappa, C., Bertram, T., Prather, K. A., and Grassian, V. H.: Analysis of organic anionic surfactants in fine (pm2.5) and coarse (pm10) fractions of freshly emitted sea spray aerosol, *Environmental Science & Technology*, 50 2477-2486, 10.1021/acs.est.5b04053, 2016.
- 25 Collins, D. B., Ault, A. P., Moffet, R. C., Ruppel, M. J., Cuadra-Rodriguez, L. A., Guasco, T. L., Corrigan, C. E., Pedler, B. E., Azam, F., and Aluwihare, L. I.: Impact of marine biogeochemistry on the chemical mixing state and cloud forming ability of nascent sea spray aerosol, *Journal of Geophysical Research: Atmospheres*, 118, 8553-8565, 10.1002/jgrd.50598, 2013.
- 30 Cruz, C. N., and Pandis, S. N.: Deliquescence and hygroscopic growth of mixed inorganic-organic atmospheric aerosol, *Environmental Science & Technology*, 34, 4313-4319, 10.1021/es9907109, 2000.
- 35 Dusek, U., Frank, G., Hildebrandt, L., Curtius, J., Schneider, J., Walter, S., Chand, D., Drewnick, F., Hings, S., and Jung, D.: Size matters more than chemistry for cloud-nucleating ability of aerosol particles, *Science*, 312, 1375-1378, 10.1126/science.1125261, 2006.
- 40 Facchini, M. C., Rinaldi, M., Decesari, S., Carbone, C., Finessi, E., Mircea, M., Fuzzi, S., Ceburnis, D., Flanagan, R., and Nilsson, E. D.: Primary submicron marine aerosol dominated by insoluble organic colloids and aggregates, *Geophysical Research Letters*, 35, 17814, 10.1029/2008GL034210, 2008.
- Farmer, D. K., Cappa, C. D., and Kreidenweis, S. M.: Atmospheric processes and their controlling influence on cloud condensation nuclei activity, *Chemical Reviews*, 115, 4199-4217, 10.1021/cr5006292, 2015.
- 35 Frossard, A. A., Russell, L. M., Massoli, P., Bates, T. S., and Quinn, P. K.: Side-by-side comparison of four techniques explains the apparent differences in the organic composition of generated and ambient marine aerosol particles, *Aerosol Science and Technology*, 48, v-x, 10.1080/02786826.2013.879979, 2014.
- 40 Fuentes, E., Coe, H., Green, D., and McFiggans, G.: On the impacts of phytoplankton-derived organic matter on the properties of the primary marine aerosol—part 2: Composition, hygroscopicity and cloud condensation activity, *Atmospheric Chemistry and Physics*, 11, 2585-2602, 10.5194/acp-11-2585-2011, 2011.

- Gard, E. E., Kleeman, M. J., Gross, D. S., Hughes, L. S., Allen, J. O., Morrical, B. D., Fergenson, D. P., Dienes, T., Galli, M. E., Johnson, R. J., Cass, G. R., and Prather, K. A.: Direct observation of heterogeneous chemistry in the atmosphere, *Science*, 279, 1184-1187, 10.1126/science.279.5354.1184, 1998.
- 5 Guasco, T. L., Cuadra-Rodriguez, L. A., Pedler, B. E., Ault, A. P., Collins, D. B., Zhao, D., Kim, M. J., Ruppel, M. J., Wilson, S. C., and Pomeroy, R. S.: Transition metal associations with primary biological particles in sea spray aerosol generated in a wave channel, *Environmental Science & Technology*, 48, 1324-1333, 10.1021/es403203d, 2013.
- 10 Hansson, H.-C., Rood, M., Koloutsou-Vakakis, S., Hämeri, K., Orsini, D., and Wiedensohler, A.: NaCl aerosol particle hygroscopicity dependence on mixing with organic compounds, *Journal of Atmospheric Chemistry*, 31, 321-346, 10.1023/A:1006174514022, 1998.
- Haywood, J., Ramaswamy, V., and Soden, B.: Tropospheric aerosol climate forcing in clear-sky satellite observations over the oceans, *Science*, 283, 1299-1303, 10.1126/science.283.5406.1299, 1999.
- 15 Hegg, D., Covert, D., and Jonsson, H.: Measurements of size-resolved hygroscopicity in the California coastal zone, *Atmospheric Chemistry and Physics*, 8, 7193-7203, 10.5194/acp-8-7193-2008, 2008.
- 20 IPCC: Climate change 2013: The physical science basis. Contribution of working group I to the fifth assessment report of the intergovernmental panel on climate change, Cambridge University Press, Cambridge, United Kingdom and New York, NY, USA, 1535 pp., 2013.
- Keene, W. C., Maring, H., Maben, J. R., Kieber, D. J., Pszenny, A. A., Dahl, E. E., Izaguirre, M. A., Davis, A. J., Long, M. S., and Zhou, X.: Chemical and physical characteristics of nascent aerosols produced by bursting bubbles at a model air-sea interface, *Journal of Geophysical Research: Atmospheres* (1984–2012), 112, D21202, 10.1029/2007JD008464, 2007.
- 25 Kirchman, D. L., Suzuki, Y., Garside, C., and Ducklow, H. W.: High turnover rates of dissolved organic carbon during a spring phytoplankton bloom, *Nature*, 352, 612-614, 10.1038/352612a0, 1991.
- 30 Kleefeld, C., O'Dowd, C. D., O'Reilly, S., Jennings, S. G., Aalto, P., Becker, E., Kunz, G., and de Leeuw, G.: Relative contribution of submicron and supermicron particles to aerosol light scattering in the marine boundary layer, *Journal of Geophysical Research: Atmospheres*, 107, PAR 8-1-PAR 8-13, 10.1029/2000JD000262, 2002.
- Langridge, J. M., Richardson, M. S., Lack, D., Law, D., and Murphy, D. M.: Aircraft instrument for comprehensive characterization of aerosol optical properties, part I: Wavelength-dependent optical extinction and its relative humidity dependence measured using cavity ringdown spectroscopy, *Aerosol Science and Technology*, 45, 1305-1318, 10.1080/02786826.2011.592745, 2011.
- 35 Laskina, O., Morris, H. S., Grandquist, J. R., Qin, Z., Stone, E. A., Tivanski, A. V., and Grassian, V. H.: Size matters in the water uptake and hygroscopic growth of atmospherically relevant multicomponent aerosol particles, *The Journal of Physical Chemistry A*, 119, 4489-4497, 10.1021/jp510268p, 2015.
- 40

- Lawler, M., Whitehead, J., O'Dowd, C., Monahan, C., McFiggans, G., and Smith, J.: Composition of 15–85 nm particles in marine air, *Atmospheric Chemistry and Physics*, 14, 11557–11569, 10.5194/acp-14-11557-2014, 2014.
- 5 Lee, C., Sultana, C. M., Collins, D. B., Santander, M. V., Axson, J. L., Malfatti, F., Cornwell, G. C., Grandquist, J. R., Deane, G. B., Stokes, M. D., Azam, F., Grassian, V. H., and Prather, K. A.: Advancing model systems for fundamental laboratory studies of sea spray aerosol using the microbial loop, *The Journal of Physical Chemistry A*, 119 8860–8870, 10.1021/acs.jpca.5b03488, 2015.
- 10 Lewis, E. R., and Schwartz, S. E.: *Sea salt aerosol production: Mechanisms, methods, measurements, and models—a critical review*, American Geophysical Union, 2004.
- Li, W. K.: Annual average abundance of heterotrophic bacteria and *synechococcus* in surface ocean waters, *Limnology and Oceanography*, 43, 1746–1753, 10.4319/lo.1998.43.7.1746, 1998.
- 15 Lopez-Yglesias, X. F., Yeung, M. C., Dey, S. E., Brechtel, F. J., and Chan, C. K.: Performance evaluation of the brechtel mfg. Humidified tandem differential mobility analyzer (bmi htdma) for studying hygroscopic properties of aerosol particles, *Aerosol Science and Technology*, 48, 969–980, 10.1080/02786826.2014.952366, 2014.
- 20 Massoli, P., Lambe, A., Ahern, A., Williams, L., Ehn, M., Mikkilä, J., Canagaratna, M., Brune, W., Onasch, T., and Jayne, J.: Relationship between aerosol oxidation level and hygroscopic properties of laboratory generated secondary organic aerosol (soa) particles, *Geophysical Research Letters*, 37, L24801, 10.1029/2010GL045258, 2010.
- Ming, Y., and Russell, L. M.: Predicted hygroscopic growth of sea salt aerosol, *Journal of Geophysical Research: Atmospheres*, 106, 28259–28274, 10.1029/2001JD000454, 2001.
- 25 Mochida, M., Kitamori, Y., Kawamura, K., Nojiri, Y., and Suzuki, K.: Fatty acids in the marine atmosphere: Factors governing their concentrations and evaluation of organic films on sea-salt particles, *Journal of Geophysical Research: Atmospheres* (1984–2012), 107, AAC 1-1–AAC 1-10, 2002.
- Mochida, M., and Kawamura, K.: Hygroscopic properties of levoglucosan and related organic compounds characteristic to biomass burning aerosol particles, *Journal of Geophysical Research: Atmospheres*, 109, n/a-n/a, 10.1029/2004jd004962, 2004.
- 30 Modini, R. L., Harris, B., and Ristovski, Z.: The organic fraction of bubble-generated, accumulation mode sea spray aerosol (ssa), *Atmospheric Chemistry and Physics*, 10, 2867–2877, 10.5194/acp-10-2867-2010, 2010.
- 35 Norrman, B., Zwiefel, U. L., Hopkinson, C. S., and Brian, F.: Production and utilization of dissolved organic carbon during an experimental diatom bloom, *Limnology and Oceanography*, 40, 898–907, 10.4319/lo.1995.40.5.0898, 1995.
- O'Dowd, C. D., Facchini, M. C., Cavalli, F., Ceburnis, D., Mircea, M., Decesari, S., Fuzzi, S., Yoon, Y. J., and Putaud, J.-P.: Biogenically driven organic contribution to marine aerosol, *Nature*, 431, 676–680, 10.1038/nature02959, 2004.
- 40 O'Dowd, C. D., Langmann, B., Varghese, S., Scannell, C., Ceburnis, D., and Facchini, M. C.: A combined organic-inorganic sea-spray source function, *Geophysical Research Letters*, 35, L01801, 10.1029/2007GL030331, 2008.

- O'Reilly, J. E., Maritorena, S., Mitchell, B. G., Siegel, D. A., Carder, K. L., Garver, S. A., Kahru, M., and McClain, C.: Ocean color chlorophyll algorithms for seawifs, *Journal of Geophysical Research: Oceans*, 103, 24937-24953, 10.1029/98JC02160, 1998.
- 5 Ovadnevaite, J., Ceburnis, D., Martucci, G., Bialek, J., Monahan, C., Rinaldi, M., Facchini, M. C., Berresheim, H., Worsnop, D. R., and O'Dowd, C.: Primary marine organic aerosol: A dichotomy of low hygroscopicity and high ccn activity, *Geophysical Research Letters*, 38, L21806, 10.1029/2011GL048869, 2011.
- 10 Ovadnevaite, J., Ceburnis, D., Canagaratna, M., Berresheim, H., Bialek, J., Martucci, G., Worsnop, D. R., and O'Dowd, C.: On the effect of wind speed on submicron sea salt mass concentrations and source fluxes, *Journal of Geophysical Research-Atmospheres*, 117, 10.1029/2011jd017379, 2012.
- Park, J. Y., Lim, S., and Park, K.: Mixing state of submicrometer sea spray particles enriched by insoluble species in bubble-bursting experiments, *Journal of Atmospheric and Oceanic Technology*, 31, 93-104, 10.1175/JTECH-D-13-00086.1, 2014.
- 15 Partanen, A.-I., Dunne, E., Bergman, T., Laakso, A., Kokkola, H., Ovadnevaite, J., Sogacheva, L., Baisnée, D., Sciare, J., and Manders, A.: Global modelling of direct and indirect effects of sea spray aerosol using a source function encapsulating wave state, *Atmospheric Chemistry and Physics*, 14, 11731-11752, 10.5194/acp-14-11731-2014, 2014.
- 20 Petters, M., and Kreidenweis, S.: A single parameter representation of hygroscopic growth and cloud condensation nucleus activity, *Atmospheric Chemistry and Physics*, 7, 1961-1971, 10.5194/acp-7-1961-2007, 2007.
- Pilinis, C., Pandis, S. N., and Seinfeld, J. H.: Sensitivity of direct climate forcing by atmospheric aerosols to aerosol size and composition, *Journal of Geophysical Research: Atmospheres*, 100, 18739-18754, 10.1029/95JD02119, 1995.
- 25 Pomeroy, L. R., Williams, P. J. I. B., Azam, F., and Hobbie, J. E.: The microbial loop, *Oceanography*, 20, 28-33, 10.5670/oceanog.2007.45, 2007.
- Prather, K. A., Bertram, T. H., Grassian, V. H., Deane, G. B., Stokes, M. D., DeMott, P. J., Aluwihare, L. I., Palenik, B. P., Azam, F., and Seinfeld, J. H.: Bringing the ocean into the laboratory to probe the chemical complexity of sea spray aerosol, *Proceedings of the National Academy of Sciences*, 110, 7550-7555, 10.1073/pnas.1300262110, 2013.
- 30 Pratt, K. A., DeMott, P. J., French, J. R., Wang, Z., Westphal, D. L., Heymsfield, A. J., Twohy, C. H., Prenni, A. J., and Prather, K. A.: In situ detection of biological particles in cloud ice-crystals, *Nature Geoscience*, 2, 397-400, 10.1038/ngeo521, 2009.
- 35 Quinn, P. K., Bates, T. S., Schulz, K. S., Coffman, D. J., Frossard, A. A., Russell, L. M., Keene, W. C., and Kieber, D. J.: Contribution of sea surface carbon pool to organic matter enrichment in sea spray aerosol, *Nature Geosci*, 7, 228-232, 10.1038/ngeo2092, 2014.
- Quinn, P. K., Collins, D. B., Grassian, V. H., Prather, K. A., and Bates, T. S.: Chemistry and related properties of freshly emitted sea spray aerosol, *Chemical reviews*, 10.1021/cr500713g, 2015.
- 40 Rinaldi, M., Fuzzi, S., Decesari, S., Marullo, S., Santoleri, R., Provenzale, A., Hardenberg, J., Ceburnis, D., Vaishya, A., and O'Dowd, C. D.: Is chlorophyll-a the best surrogate for organic

- matter enrichment in submicron primary marine aerosol?, *Journal of Geophysical Research: Atmospheres*, 118, 4964-4973, 10.1002/jgrd.50417, 2013.
- 5 Saxena, P., Hildemann, L. M., McMurry, P. H., and Seinfeld, J. H.: Organics alter hygroscopic behavior of atmospheric particles, *Journal of Geophysical Research: Atmospheres* (1984–2012), 100, 18755-18770, 10.1029/95JD01835, 1995.
- Schmidt, G. A., Ruedy, R., Hansen, J. E., Aleinov, I., Bell, N., Bauer, M., Bauer, S., Cairns, B., Canuto, V., and Cheng, Y.: Present-day atmospheric simulations using giss modele: Comparison to in situ, satellite, and reanalysis data, *Journal of Climate*, 19, 153-192, 2006.
- 10 Sellegri, K., Villani, P., Picard, D., Dupuy, R., O'Dowd, C., and Laj, P.: Role of the volatile fraction of submicron marine aerosol on its hygroscopic properties, *Atmospheric Research*, 90, 272-277, 10.1016/j.atmosres.2008.04.004, 2008.
- Shaw, S. L., Gantt, B., and Meskhidze, N.: Production and emissions of marine isoprene and monoterpenes: A review, *Adv. Meteorol.*, 2010, 10.1155/2010/408696, 2010.
- 15 Skop, R. A., Viechnicki, J. T., and Brown, J. W.: A model for microbubble scavenging of surface-active lipid molecules from seawater, *Journal of Geophysical Research: Oceans* (1978–2012), 99, 16395-16402, 10.1029/94JC01199, 1994.
- Stefan, R. L., and Szeri, A. J.: Surfactant scavenging and surface deposition by rising bubbles, *Journal of colloid and interface science*, 212, 1-13, 10.1006/jcis.1998.6037, 1999.
- 20 Stier, P., Feichter, J., Kinne, S., Kloster, S., Vignati, E., Wilson, J., Ganzeveld, L., Tegen, I., Werner, M., and Balkanski, Y.: The aerosol-climate model echam5-ham, *Atmospheric Chemistry and Physics*, 5, 1125-1156, 2005.
- Stokes, M. D., Deane, G. B., Prather, K., Bertram, T. H., Ruppel, M. J., Ryder, O. S., Brady, J. M., and Zhao, D.: A marine aerosol reference tank system as a breaking wave analogue for the production of foam and sea-spray aerosols, *Atmos. Meas. Tech.*, 6, 1085-1094, 10.5194/amt-6-1085-2013, 2013.
- 25 Stokes, R., and Robinson, R.: Interactions in aqueous nonelectrolyte solutions. I. Solute-solvent equilibria, *The Journal of Physical Chemistry*, 70, 2126-2131, 10.1021/j100879a010, 1966.
- Sultana, C. M., Collins, D. B., Lee, C., Axson, J. L., Santander, M. V., and Prather, K. A.: Exploration of the effect of biological activity on the chemical mixing state of sea spray aerosols during a laboratory phytoplankton bloom, In Prep.
- 30 Tseng, R. S., Viechnicki, J. T., Skop, R. A., and Brown, J. W.: Sea-to-air transfer of surface-active organic compounds by bursting bubbles, *Journal of Geophysical Research: Oceans* (1978–2012), 97, 5201-5206, 10.1029/91JC00954, 1992.
- Vaishya, A., Ovadnevaite, J., Bialek, J., Jennings, S. G., Ceburnis, D., and O'Dowd, C. D.: Bistable effect of organic enrichment on sea spray radiative properties, *Geophysical Research Letters*, 40, 6395-6398, 10.1002/2013GL058452, 2013.
- 35 Vesna, O., Sjogren, S., Weingartner, E., Samburova, V., Kalberer, M., Gäggeler, H., and Ammann, M.: Changes of fatty acid aerosol hygroscopicity induced by ozonolysis under humid conditions, *Atmospheric Chemistry and Physics*, 8, 4683-4690, 10.5194/acp-8-4683-2008, 2008.

- 5 Wang, X., Sultana, C. M., Trueblood, J., Hill, T. C. J., Malfatti, F., Lee, C., Laskina, O., Moore, K. A., Beall, C. M., McCluskey, C. S., Cornwell, G. C., Zhou, Y., Cox, J. L., Pendergraft, M. A., Santander, M. V., Bertram, T. H., Cappa, C. D., Azam, F., DeMott, P. J., Grassian, V. H., and Prather, K. A.: Microbial control of sea spray aerosol composition: A tale of two blooms, *ACS Central Science*, 1, 124-131, 10.1021/acscentsci.5b00148, 2015.
- Wise, M. E., Surratt, J. D., Curtis, D. B., Shilling, J. E., and Tolbert, M. A.: Hygroscopic growth of ammonium sulfate/dicarboxylic acids, *Journal of Geophysical Research: Atmospheres*, 108, 10.1029/2003jd003775, 2003.
- 10 Zhang, X., Massoli, P., Quinn, P. K., Bates, T. S., and Cappa, C. D.: Hygroscopic growth of submicron and supermicron aerosols in the marine boundary layer, *Journal of Geophysical Research: Atmospheres*, 119, 8384-8399, 10.1002/2013JD021213, 2014.
- Zhao, W. X., Hopke, P. K., and Prather, K. A.: Comparison of two cluster analysis methods using single particle mass spectra, *Atmospheric Environment*, 42, 881-892, 10.1016/j.atmosenv.2007.10.024, 2008.

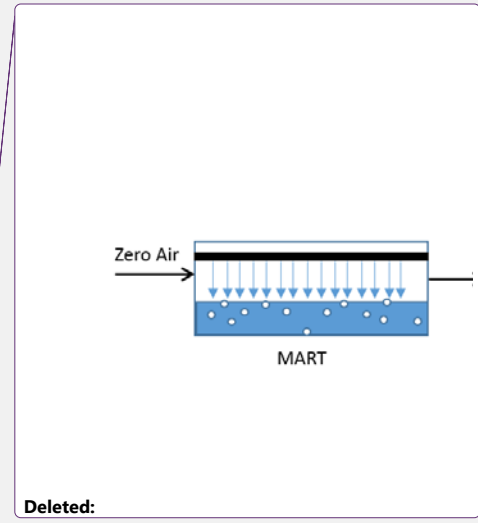
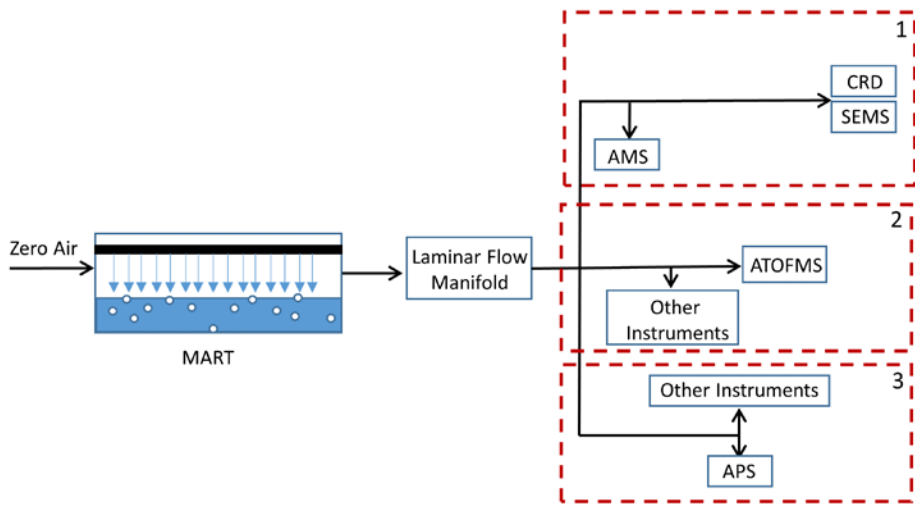
15

**Table 1.** Summary of all instrumentation used in this study.

Sampling Group	Group MART Flow Rates (LPM) Input/Output	Group Sampling Duration (hours)	Group Sampling Time After Group #1 (hrs)	Instrument/Method	Property Measured	Reference
<i>Particle Measurements</i>						
1	4.7 /3.7	1.5	0	UCD Cavity Ringdown Spectrometer (CRD)	Light extinction by dry (<20% RH) and humidified (RH ~85%) particles	(Langridge et al., 2011; Cappa et al., 2012)
1	4.7 /3.7	1.5	0	Scanning Electrical Mobility Analyzer (SEMS)	Dry particle mobility size <a href="#">distributions from <math>d_{p,m} = 15</math> to 1000 nm</a>	<b>Deleted:</b> distributions ( <b>Deleted:</b> - <b>Deleted:</b> )
1	4.7/3.7	1.5	0	High Resolution Time of Flight Aerosol Mass Spectrometer (HR-ToF-AMS)	Bulk concentrations of non-refractory particulate components of dry particles from $d_{va} = 90$ nm to 700 nm	(Canagaratna et al., 2007)
2	3.9/2.9	2.0	9	Aerosol Time of Flight Mass Spectrometer (ATOFMS)	Composition and number concentration of dried individual particles from $d_{va} = 300$ nm to 3000 nm	(Gard et al., 1998; Pratt et al., 2009)
3	6.3/5.3	1.0	4.5	Aerodynamic Particle Sizer (APS)	Dry particle aerodynamic size distributions (0.7-20 $\mu$ m)	
<i>Waterside Measurements</i>						
				Aquafloor handheld portable fluorimeter	Chlorophyll-a	
				High temperature combustion <a href="#">Epifluorescence microscopy</a>	Dissolved organic carbon <a href="#">Heterotrophic bacteria concentrations</a>	

**Table 2.** Seawater conditions at the time of collection

Date	Time	Chlorophyll-a (ug/L)	Water Temp. (°C)	Pressure (dbar)	Salinity (PSU)
8 July	12:00	0.998	23.1214	3.389	33.546
19 July	12:00	2.171	20.7463	3.567	33.6051



Deleted:

**Figure 1.** Experimental schematic for MART sampling during the IMPACTS 2014 study, with boxes labeled 1, 2, and 3 corresponding to different sampling configurations.

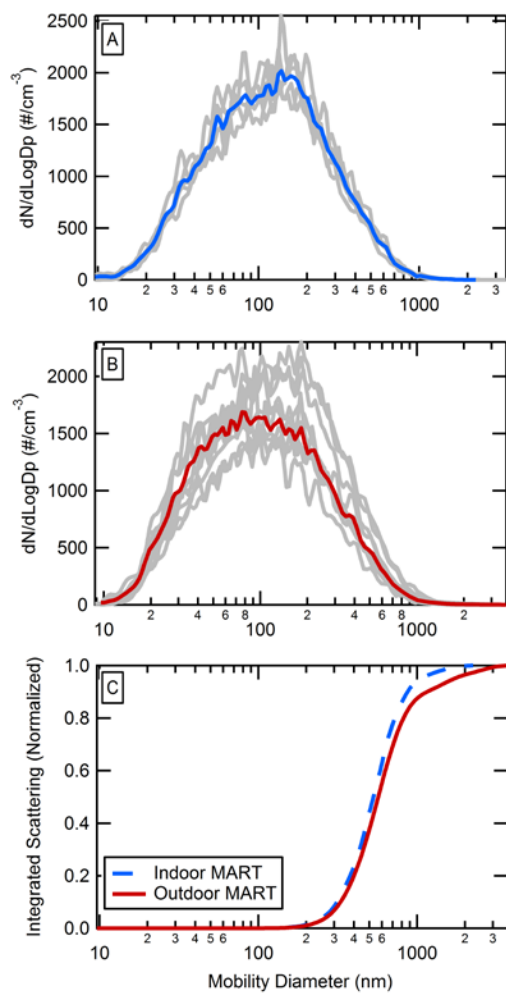


**Figure 2.** Single (grey) and average (red or blue) number-weighted merged size distributions for the (A) “indoor” and (B) “outdoor” MARTs averaged over the MART sampling period (1.5 hours) and (C) normalized integrated scattering as a function of dry mobility diameter for the merged size distribution. The optically-weighted median diameters are 530 nm for the indoor MART and 570 nm for the outdoor MART.

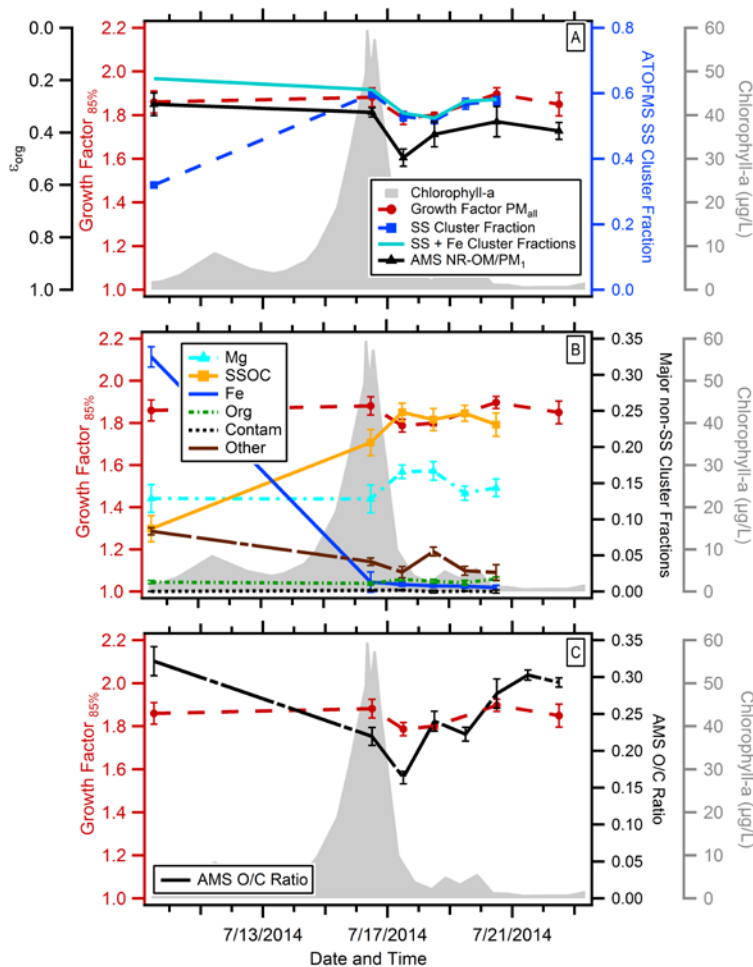
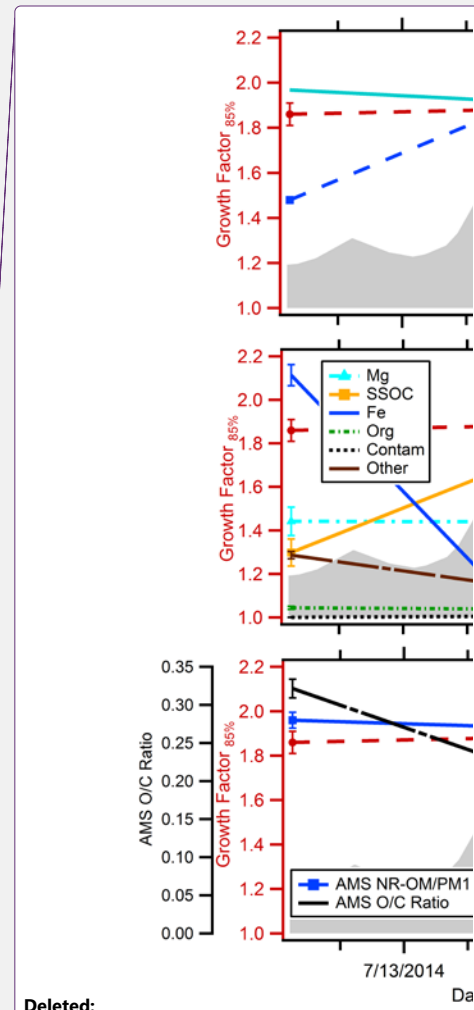


**Figure 3.** Time series for the indoor MART chlorophyll-a (gray),  $PM_{all}$   $GF(85\%)$  (red circles), and **(A)** organic volume fraction ( $\epsilon_{org}$ ) estimated from AMS non-refractory organic matter (NR-POM)/  $PM_1$  mass (solid black line), ATOFMS sea salt (SS) cluster fractions (blue dashed line), and ATOFMS SS + Iron type (Fe) cluster fractions **(B)** dominant non-sea salt cluster fractions magnesium (Mg) type (dashed turquoise line), Fe, “Other” type, and contamination (black line) and sea salt with organic carbon (SSOC) (orange line) cluster fractions, and **(C)** the AMS O/C ratio (dashed black line). Note that the axis for  $\epsilon_i$  is reversed to facilitate comparison to  $GF(85\%)$  values. The reported standard deviations for all properties is  $1\sigma$  of the individual measurements over each sampling period.



Deleted:

Deleted: )

Deleted: ratio of non-refractory organic matter (NR-POM)/  $PM_1$  mass (solid blue line) and

Deleted: NR-POM/ $PM_1$

Deleted: uncertainties

Deleted:  $1\sigma$

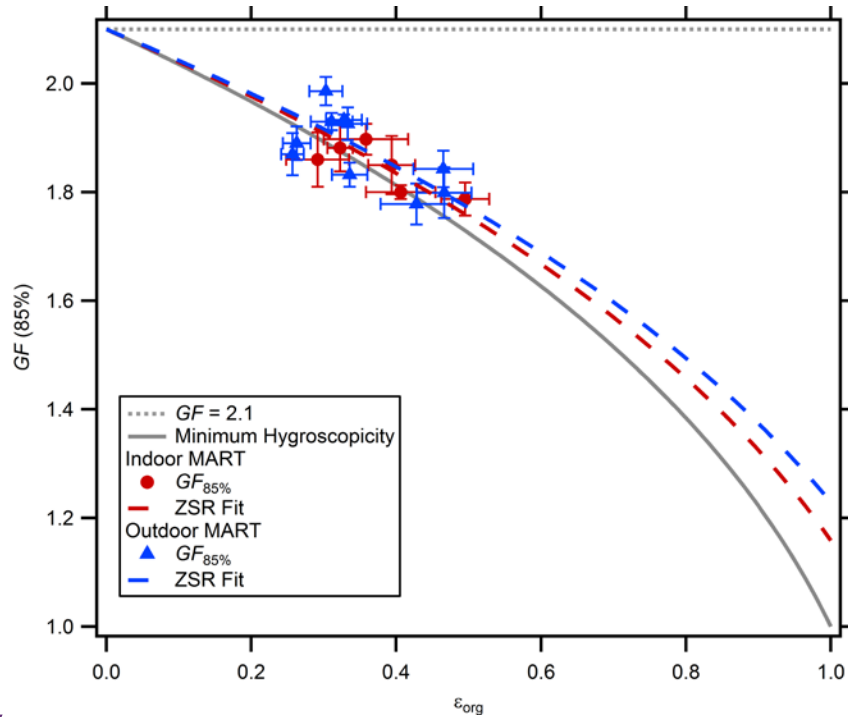
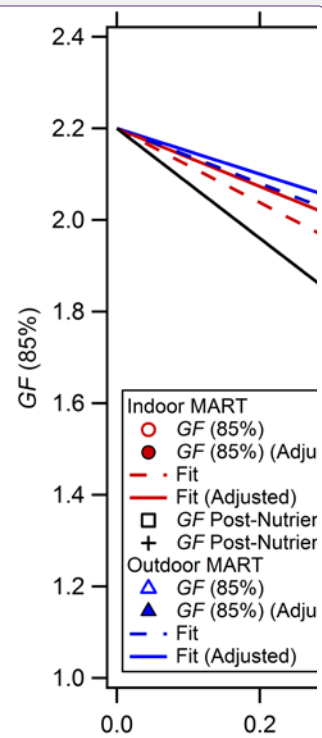


**Figure 4.**  $PM_{all}$   $GF(85\%)$  as a function of the fraction of organic volume fraction estimated from AMS non-refractory organic matter (NR-POM)/  $PM_{1, mass}$  for the indoor (red circles) and the outdoor (blue triangles) MARTs. ZSR fits to the data using Equation 5 are shown for the indoor (dashed red line) and outdoor (dashed blue line) MARTs, assuming  $GF_{sea\ salt}(85\%) = 2.1$  (dotted grey line). The overall retrieved  $GF_{org}(85\%)$  values were  $1.16 \pm 0.09$  and  $1.23 \pm 0.10$  for the indoor and outdoor MARTs, respectively. The grey solid line connecting  $GF(85\%) = 2.1$  and  $GF_{org}(85\%) = 1.0$  provides the minimum value expected for any combination of  $GF(85\%)$ .



**Deleted:**

**Deleted:** SS particles (equivalent to  $1 - f_{SS,avg}$ )... refractory organic matter (NR-POM)/  $PM_{1, mass}$  for the indoor (open red circles) and the outdoor (open blue triangles) MARTs. Also shown as solid symbols are the  $GF(85\%)$  values as a function of  $1 - f_{SS^*}$ , where  $f_{SS^*}$  is the size-adjusted SS-type particle fraction (see main text for details)... ZSR fits to the data using Equation 5 are shown, assuming  $GF_{SS}(85\%) = 2.2$ ... for the indoor overall (red dashed red line), outdoor overall (blue dashed line), indoor adjusted (red solid line),... and outdoor adjusted (...dashed blue solid ...ine) MARTs... assuming  $GF_{sea\ salt}(85\%) = 2.1$  (dotted grey line). The overall retrieved  $GF_{non-SS}...GF_{org}(85\%)$  values were  $1.39...6 \pm 0.03...9$  and  $1.60 \pm ...3 \pm 0.03...0$  for the indoor and outdoor MARTs, respectively. The adjusted  $f_{SS,0.75\ \mu m}$  retrieved  $GF_{non-SS}(85\%)$  values were  $1.57 \pm 0.03$  and  $1.70 \pm 0.03$  for the indoor and outdoor MARTs, respectively. The black...rey solid line connecting  $GF_{SS}...F(85\%) = 2.2$ ... and  $GF_{non-SS}...F_{org}(85\%) = 1.0$  provides the minimum value expected for any combination of SS and non-SS particles. The post-nutrient ... $F(85\%)$  corresponding to  $f_{SS}$  (open black square) and  $f_{SS+Fe}$  (black cross) are shown for reference, but not included in the fits.

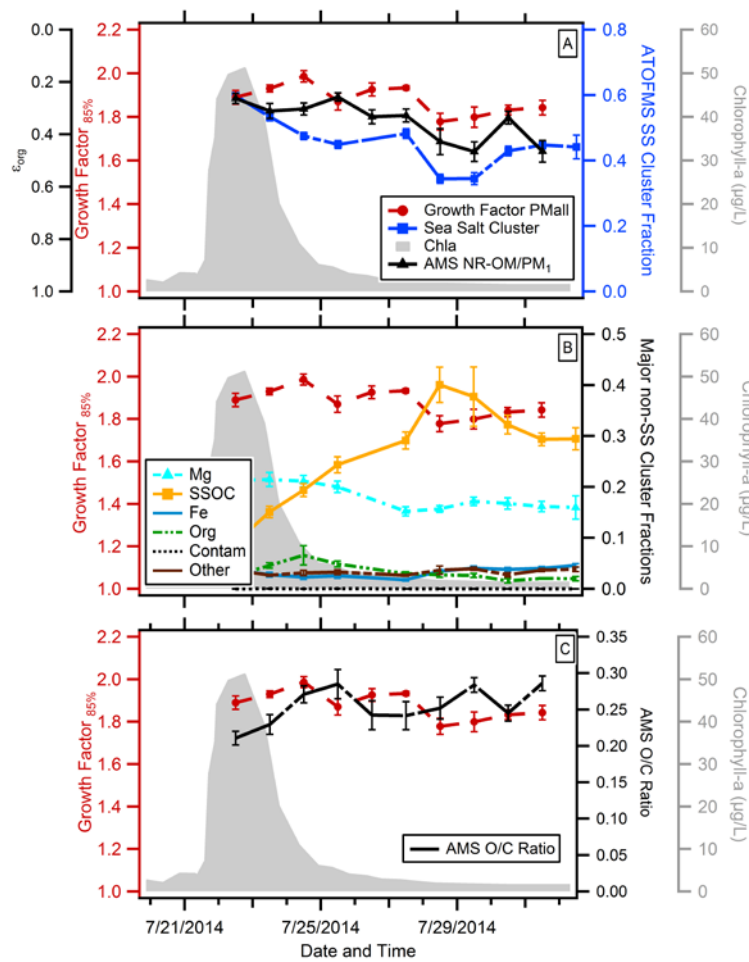
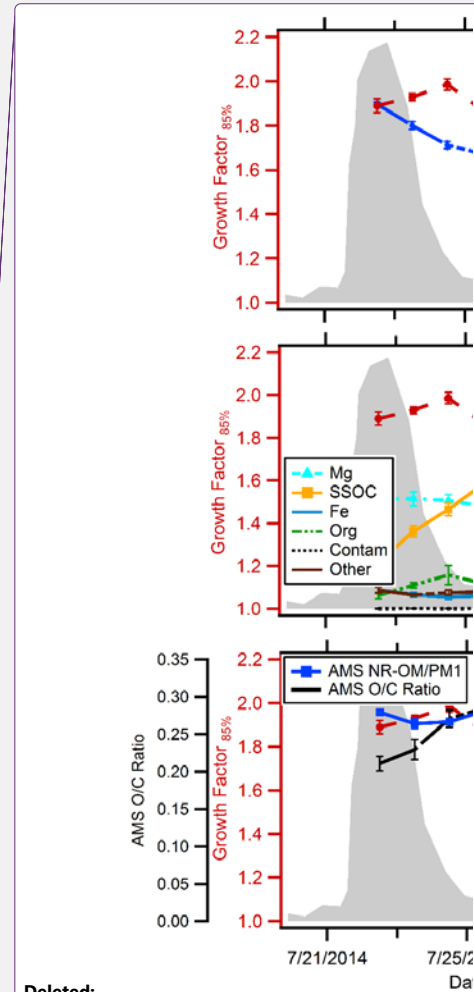
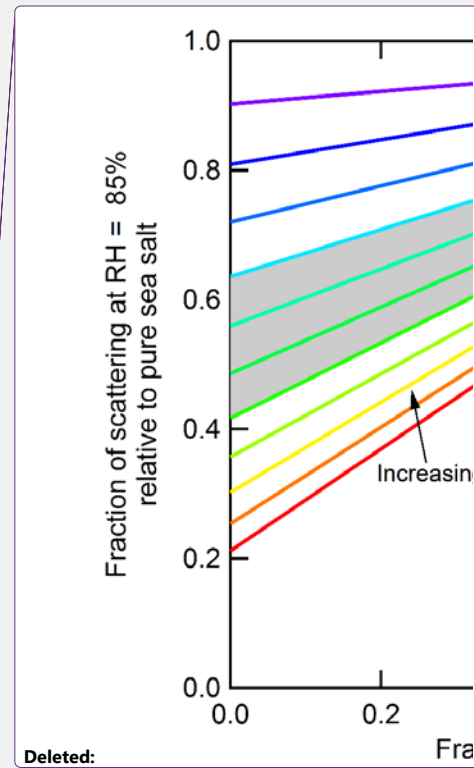
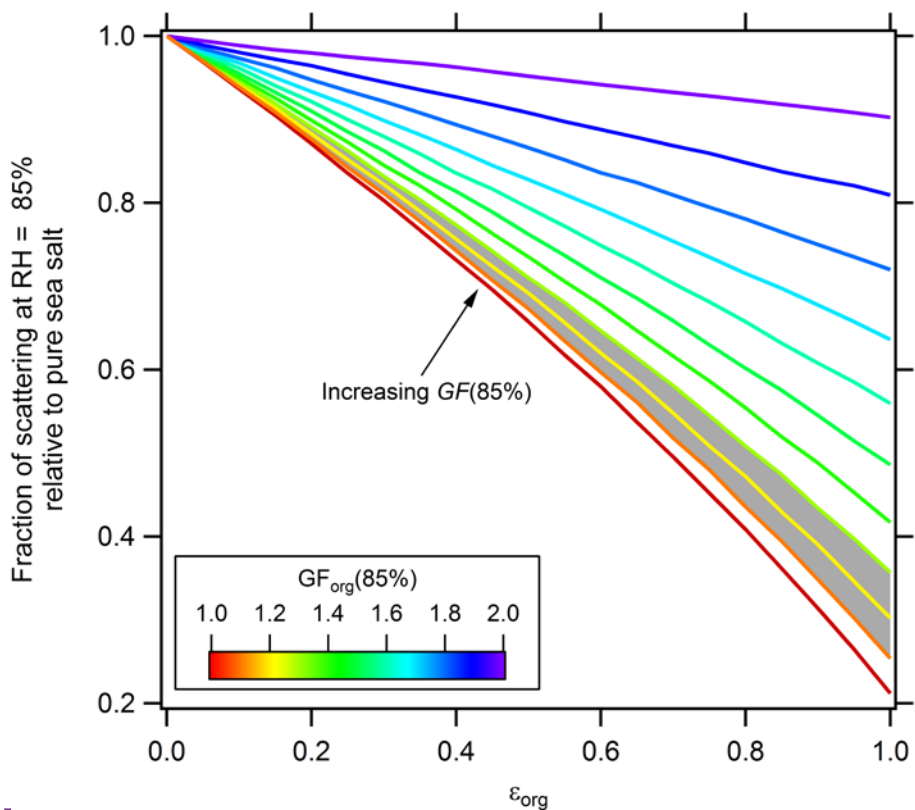


Figure 5. Same as Figure 3 above, but for the outdoor MART.



Deleted:



**Figure 6.** Calculated fraction of scattering relative to pure sea salt particles at 85% RH as a function of  $\epsilon_{org}$ , assuming the OM component of the SSA particles have the same, constant hygroscopicity and a refractive index of 1.55 and the SSA particles follow the ZSR mixing rules. The different curves are colored according to the assumed  $GF_{org}(85\%)$  value, ranging from 1.0 to 2.0, given  $GF_{sea\ salt}(85\%) = 2.1$ . The gray band shows the range of  $GF_{org}$  values indicated by the current measurements.

- Deleted: number fraction
- Deleted: SS-type
- Deleted: , assuming all non-SS particle types
- Deleted: .
- Deleted:  $GF_{non-SS}$
- Deleted:  $GF_{SS}$
- Deleted:  $GF_{non-SS}$

## Supplementary Online Material for “Linking variations in sea spray aerosol particle hygroscopicity to composition during two microcosm experiments”

Sara D. Forestieri<sup>1</sup>, Gavin C. Cornwell<sup>2</sup>, Taylor M. Helgestad<sup>1</sup>, Kathryn A. Moore<sup>2</sup>, Christopher Lee<sup>2</sup>, Gordon A. Novak<sup>3</sup>, Camille M. Sultana<sup>2</sup>, Xiaofei Wang<sup>2</sup>, Timothy H. Bertram<sup>2,3</sup>, Kimberly A. Prather<sup>2,4</sup>, Christopher D. Cappa<sup>1,\*</sup>

<sup>1</sup>Department of Civil and Environmental Engineering, University of California, Davis, CA 95616

<sup>2</sup>Department of Chemistry and Biochemistry, University of California, San Diego, La Jolla, CA 92093

<sup>3</sup>Department of Chemistry, University of Wisconsin, Madison, WI 53706

<sup>4</sup> Scripps Institution of Oceanography, 9500 Gilman Drive, La Jolla, CA 92093

\* Correspondence to: E-mail: [cdcappa@ucdavis.edu](mailto:cdcappa@ucdavis.edu)

The supplementary material consists of six figures that provide additional support for the conclusions presented in the paper.

**Deleted:** Supporting Materials: ¶

**Deleted:** mesocosm

**Deleted:** Cornwell<sup>5</sup>

**Deleted:** Moore<sup>3</sup>, Chris Lee<sup>3</sup>

**Deleted:** Novak<sup>4</sup>

**Deleted:** Sultana<sup>3</sup>

**Deleted:** Wang<sup>3</sup>

**Deleted:** Bertram<sup>3,4</sup>

**Deleted:** Prather<sup>3</sup>

**Deleted:** <sup>2</sup> Chemistry Department, University of Iowa, IA, 52242¶  
<sup>3</sup>

**Deleted:** <sup>4</sup>

**Deleted:** .

**Table S1. Summary of uncertainties for growth factor (GF) retrieval.**

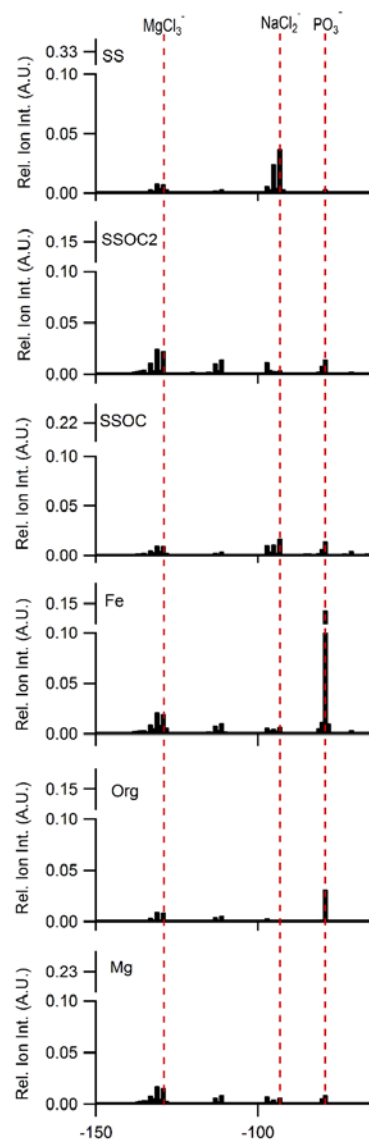
Parameter	Default Value	Perturbation	$\Delta$ GF	% $\Delta$ GF
f(RH)	3.7	0.5 (7%) <sup>#</sup>	0.05	2.6%
Relative Humidity	85%	1.2%/0.03% (see Table 2)	0.05/0.01 <sup>§</sup>	2.4%/0.5%
Refractive Index	1.55	0.04	0.05	2.7%
Particle Diameter	Distribution with mode $\equiv$ ~112 nm	+1%	0.01	<1%

<sup>§</sup>  $\Delta$ GF values were calculated using Kappa-Kohler equation and assuming a  $\kappa$  value of 1.3 [Petters and Kreidenweis, 2007].

**Table S2. Measured and actual GFs for pure substances and the implied error in the measured RH.**

	Observed	Actual	$\Delta$ RH
NaCl	2.09	2.1	0.03%
Ammonium Sulfate	1.59	1.55	1.2%

Uncertainties in the measured f(RH), relative humidity, refractive index, and diameter that contribute to the overall uncertainty in GF retrieval are provided in Table S1. The uncertainty in the CRD extinction is ~5% at 532 nm and the fundamental performance of the CRD method for wet particles is not changed. Therefore, the propagated uncertainty of f(RH) ( $=b_{ext_{wet}}/b_{ext_{dry}}$ ) =  $\sqrt{0.05^2 + 0.05^2} = 7\%$ . Two estimates for uncertainty in relative humidity were based on the hygroscopic growth factors of pure NaCl and pure ammonium sulfate generated from a TSI atomizer. The measured values were compared to literature values to infer the error in RH (see Table 2). The refractive index used in this study is appropriate for NaCl. However, refractive index of sea salt mixed with marine derived organic matter is not well known, but a value of 1.48 reported by Nessler et al. [2005] for organic matter has been used in many recent studies [Partanen et al., 2014; Vaishya et al., 2013] for marine derived organic matter. The refractive index of the mixture is likely to be somewhere in between. Assuming that organic matter is 50% of the particles by volume (consistent with the ensemble average fraction reported in this manuscript), the volume-



**Deleted:** Figure S. Dual polarity ATOFMS Mass Spectra for the major cluster types

weighted refractive index is 1.51. GF values were retrieved with a refractive index of 1.51 and compared to the GF values retrieved using the default value of 1.55 to assess the uncertainty in the refractive index. The uncertainty of 1% for the measured diameter was determined during the experiments in which a 2<sup>nd</sup> DMA size-selected particles 100-300 nm.

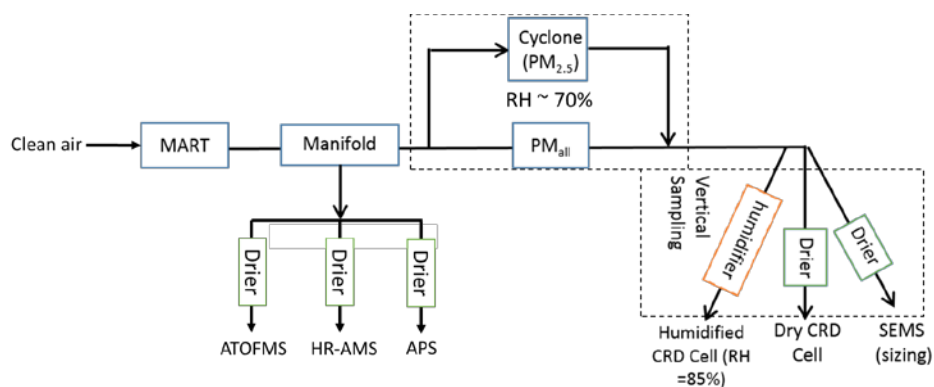


Figure S1. A detailed schematic of the general sampling scheme for the online instruments. Note that not all instruments sampled at the same time (see Table 1). Particles sampled from the MART passed through a manifold from which they were subsampled to the various instrumentation. All instruments included an upstream drier and sampled dried particles. The driers and humidifiers for the CRD and SEMS sampling group (Group 1) were oriented vertically. The particles sampled to the CRD and SEMS alternately passed through a PM<sub>2.5</sub> cyclone. The RH at this point was ~70%.

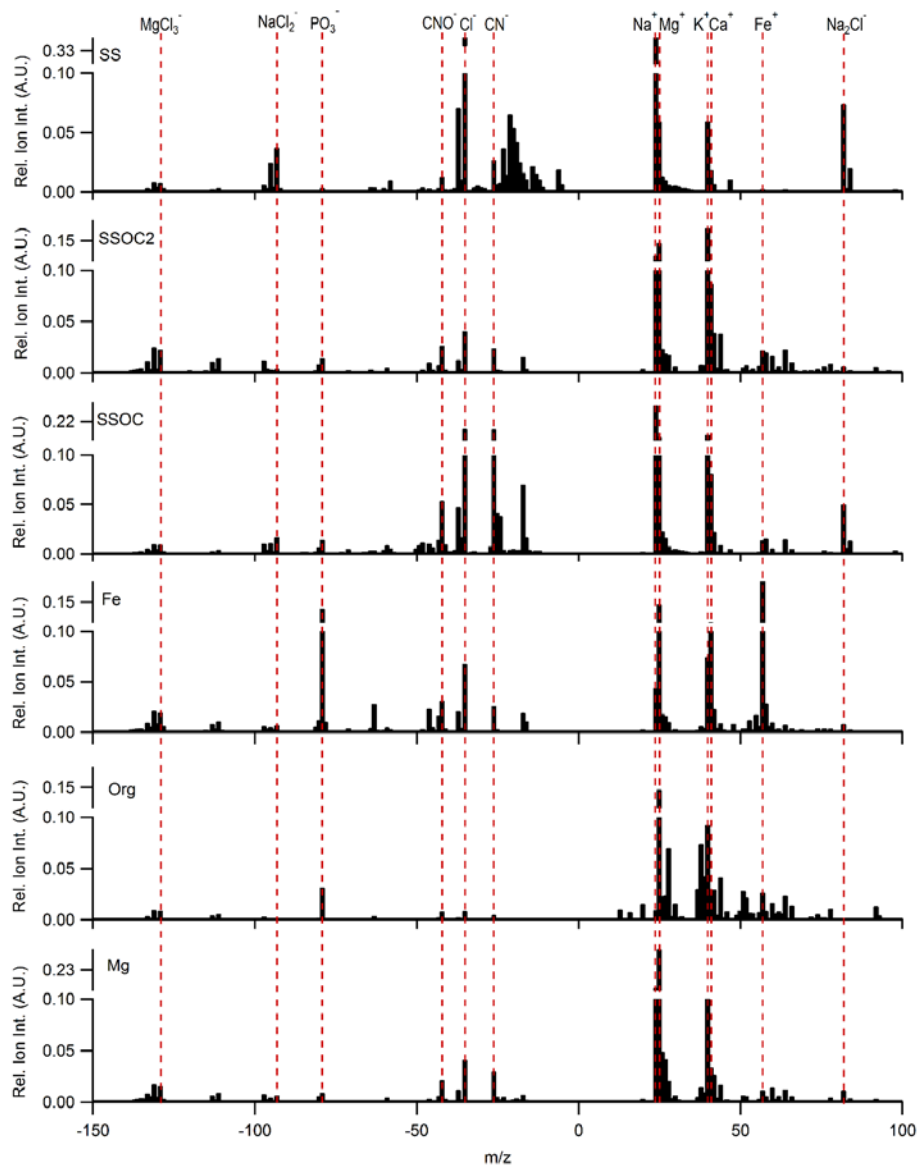


Figure S2. Dual polarity ATOFMS Mass Spectra for the major spectra categories: sea salt (SS), sea salt with organic carbon (SSOC and SSOC2), Iron (Fe), Organic (Org), and Magnesium (Mg) types.

Deleted: clusters

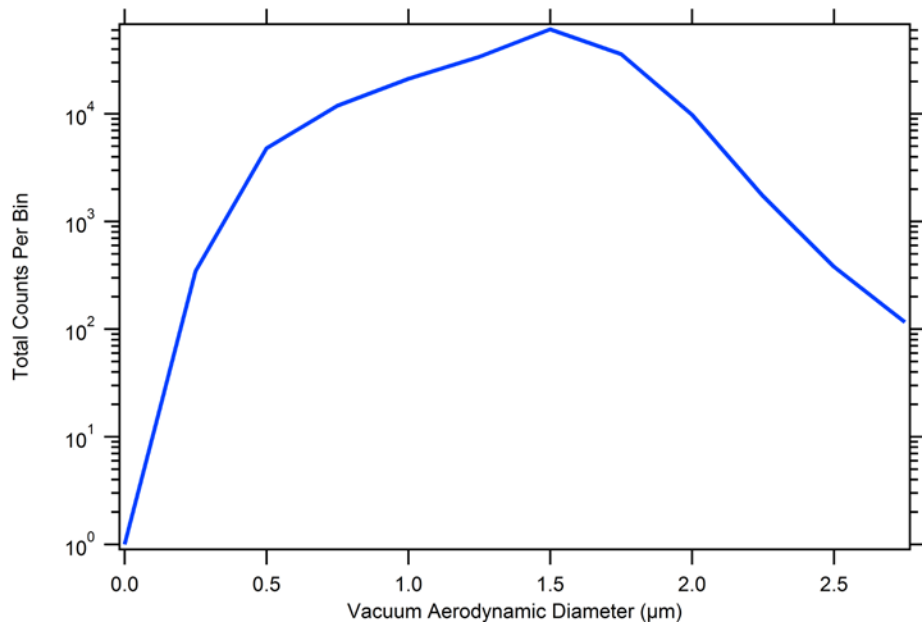


Figure S3. Size-resolved ATOFMS particle counts.

Deleted: S.

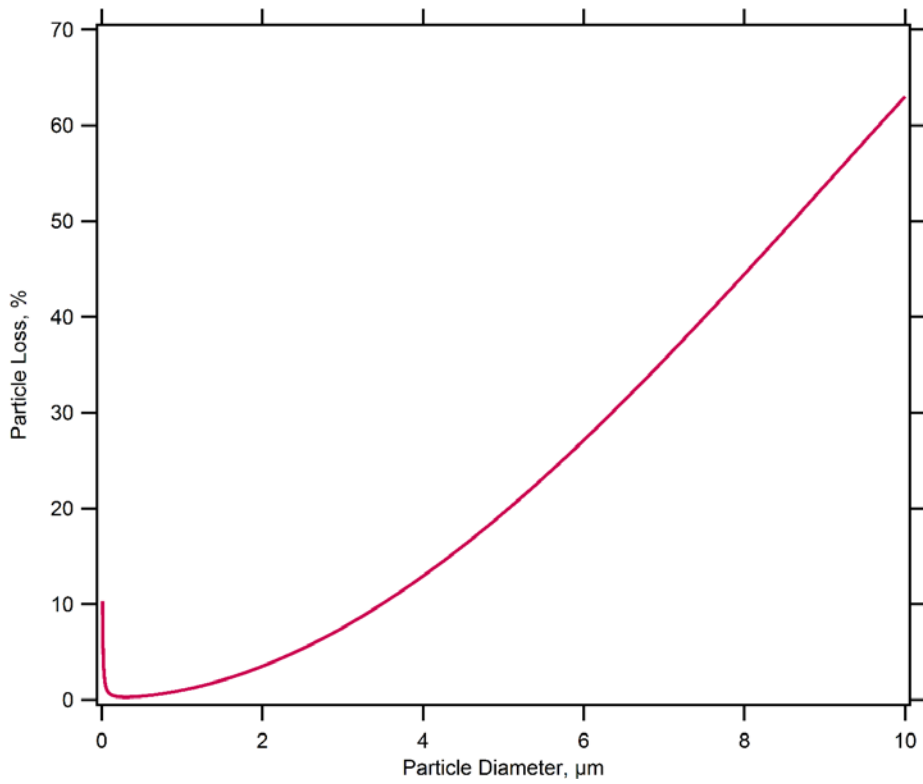


Figure S4. Predicted particle losses for particles travelling from the MART outlet to the MART manifold for a sampling line 10' in length and 3/8" in diameter. The Particle Loss Calculator of [Von der Weiden et al., 2009] as used.

Deleted: S.

Field Code Changed

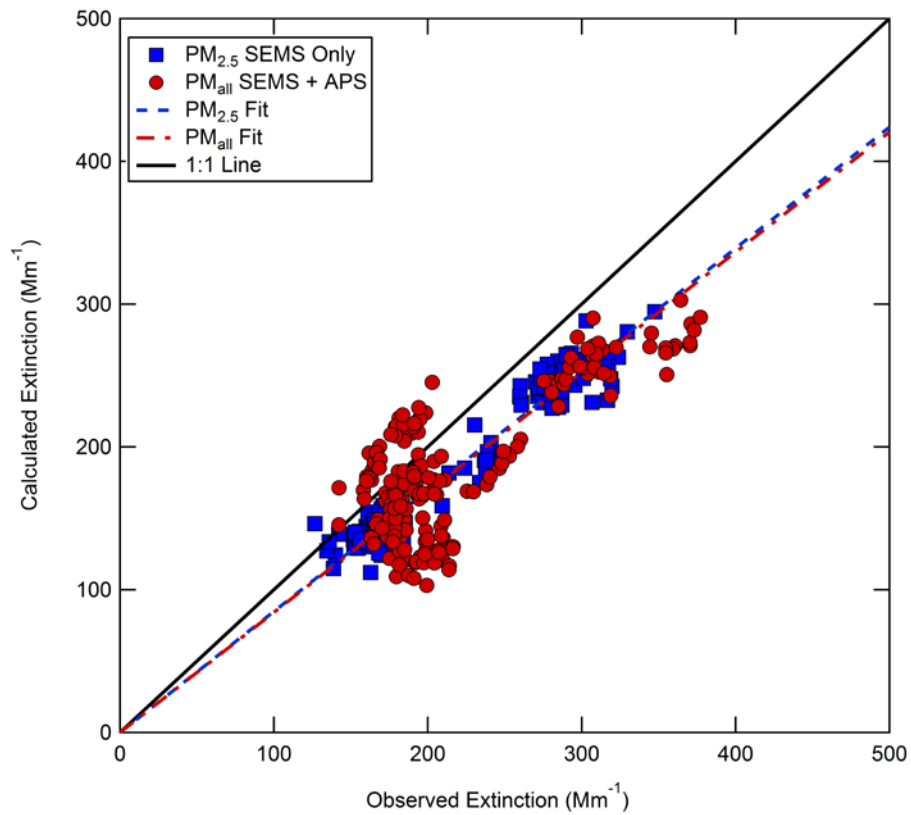


Figure S5. Calculated extinction using SEMS size distributions (real RI = 1.55) for  $PM_{2.5}$  and SEMS+APS size distributions as a function of the observed CRD extinction for the 2014 MART experiments. Slopes for linear fits (with the intercept fixed at 0) of calculated extinction as a function of observed extinction were 0.85 and 0.84 for  $PM_{2.5}$  and  $PM_{all}$ , respectively. A 1:1 line is provided for reference.

Deleted: s.

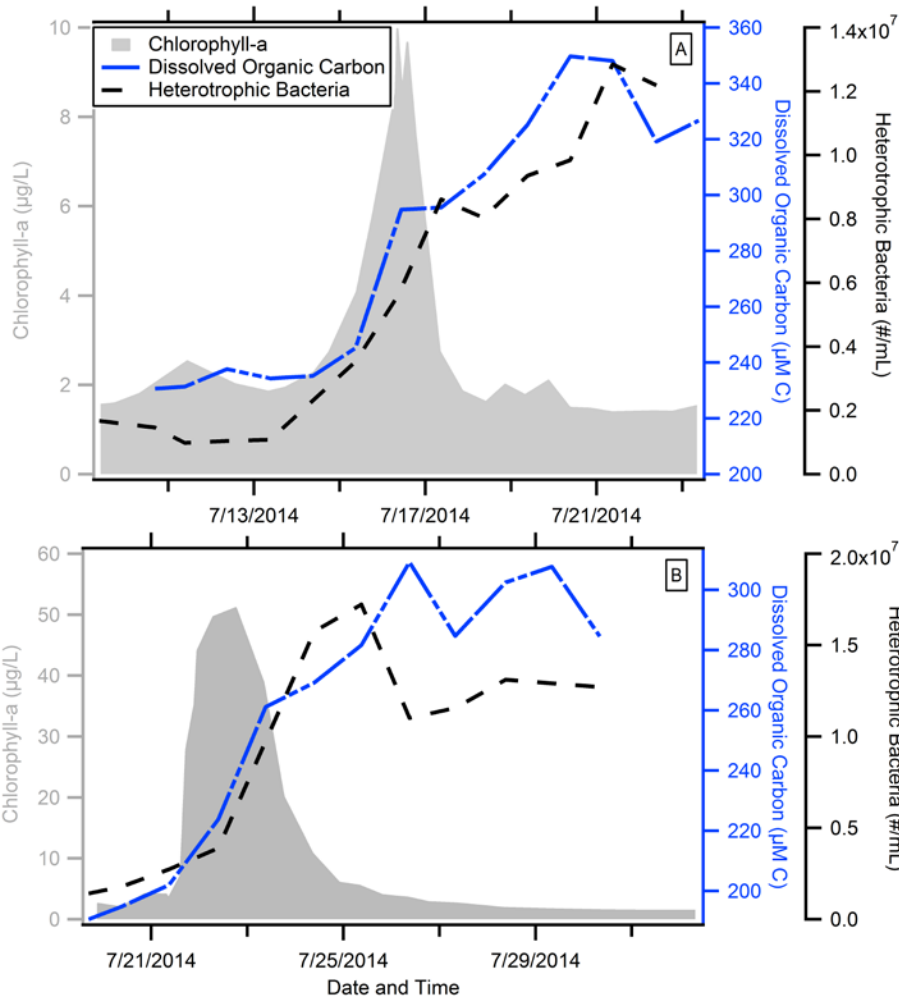


Figure S6. Time series of concentrations of dissolved organic carbon (DOC; µM C), heterotrophic bacteria (#/mL), and chlorophyll-a concentrations (µg/L) in the seawater water for the (A) indoor and (B) outdoor MARTs.

Deleted: S.

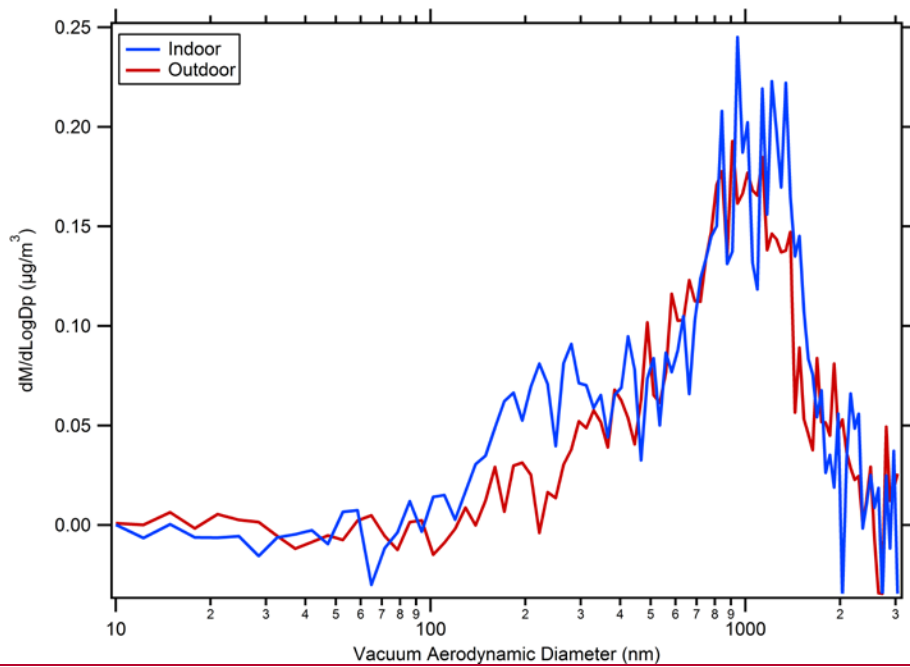
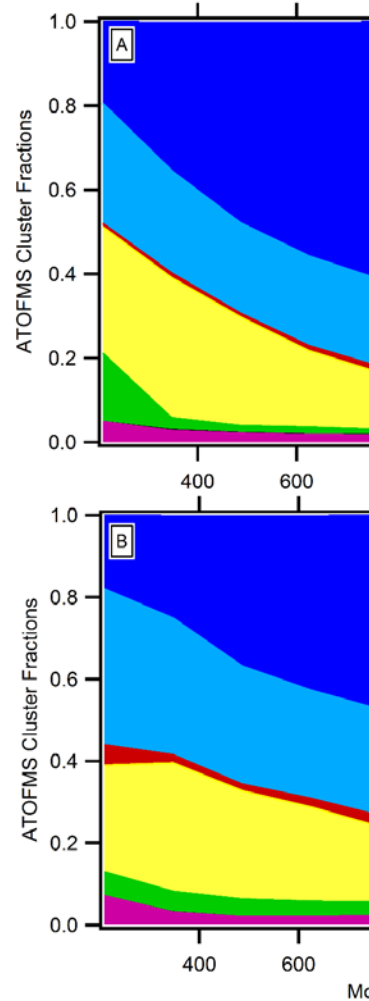


Figure S7. AMS m/z 43 particle time of flight (pTOF) mass distributions for the indoor (blue) and outdoor (red) MARTS.



**Deleted:** Figure S. ATOFMS cluster fractions of sea salt (SS; dark blue), sea salt with organic carbon (SSOC; light blue), magnesium type (Mg; light yellow), iron type (Fe; red), organic (ORG; green), contamination (black), and "other" (magenta) as a function of mobility diameter averaged for (A) MART A and (B) MART B. Note the enrichment in non-SS cluster fractions at mobility diameters < 1 µm. Vacuum aerodynamic diameters have been adjusted to mobility diameters assuming spherical particles with a density of 1.8 g cm<sup>-3</sup>. Vacuum aerodynamic diameter ( $d_{p,a}$ ) was converted to mobility diameter ( $d_{p,m}$ ) using the equation  $d_{p,m} = d_{p,a}/1.8$ .

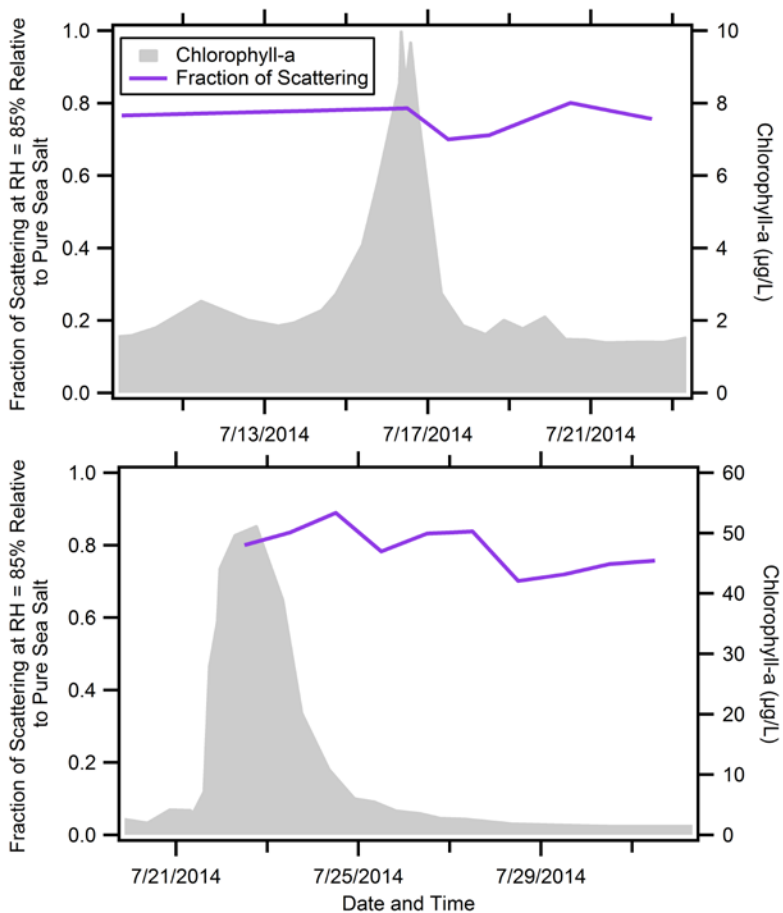


Figure S8. Calculated fraction of scattering relative to pure sea salt particles at 85% RH as a function of time for the two microcosm experiments.

DeCarlo, P. F., J. G. Slowik, D. R. Worsnop, P. Davidovits, and J. L. Jimenez (2004), Particle morphology and density characterization by combined mobility and aerodynamic diameter measurements. Part 1: Theory, *Aerosol Science and Technology*, 38(12), 1185-1205.

Nessler, R., E. Weingartner, and U. Baltensperger (2005), Adaptation of dry nephelometer measurements to ambient conditions at the Jungfraujoch, *Environmental science & technology*, 39(7), 2219-2228.

Partanen, A. I., et al. (2014), Global modelling of direct and indirect effects of sea spray aerosol using a source function encapsulating wave state, *Atmospheric Chemistry and Physics*, 14(21), 11731-11752.

Petters, M., and S. Kreidenweis (2007), A single parameter representation of hygroscopic growth and cloud condensation nucleus activity, *Atmospheric Chemistry and Physics*, 7, 1961-1971.

Vaishya, A., J. Ovadnevaite, J. Biialek, S. G. Jennings, D. Ceburnis, and C. D. O'Dowd (2013), Bistable effect of organic enrichment on sea spray radiative properties, *Geophysical Research Letters*, 40(24), 6395-6398.

Von der Weiden, S., F. Drewnick, and S. Borrmann (2009), Particle Loss Calculator—a new software tool for the assessment of the performance of aerosol inlet systems, *Atmos. Meas. Tech*, 2(2), 479-494.